Tactile Perception in Robots:
From the Somatic Alphabet to the Realization of a Fully "Sensitive Skin"

by

Walter Daniel Stiehl

Submitted to the Department of Mechanical
Engineering in Partial Fulfillment of the
Requirements for the Degree of

Bachelor of Science

at the

Massachusetts Institute of Technology

June 2003

© 2003 Walter Daniel Stiehl
All rights reserved

The author hereby grants to MIT permission to reproduce and to distribute publicly paper and electronic copies of this thesis document in whole or in part.

Signature of Author……
Department of Mechanical Engineering
May 9, 2003

Certified by……
Cynthia Breazeal
LG Group Career Development Professor
Assistant Professor of Media Arts and Sciences
Thesis Supervisor

Accepted by……...……
Professor Ernest G. Cravalho
Chairman, Undergraduate Thesis Committee

Acknowledgements

This thesis would not have been possible without the incredible opportunities, knowledge, and support I have received from a great number of people.

To my parents, Alan and Elaine Stiehl, who have always believed in my work and done everything they could to support me. To Aunt Barbara, whose generous gift of a new computer helped to create this thesis and made the solid modeling and computation that much easier. To Pop Pop and Grandma Stiehl, who while at times didn't quite understand what I was working on, still provided me with their love and support. To my uncles, Donald, Chris, and Dick, and my aunts, Beverly, Diana and Carol, who during family get togethers gave not only great meals to a tired student, but also provided good natured support. To Shannon for her love and support. To Papa, Nana and Uncle Phil, who let a young 12 year old take over their basement so he could begin to experiment with plaster molds, casting and sculpture. No matter where I end up in life I will always consider the basement on Thurston St. as my first Creature Shop.

I have had the great opportunity to work and learn from a great many talented people in the special effects industry. Their instruction has changed the way in which I approach art and design, and their influence is seen throughout this thesis. To Tate Holland, John Bailey, Paul Thompson, Karl Zundel and the other instructors and staff of mud – the Make-Up Designory in Burbank, California. Karl, I am truly grateful for your instruction and guidance not only during the months of class but afterwards as well. I will always consider you a mentor and a friend. To Tom McLaughlin, whose Silicone Art Seminar and Workshop taught me a great deal about silicone and began to generate some of the ideas and applications demonstrated in this thesis. To Stan Winston, Richard Landon, Lindsay MacGowan, Alan Scott, Jon Dawe, Al Sousa, Keith Marbory, and the other members of the Leonardo team at Stan Winston Studio. Their guidance both during my time at the studio while Leonardo was being constructed and through phone calls and e-mail afterwards was incredibly beneficial. Without the mechanical design and materials help provided by Richard, Lindsay, Alan, Keith, and J.D. this thesis would not have been possible. I am truly grateful to be part of collaboration with such a talented group of artists and engineers.

To Professor Steve Benton for first opening the world of the Media Lab to me when he answered my father's request for a tour of the Media Lab while I was deciding between MIT and other colleges. I am very happy to say that my decision to come to MIT was made practically on the spot. To Bill Tomlinson, whose first enthusiastic words to me while on that tour were "You know how to do latex? We could use someone to make us a latex chicken…." And thus began my entry into the Media Lab. To Professor Bruce Blumberg who took a chance by giving a 17-year-old high school graduate the task of creating a series of chickens for the Swamped! SIGGRAPH '98 Demo. Now as I look back, I realize how much faith he and Bill must have had in me; for this I am truly grateful. To Robert Burke, Marc Downie, Scott Eaton, Damian Isla, Yuri Ivanov, Michael Patrick Johnson, Ben Resner, Matt Berlin, Michal Hlavac, Chris Kline, Ken Russell, Jed Wahl, Andrew Wilson, Song-Yee Yoon, Delphine Nain, Aileen Kawabe and the other members of the Synthetic Characters Group with whom I have had the privilege to work. Special thanks goes to Rob and Scott who worked together with me to bring to life Rufus, the first computer controlled animatronic character I worked on. Many of the

ideas in this thesis first began to gel from the desires of wanting to "touch" Rufus and scratch his head and have him respond.

To Professor Joe Paradiso and the other members of the Responsive Environments Group, especially Mark Feldmeier, Josh Lifton, Hong Ma, Stacy Morris, and Ari Benbasat, who each provided helpful answers to various questions during the design and construction of this thesis. Special thanks to Joe and Josh for their work on MAS.965 – this class provided much of the initial research used for the third chapter of this thesis.

To Professor Christopher Moore and the members of his research lab – Cheryl Ann Cheney, Jason Ritt, Mark Lawrence Andermann, Catherine Garabedian, and Catherine Kerr. Without their knowledge of human skin, much of the focus of this thesis and a large portion of Chapter 2 would not have been possible. I look forward to many more discussions on skin as my work continues. To Professor Sue Corkin, my advisor in Brain and Cognitive Sciences, and the other members of the faculty of Brain and Cognitive Sciences with whom I have had the opportunity to learn from. To the faculty and staff of Mechanical Engineering, especially Professor Woodie Flowers, Professor Dave Wallace, Professor Warren Seering, Professor Sang-Gook Kim, Professor Sanjay Sarma, Professor Ernesto Blanco, and Professor Alexander Slocum, whose guidance and instruction through the design subjects of 2.007, 2.008, 2.72, and 2.009 greatly influenced the design approaches of this thesis.

Finally, to Professor Cynthia Breazeal for believing in me and in the importance of a sense of touch for robotics and allowing me the incredible opportunities I have had so far working with her. To Matt Hancher, for countless answers to a bevy of electronics questions and networking issues. To John McBean and Jeff Lieberman who provided another viewpoint during the difficult phases of the mechanical design and often helped to narrow down the approach. To Josh Strickon for his guidance in the initial software design of this thesis and to Jesse Gregory for further help. To the other members of the group - Corey Kidd, Andrew 'Zoz' Brooks, Heather Knight, Hans Lee, Blake Brasher, Dan McAnulty, Michael Wolf, and Janette Fong, who all provided help in various other ways during the creation of this thesis. I can truly say the last two years at One Cambridge Center have been an enjoyable experience.

Most importantly, to the brewers of coffee everywhere, especially Starbucks, Au Bon Pain, Arrow Street Crepes, and Dunkin Donuts for providing the fuel necessary for countless late nights of writing, molding, pouring, designing, programming, mixing, wiring….

CONTENTS

ACKNOWLEDGEMENTS II
LIST OF TABLES VI
LIST OF FIGURES VII
ABSTRACT X
1. MOTIVATION: WHY TOUCH? 1
2. TOUCH IN HUMANS AND ANIMALS – LESSONS FROM NEUROSCIENCE 4
2.1 Introduction 4
2.2 Essential Terminology and Concepts 4
2.3 Skin – The Largest Sensory Organ 8
2.4 Receptor Types of Somatic Sensation 10
2.5 Properties of the Stimulus Encoded at the Periphery 17
2.6 Pathway from Receptor to Cortex 20
2.7 The Somatosensory Cortex 26
2.8 Other Findings from Studies of Humans 36
2.9 Argument for the Somatic Alphabet 36
3. TOUCH IN ROBOTICS 38
3.1 Introduction 38
3.2 "Sensitive Skin": Moving Beyond the Robotic Gripper 38
3.3 Tactile Sensing in Robotics: A Survey of Approaches 39
3.4 Sensitive Robotic Fingers and Hands 40
3.5 How the "Alphabet" Framework Could Be Applied to Robotics 44
4. OVERVIEW OF THE DESIGN 46
4.1 Leonardo, a Sociable Robot 46
4.2 Design Constraints and Challenges 47
4.3 The "Pixel" Platform 49
5. ELECTROMECHANICAL DESIGN OF THE NEW "PIXEL" HAND 51
5.1 Modifications of the "Pixel" Hand 51
5.2 Sensors, Wiring, and Circuit Boards 53
5.3 Mechanical Design of the New "Pixel" Hand 64
5.4 Assembly of Components 75
6. ELECTRONICS 82
6.1 Overview of the Electronic System 82
6.2 Sensor Selection and Performance 83
6.3 The Arm Developer 64-Channel A/D Board 86
6.4 The Motor Control System 89
7. SYNTHETIC SILICONE SKIN 91
7.1 Why give a Robot Skin? 91
7.2 Types of Silicone 94
7.3 Molds for the Hand and Fingertips 95
7.4 Silicone Formulas for Experimentation and Durometer Tests 103
8. COMPUTATION 110
8.1 Overview 110
8.2 Framework Designed for Expansion 111
8.3 Peripheral Coding 113

8.4 Higher Cortical Processing 114
9. CONCLUSIONS AND FUTURE WORK 117
9.1 Conclusions 117
9.2 Future Work 117
9.3 Potential Uses of "Sensitive Skin" Beyond Robotics 119
REFERENCES 121
APPENDIX A: PIC CODE 128

List of Tables

Table 2-1. Somatic Sensation Receptor Types 11
Table 2-2. Mechanoreceptors in Glaborous Skin 12
Table 5-1. The Number of Sensors per Region. 57
Table 7-1. Silicone Formulas used in Experiments.. ……..105
Table 7-2. The Durometer Conversion Chart 107

List of Figures

Figure 2-1. The Views of the Brain and Body 5
Figure 2-2. Divisions of the Central Nervous System. 6
Figure 2-3. Three Views of the Human Brain 7
Figure 2-4. Brodmann's Areas. 8
Figure 2-5. Sectional View of the Skin. 9
Figure 2-6. Sectional View of Hairy and Glaborous Skin with Mechanoreceptors Highlighted. 10
Figure 2-7. Responses of Slowly Adapting (SA) and Rapidly Adapting (RA) Receptors to an Indented Probe 13
Figure 2-8. Measures of Spatial Acuity on Different Body Sites 16
Figure 2-9. Response of Single Human Mechanoreceptors to Scanned Braille Characters. 17
Figure 2-10. The Response of an SA Fiber to a Flat Plate and to Selected Cylindrical Bars of Different Radii of Curvature Indented in the Skin 18
Figure 2-11. The Response of an RA Fiber to a Flat Plate and to Selected Cylindrical Bars of Different Radii of Curvature Indented into the Skin. 19
Figure 2-12. The Morphology of a Dorsal Root Ganglion Cell. 20
Figure 2-13. Types of Peripheral Nerve Fibers through which Somatic Information can Travel 21
Figure 3-1. Three Different Robotic Fingertips with Tactile Sensing..... .41
Figure 3-2. Schematic of the Deformable Finger Tactile Sensor 41
Figure 3-3. Camera view of membrane. 42
Figure 4-1. Leonardo..... . .46
Figure 4-2. Mechanical Design of Leonardo's Hand. 48
Figure 4-3. Images of Robotic Hands 49
Figure 4-4. The Arm "Pixel" Platform.. 50
Figure 5-1. Comparison of "Pixel" Hand to Leonardo's Hand 51
Figure 5-2. The Routing of the Kevlar Cable in the "Pixel" Hand 52
Figure 5-3. Dual Layer Design for the New "Pixel" Hand 53
Figure 5-4. Dimensions of the Interlink Model #400 FSR 54
Figure 5-5. The Four Hand Tools Used to Crimp the Solder Tabs to the Cut FSRs 55
Figure 5-6. The Modified and Unmodified FSR 55
Figure 5-7. Two Views of the Original Solid Model used for Sensor Placement 56
Figure 5-8. Protel Screen Shot of the Design of the Side Circuit Board. 58
Figure 5-9. Protel Screen Shot of the Palm Circuit Board Design 58
Figure 5-10. Protel Screen Shot of the Back of Hand Circuit Board Design. 59
Figure 5-11. Final Side Sensor Board with Sensors Mounted 60
Figure 5-12. Final Palm Sensor Board with Sensors Mounted 60
Figure 5-13. Final Palm Sensor Board with Sensors Mounted 60
Figure 5-14. The Graphical Depiction of the Spacer Problem and Solution.. 61
Figure 5-15. The Mounted Fingertip FSRs. 62
Figure 5-16. The Protel Screen Shot and Actual Mid-Plane Circuit Board 63
Figure 5-17. Wiring Diagram for FSR Signal from Sensor to A/D Board. 64
Figure 5-18. The Fingertips 65

Figure 5-19. Two Types of Fingertip Vertibrae..... 66
Figure 5-20. The Assembled Finger 67
Figure 5-21. The Wiring Path in the Fingertip 68
Figure 5-22. Top View of Hand..... 69
Figure 5-23. Front View of the Hand..... 70
Figure 5-24. Isometric View of Hand Part..... 71
Figure 5-25. Another View of the Hand Part..... 72
Figure 5-26. The Mid-Plane Plate..... 73
Figure 5-27. The Mid-Plane Plate in the Hand.. 73
Figure 5-28. The Top Plate. 74
Figure 5-29. Top Plate on Top of Hand with Mid-Plane Plate.. 75
Figure 5-30. Hand with Fingers. 76
Figure 5-31. Mid-Plane Circuit Board Mounted in Hand. 77
Figure 5-32. The Assembled Hand – Palm View 78
Figure 5-33. The Assembled Hand – Back of Hand View 78
Figure 5-34. The Assembled Hand – Side View 79
Figure 5-35. The Assembled Hand and Arm 80
Figure 5-36. The Assembled Hand - Grip 81
Figure 6-1. Diagram of Electronic Pathways……82
Figure 6-2. A Section of the Spinal Cord Showing Dorsal and Ventral Roots 83
Figure 6-3. Construction of the FSR Sensor 84
Figure 6-4. The Response of a Model #402 to Applied Loads. 84
Figure 6-5. How a Potentiometer Encodes Joint Angle from. 85
Figure 6-6. The 64-Channel A/D Board. 86
Figure 6-7. The Flow of Information through the 64-Channel A/D Board. 87
Figure 6-8. The Non-Inverting Op Amp Circuit Used to Increase the Resolution of the Potentiometer. 87
Figure 6-9. Voltage Divider Circuit Used with FSRs. 88
Figure 6-10. Positive Logic Engineering's ASC16 16-Axis Advanced Servo Controller. 90
Figure 7-1. Examples of Realistic Prostheses……...92
Figure 7-2. Three Different Facial Expressions of Hiroshi Kobayashi's Face Robots .. 93
Figure 7-3. Public Anemone Shown at SIGGRAPH 2002 in San Antonio Texas. 93
Figure 7-4. The New "Pixel" Hand with Attached Silicone Pieces..... 96
Figure 7-5. The Silicone Glove Mold.. 97
Figure 7-6. The Assembled Glove Mold. 98
Figure 7-7. The Cured Silicone Glove 99
Figure 7-8. Mold of Aluminum Fingertip. 100
Figure 7-9. The Mold and Cast of the Fingertip Core 100
Figure 7-10. The Fingertip Sculpt. 101
Figure 7-11. The Silicone Fingertip Mold. 101
Figure 7-12. Fingertip Molds with Silicone Injected into Them. 102
Figure 7-13. The Silicone Fingertip. 103
Figure 7-14. The Measurement of the Durometer of the Twelve Silicone Samples. 104
Figure 7-15. Plot of Durometer as a Function of Silicone Fluid Percentage. 106
Figure 7-16. Common Medical Grade Silicones Used in Prosthetic Work 108

Figure 8-1. The Theoretical Location of the "Virtual Somatosensory Cortex" in Leonardo. 110
Figure 8-2. Computational Framework of the "Pixel" Arm/Hand. 111
Figure 8-3. Hierarchical Organization from Sensor Level to Cortex. 112
Figure 8-4. The Response of a Single FSR to Finger Taps.. 113
Figure 8-5. An Initial Evaluation of the Possibility of the Formation of Cortical Neurons from Individual Sensors. 115

Abstract

The sense of touch is the most basic sensory system in humans, yet little work has been done to emulate the somatic senses in the field of robotics. This thesis describes an initial step toward the realization of a fully "sensitive skin" for robots in which somatic sensors of varying modalities such as touch, temperature, pain, and proprioception combine, as if letters in an alphabet, to create a more vivid depiction of the world and foster richer human robot social interactions. A new "sensitive" hand is created to begin to explore the importance of touch and the formation of the somatic alphabet in the context of Leonardo, a sociable robot created through collaboration between the Robotic Life Group at the MIT Media Lab and Stan Winston Studio. Forty-three force sensing resistors are mounted on the fingers, palm, side, and back of the hand. The hand and fingertips are covered in a very lifelike silicone "skin" which not only improved sensor performance but also increased the illusion of life. From initial tests the populations of these sensors show the potential for similar performance to both the mechanoreceptors in human skin and the cortical neurons in the somatosensory cortex. Thus the force sensing resistors can be used as part of the formation of the somatic alphabet.

1. Motivation: Why Touch?

> "The skin is the largest sensory organ of the body, and the tactile system is the earliest sensory system to become functional is all species thus far studied – human, animal, and bird. Perhaps next to the brain, the skin is the most important of all our organ systems." (Montagu 1986, pg 4)

> "In discussing prostheses, (John) Chapin noted that remarkable developments have been made in eliciting viable neuronal control of a robotic arm, but, 'what is still lacking is the sensation of touch to make the control process truly useful.'"(Ferrier, Lozano et al. 2002, pg 1632)

> "To operate in an unstructured environment, every point on the surface of a moving machine must be protected by this point's 'own' local sensing." (Lumelsky, Shur et al. 2001, pg 43)

Right now, as you sit in a chair, reading this thesis, your skin is encoding the world around you. Signals from these different sensors are traveling up your spinal cord and into your brain where they are being processed into the sensations of the chair that you feel, the temperature of the room you are sitting in, the smoothness of the surface of this paper or the sharpness of its edge when you turn the page, and even the vibration coming from a neighbor's subwoofer. Now close your eyes and scan your fingers across the area around you. How much of the world around you can you construct from the sense of touch alone? Most likely you will find that you can still recognize the objects on your desk. This simple illustration shows how our sense of touch is always present in our lives.

Now, imagine a world without touch. How difficult would it be to function in your everyday life? For some people this is an all too difficult reality. The book *Pride and a Daily Marathon* (Cole 1995) describes the life of Ian Waterman, who in 1971 lost all sensation of light touch and kinesthesis below the neck due to a viral infection (Craig and Rollman 1999). His accounts describe the reliance on vision to control all his movements; for example, when the lights go out he falls to the floor. Other diseases, such as multiple sclerosis also destroy the sense of touch. Jacqueline Du Pre lost her sense of touch in her hands while performing a concert, and had to finish her cello piece using vision to guide her fingers as she played (Field 2001). Losing the sense of touch can also be dangerous in the sense of a loss of pain responsiveness. People with a congenital absence of pain disorder usually die young due to infections from wounds or tissue deterioration suffered from failing to remove hands from a hot stove, chewing on their tongues while eating, or failing to shift body posture to relieve the strain on muscles and joints (Gray 1999, pg 257). Thus touch is necessary for not only our survival, but also in every moment of our daily lives.

It is remarkable that touch, the "mother of all senses," has historically received little interest, especially when compared to vision (Heller 1991). So it does not seem surprising that the field of robotics has also largely ignored the benefits of a sense of touch in favor of vision. As will later be discussed in Chapter 3, touch systems, if employed in robotics at all, often are seen in the realm of object manipulation to detect

slip or to keep a proper pressure during grip. These uses are only a small portion of the ways in which touch can be beneficial to a robot.

A sense of touch over the entire surface of a robot can help to protect it from damage. Vision alone is not sufficient due to the problems of occlusion (Lumelsky, Shur et al. 2001). Vision and touch can be combined to form stronger percepts. A simple example is in the case of distinguishing between two objects: vision could detect the color, shape, and location while touch could be used to detect the softness, roughness, temperature, vibration, or mass of the object. Full body touch can help to convey the "illusion of life." No matter how lifelike the movement of a robot may appear, if it is touched and does not respond, the illusion is instantly broken. In the context of human robot interaction, touch can be used to help guide the robots body into new positions. For example, a sense of touch can help distinguish between when a person places his or her hand around the robot's arm to guide it to an object and the impact felt by the arm bumping into a wall or an object.

Touch also can provide affective content which a robot could use for learning or interaction. As robots become more sociable in their behavior and organic in their appearance, the sense of touch can hold a much greater emotional meaning. Robots which are soft, expressive, and lovable begged to be touched by people, especially children. This touch can be used for reward, such as patting the robot on the head much like a pet, for play, such as tickling the robot to get a response, or to illicit a reaction, for example tapping the robot on the shoulder to get its attention. Additionally the robot can convey emotions based on its sense of touch. For example, if the robot is "sad," touch can be used to cheer it up through hugs, tickles, or pats on the head. These are only a few of the many examples in which a full body sense of touch can be beneficial to the field of robotics and the related field of prosthetics.

The goal of this thesis is to begin to explore the potential ways in which a full body sense of touch, based on the brain and cognitive neuroscience understanding of human and animal somatic senses, can be employed in an anthropomorphic robot. To begin this exploration, the hand was chosen as the first region of the body to be sensed due to the fact that the human hand has a very high sensor density, as will be discussed in Chapter 2, and the use of tactile sensors in a robotic hand is important for manipulation (Howe 1994). Pressure, i.e. a sense of "touch," was selected as the first modality to explore due to the fact that much of this system has been studied, as will also be discussed in Chapter 2, and many types of pressure sensors exist, as will be shown in Chapter 3. The hope is that similar algorithms developed for the hand, such as orientation and direction of motion across the surface of the skin, can be applied to other regions of the robot's body as well. In addition, other modalities such as temperature and pain will later be explored as well to help build the somatic alphabet for a robot, as will be discussed in Chapter 2.

Chapter 2 discusses the sense of touch in human and animals, based upon the work done in the fields of brain and cognitive neurosciences and neuroanatomy. The path from receptor through the spinal cord and finally into the brain for higher level processing as well as the different types of receptors and cortical neurons is described in detail. Throughout this chapter, the focus is on the idea of a "somatic alphabet" in which our perception of the world around us through our somatic senses is not due to a single

"somatic sensor" but rather an alphabet of these different types or sensors and methods of processing which all combine to form the words and sentences of our perception.

Chapter 3 begins with a discussion of the idea of the creation of a "Sensitive Skin" originally proposed in (Lumelsky, Shur et al. 2001). From this initial discussion, a survey of the different types of sensors available for detecting the different somatic modalities will be presented. The implementation of some of these sensors in robotic fingers and hands will be described as well. At the end of this chapter a discussion of how the "somatic alphabet" can be applied to robotics.

Chapter 4 begins the discussion of the current approach. The Leonardo robot, for which this work is ultimately geared, and the "pixel" platforms, on which the current implementation is based, are described. From Chapters 5 through 8, the current design is described in detail. The mechanical and electrical design of the new "pixel" hand is discussed in Chapter 5. The selection of sensors as well as the design of the 64-channel analog-to-digital converter for use with these sensors is presented in Chapter 6. Chapter 7 details the creation of synthetic silicone skins which will be placed over the sensors. Finally, the computational processing of sensory information will be outlined in Chapter 8. Chapter 9 provides a conclusion of the work completed in this thesis and states a series of objectives which need to be completed in the future on the way to a fully "sensitive skin."

2. Touch In Humans and Animals – Lessons from Neuroscience

2.1 Introduction

Our skin is the largest sensory organ of our body. It acts as a shield, protecting us from bacteria and infection. It is capable of detecting skin indentations as small as 1μm (Nolte 2002). Layers of skin are constantly being regrown and replaced, yet there are no changes in our perception. Throughout the body, skin has a rich variety of different properties including stiffness, texture, sensory innervation and color to name a few. But most importantly, the sense of touch, so intimately linked to our skin, is the first of the sensory systems to develop. Before a human embryo is less than 6 weeks old and has not yet formed eyes to see or ears to hear, the sense of touch is highly developed. Even as early as nine weeks in the womb, the fetus will close its fingers in a gripping motion if its palm is touched. (Montagu 1986). Clearly skin and the sense of touch are an engineering marvel of nature.

In order to design a biologically inspired sense of touch system for robots it is important to first understand how humans and animals are able to perceive the world around them through a sense of touch. In this chapter, the biological sensors, the mechanoreceptors, which transduce the physical world into information that the brain can understand, will be described. Next, the wiring from sensor to somatosensory cortex, the processing center of touch in the brain, will be illustrated. After this discussion, the focus will be placed on the somatosensory cortex and its organization and processing. Finally, experiments in haptics and other fields which shed light onto how different modalities are combined will be discussed.

Central to this discussion is the notion that there is not one single "somatic" sensor, but rather our perception of the world around us through touch is due to the combinations of many different types of sensors, each specially designed for a specific function. In many ways, one can imagine each sensor and way of processing the information from each sensor as letters in an alphabet. While each letter may convey some information, the combination of each letter into words and sentences can have much greater meaning. Thus percepts can be formed from the arrangements of these "letters."

2.2 Essential Terminology and Concepts

Before entering into a discussion of the brain, it is important to describe a few key concepts and terms which will be used throughout the chapter. This section is intended to help those who have never studied neuroscience or neuroanatomy.

There are a series of terms which provide a way to visualize the three-dimensional structure of the brain and the body through a series of two-dimensional slices as shown in Figure 2-1. The three planes are the **saggital** (dividing the body into left and right sides), the **coronal** (dividing the body into front and back), and the **horizontal** (dividing the body into top and bottom) planes. In addition to these slices there are also a series of terms used for orientation in the brain. To determine where with respect to the middle of

the plane one is looking the terms **medial** (towards the middle) and **lateral** (towards the side) are used. For example, a mid-saggital slice would cut the brain directly down the center as shown in Figure 2-1. Other orientation terms differentiate between the head end (either **anterior, cephalic, or rostral** can be used) and the tail end (either **caudal** or **posterior)** of the body. For example, the caudate equina is the collection of spinal nerve roots at the base of the spinal cord. Along the midline of the body, i.e. the trunk of the body, is referred to as **proximal** and the periphery, i.e. moving towards the fingers or toes, is referred to as **distal**. The terms **dorsal** (toward or at the back) and **ventral** (toward or at the belly or front) are used to describe both four- and two-legged animals. However, because of the original usage in animals, and to allow for consistency across species to humans, the terms dorsal and ventral are also used to describe the top of the brain, dorsal, and the bottom of the brain, ventral. This makes sense if one thinks of placing a human on all fours with head forward like an animal; thus now the back of the body and top of the brain are parallel to each other.

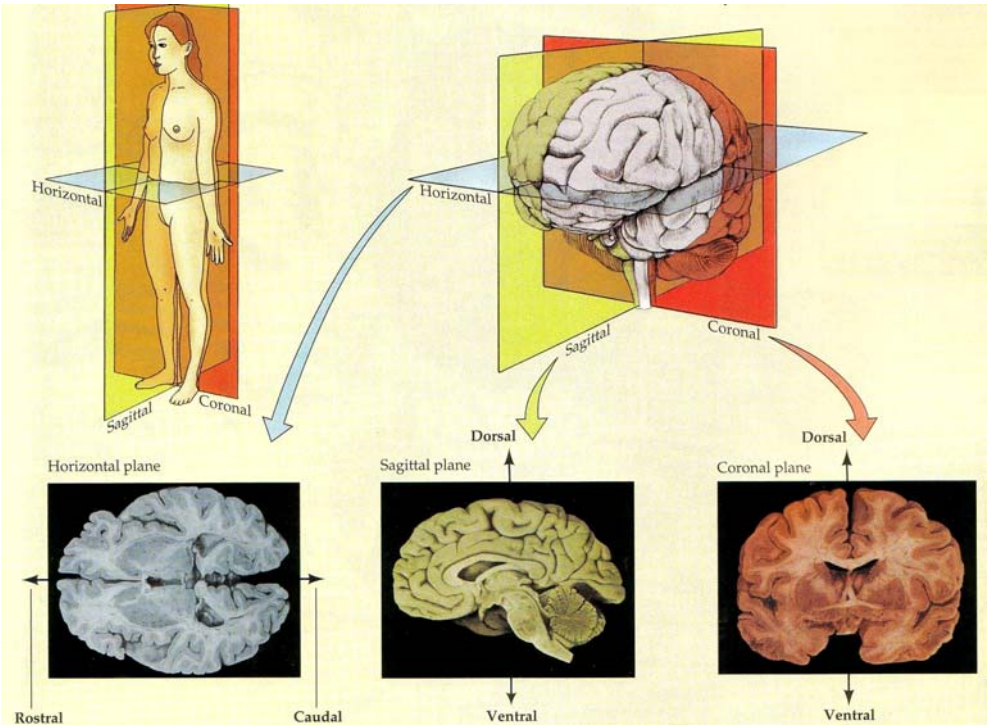

Figure 2-1. The Views of the Brain and Body. (Rosenzweig, Breedlove et al. 2002, pg 37)

There are two major divisions of the nervous system – the central and peripheral nervous system. The central nervous system (CNS) consists of the brain and the spinal cord. The peripheral nervous system (PNS) consists of the cranial nerves (a series of nerves which originate in the head and as such bypass the spinal cord and connect directly to the brain), the spinal nerves (the series of nerves which connect to the spinal cord at its different levels), and the autonomic nervous system. A visual depiction of the division between the systems appears in Figure 2-2.

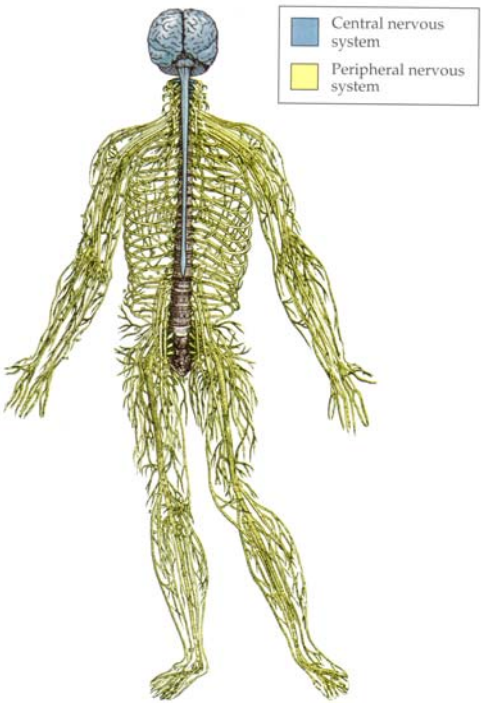

Figure 2-2. Divisions of the Central Nervous System. The Central Nervous System (CNS) is shown in blue, the Peripheral Nervous System (PNS) is shown in yellow. (Rosenzweig, Breedlove et al. 2002, pg 36)

While the majority of this discussion of the sense of touch in humans will deal primarily with one brain region, the somatosensory cortex also referred to as the postcentral gyrus, for purposes of orientation and relationship to other major structures of the brain it is worthwhile to spend some focus on the major regions of the brain. The cerebral hemispheres (the two halves of the brain) can be divided into 4 regions or lobes as indicated in Figure 2-3.

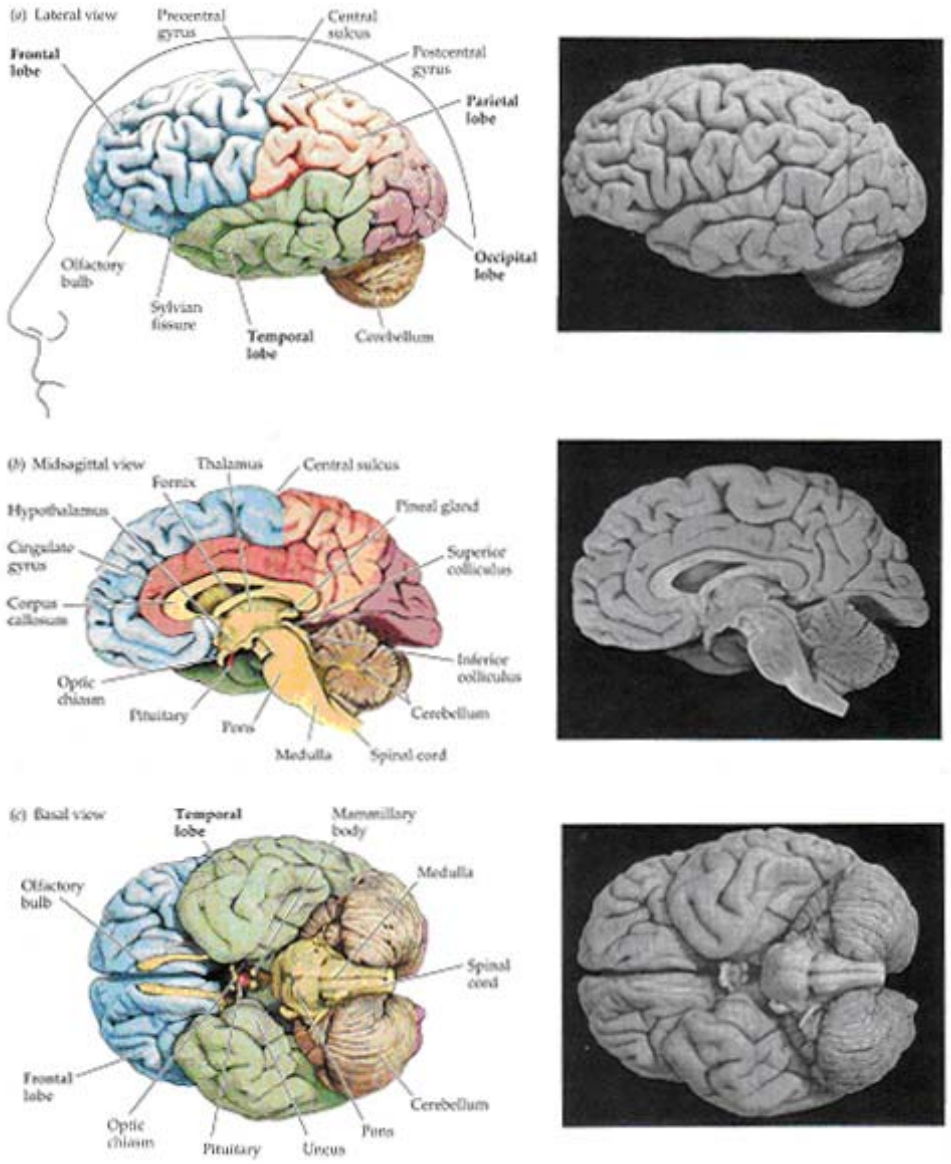

Figure 2-3. Three Views of the Human Brain. The postcentral gyrus is located in (a). (Rosenzweig, Breedlove et al. 2002, pg 42)

The four lobes consist of the temporal lobe, the occipital lobe, the parietal lobe, and the frontal lobe. The postcentral gyrus can be clearly seen in (a) of Figure 2-3 at the top of the brain caudal to the central sulcus. Of other special note, the primary motor cortex (the postcentral gyrus) sits directly across the central sulcus from the postcentral gyrus.

In addition to the division of the brain based on the four major lobes of the cerebral hemispheres, another method was done in 1909 by Korbinian Brodmann, who divided the brain into 46 regions based on structural differences as shown in Figure 2-4.

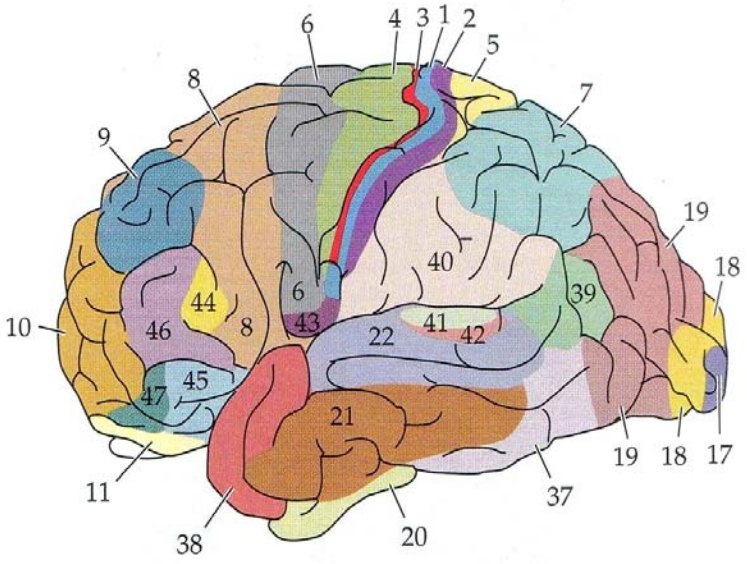

Figure 2-4. Brodmann's Areas. (Rosenzweig, Breedlove et al. 2002, pg 49)

While the divisions were based on structure, many researchers use his numbering schemes because they also correlate with function. Of particular mention are areas 3, 1, and 2 which form the somatosensory cortex, areas 5 and 7 which form the somatosensory association cortex, and area 4 which forms the motor cortex.

2.3 Skin – The Largest Sensory Organ

The skin is by far the largest sensory organ of the body. An average-sized adult human has a total skin surface area of 1.8 square meters, which is almost 1000 times the size of the area of the two retinas of the eyes, a density of 1250 kg/m^3 and weighs approximately 5 kg (Sherrick and Cholewiak 1986). It varies in thickness from $1/10^{th}$ of a millimeter to 3 or 4 millimeters in sections, with the thickest regions being the palms of the hands and the soles of the feet and thinnest on the eyelids (Montagu 1986). There are two major types of skin in the body of humans and other animals – glaborous, found on the palm of the hand and sole of the foot, and hairy, found on almost every other part of the body.

The skin itself consists of a series of layers as shown in Figure 2-5.

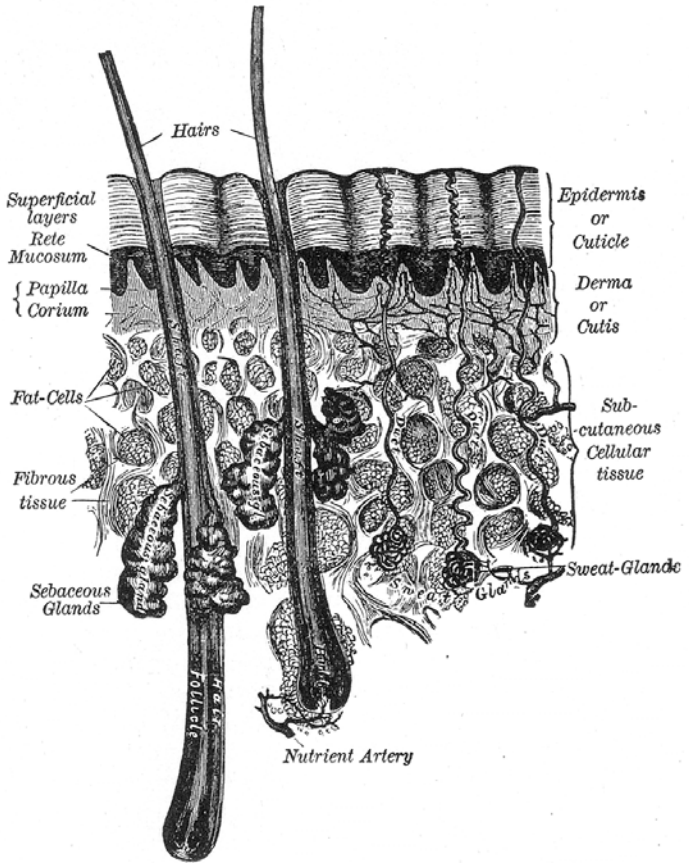

Figure 2-5. Sectional View of the Skin. (Gray 1977, pg 1136)

The epidermis or cuticle consists of two layers. The upper layer is the corneum, which consists of tough anuclear cells that are lost through friction and natural growth. Below this layer in the epidermis is the germinative layer which replaces the lost corneum cells. Below the epidermis is the dermis, also referred to as the cutis or corium. In the dermis are found the papillae, which are the irregularities which are responsible for the fingerprint patterns of the hands and feet. Beneath the dermis are found the sweat glands, hair follicles, and sebaceous glands.

The layered structure of the skin shown in Figure 2-5 highlights the physical makeup of the skin, but does not indicate the types of sensors found in the skin that respond to touch and other stimuli. Figure 2-6 shows another view of the skin, this time with an emphasis placed on the location of the mechanoreceptors.

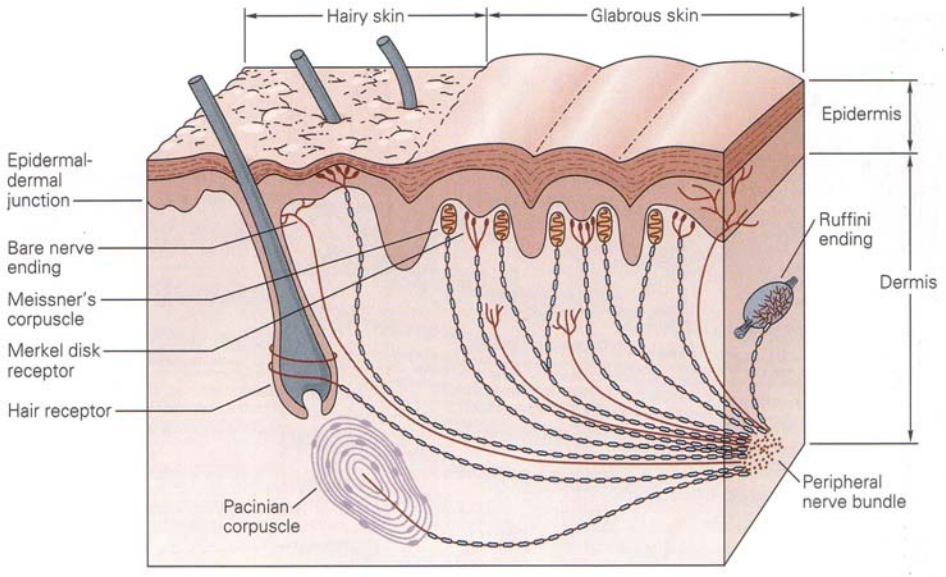

Figure 2-6. Sectional View of Hairy and Glaborous Skin with Mechanoreceptors Highlighted. (Kandel, Schwartz et al. 2000, pg 433)

As can be clearly seen from this figure, there are a wide variety of mechanoreceptors in the skin, each with a different location and preferred stimulus. Thus, by analyzing the outputs of each type of sensor an accurate depiction of the stimulus can be determined. In the next section, an in-depth discussion of the types of mechanoreceptors and what information they encode will be provided.

2.4 Receptor Types of Somatic Sensation

Our perception of the world around us through the somatic senses is due to the wide variety of receptors in our skin. Thus there is not one solitary "somatic sensor" but rather a collection of different sensors each encoding a specific type of stimulus. Each type of sensor can be classified as one of four types, each responding to a different modality. The first class of sensors are the discriminative touch sensors, which are used to recognize the properties of objects such as size, shape, and texture as well as the movement of these objects across the skin. It is this class of objects that the discussion of this section will largely focus on as it most closely correlates to the sensors used for the robotic hand that is the subject of this thesis. Another class of receptors is those that deal with proprioception, the sense of limb and body movement and static position. The third class of receptors are those that deal with pain or itch, the nocioceptive receptors. The final class are those that deal with temperature, a sensation of either warmth or cold. Table 2-1 shows a summary of the receptor types responsible for somatic sensations.

Table 2-1 Somatic Sensation Receptor Types adapted from (Kandel, Schwartz et al. 2000, pg 432)

Receptor Type	Fiber Name	Modality
Cutaneous and subcutaneous mechanoreceptors		Touch
Meissner's corpuscle	RA	Stroking, fluttering
Merkel disc receptor	SAI	Pressure, texture
Pacinian corpuscle	PC	Vibration
Ruffini ending	SAII	Skin Stretch
Hair-tylotrich, hair-guard	G1, G2	Stroking, fluttering
Hair-down	D	Light Stroking
Field	F	Skin Stretch
Thermal Receptors		Temperature
Cool receptors	III	Skin cooling (25ºC)
Warm receptors	IV	Skin warming (41ºC)
Heat nociceptors	III	Hot temperatures (>45ºC)
Cold nociceptors	IV	Cold temperatures (<5ºC)
Nociceptors		Pain
Mechanical	III	Sharp, pricking pain
Thermal-mechanical	III	Burning pain
Thermal-mechanical	IV	Freezing pain
Polymodal	IV	Slow, burning pain
Muscle and skeletal mechanoreceptors		Limb proprioception
Muscle spindle primary	Ia	Muscle length and speed
Muscle spindle secondary	II	Muscle stretch
Golgi tendon organ	Ib	Muscle contraction
Joint capsule mechanoreceptors	II	Joint angle
Stretch-sensitive free endings	III	Excess stretch or force

Another common grouping is based upon the two classes of somatic sensation. The first class, epicritic sensations, concerns the fine aspects of touch such as topognosis (detecting a gentle touch and determining where on the body it occurred), discerns the frequency and amplitude of vibration, resolving spatial details such as texture and two-point discrimination (the distance between two simultaneously touched points on the skin) and stereognosis (recognizing the shape of objects grasped in the hand). This class uses the encapsulated mechanoreceptors. The second class are the protopathic sensations, which are mediated by bare nerve ending receptors. This class of sensation involves pain and temperature. It is also important to note that pain also includes the sensations of itch and tickling. For a further discussion of pain see (Rollman 1991; Kandel, Schwartz et al. 2000 ch. 24). For a further discussion of temperature sensing see (Stevens 1991; Craig and Rollman 1999). For a further discussion of muscle and skeletal mechanoreceptors see (Clark and Horch 1986).

There are four main types of mechanoreceptors which have been found in glaborous skin. These receptors can be arranged in a grid along two different axes as shown in Table 2-2. One axis corresponds to adaption, which is how a receptor responds to a sustained stimulus. The second axis refers to the receptive field size, or how large of an area on the skin a receptor wiil be sensitive to.

Table 2-2. Mechanoreceptors in Glaborous Skin. Adapted from (Kandel, Schwartz et al. 2000)

	Slowly Adapting (SA)	Rapidly Adapting (RA)
Small Receptive Field (Superficial Layers)	Merkel disk receptors	Meissner's corpuscles
Large Receptive Field (Deep Layers)	Ruffini endings	Pacinian corpuscles

There are two types of adaption – rapidly and slowly adapting. Rapidly adapting, or RA, receptors respond primarily to the changes in a stimulus, thus in many ways one can think of such receptors as functioning as a derivative indicating the changes in or movement of a stimulus. They fire at a rate proportional to the speed of motion and their duration of activity corresponds to the duration of motion (Kandel, Schwartz et al. 2000 pg 438). Slowly adapting, or SA, receptors encode a static position and are capable of doing so continuously over a period of several minutes. However there is some gradual decay, which is obvious from everyday experience, as you don't feel you clothing on your body after a while. In fact, the amount that a slowly adapting receptor fires has been shown to indicate how rapidly the pressure is applied to the skin (initially) and then in steady-state shows a level proportional to skin indentation (Kandel, Schwartz et al. 2000 pg 438). The responses of both rapidly and slowly adapting receptors to a probe touching the skin are shown in Figure 2-7.

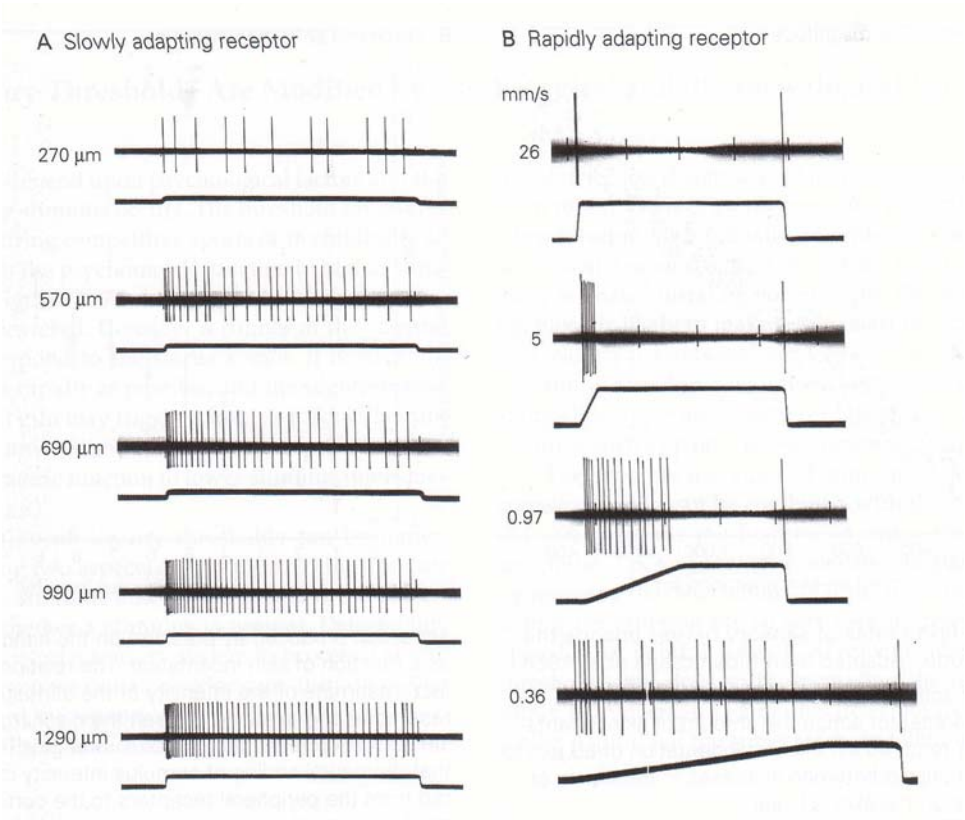

Figure 2-7. Responses of Slowly Adapting (SA) and Rapidly Adapting (RA) Receptors to an Indented Probe from (Kandel, Schwartz et al. 2000, pg. 424). In each image the response of the receptor is shown by a series of vertical bars (spikes) corresponding to each time that cell fires in response to the presented stimulus. Beneath the spike train is the time profile of the stimulus, with a step increase indicating that the probe was indented into the skin and a step decrease indicating that the probe was removed. In A, the response of a slowly adapting receptor is shown. As can be seen clearly from the figure, as indentation increases (indicated by a depth in µm) the firing rate (indicated by the number of vertical bars per interval) increases. It is also important to note that there is a greater density of spikes, i.e. a faster firing rate as the stimulus is applied. In B, the response of a rapidly adapting receptor is shown. As can be shown, the cell responds to changes in stimulus, as indicated by the ramp. The cell fires only while the skin is indented and finally when the stimulus is removed. It is silent otherwise.

The location and depth of a mechanoreceptor in the skin influence the receptive field size, which can be characterized as punctate for a small receptive field with a sharply defined boundary and diffuse for a larger field with less definition of boundary (Sekuler and Blake 2002). While the act of pressing into the skin with a probe, as shown in Figure 2-7, may seem like a simple stimulus, the complexity of the skin causes very different reactions in different locations in the skin. This is due to the fact that the deforming skin layers are "viscoelastic." Thus due to the viscous nature of the skin, when it is touched energy from the contact point will be transmitted through the skin.

However, the elastic nature of the skin means that some of this energy will be stored and then used to return the skin to its original shape (Cholewiak and Collins 1991). In addition the path from stimulus to receptor is often filled with obstacles such as blood vessels, bone, fat cells or other types of obstructions as shown in Figure 2-5. Each obstacle may actually distort the signal before it reaches the receptor (Cholewiak and Collins 1991). Thus the "image" that each sensor "sees" may be very different from the original "image" of the stimulus. The receptors closer to the skin surface, in the papillary ridges of the superficial layers of the skin, such as the Meissner corpuscle and Merkel disk receptor, shown in Figure 2-6, have a small receptive field which is more finely tuned. In contrast, those deep in the skin, such as the Pacinian corpuscle and the Ruffini endings, also shown in Figure 2-6, have a much wider receptive field, but have less spatial sensitivity. Often such receptors will have a region directly above them in which sensitivity is greatest.

The physical properties of each receptor also dictate how it responds to a stimulus. The Meissner's corpuscle, RA, is actually mechanically coupled to the papillary ridge edge as shown in Figure 2-6, which allows for a high degree of sensitivity. It has a layered structure, in which the sensory nerve terminal is wrapped around and in between layers of stacked epithelial cells, each oriented in the direction perpendicular to the long axis of the cell. A thin outer capsule surrounds the stack. When vertical pressure is applied to a dermal papilla, the nerve endings are compressed between the stack and thus, the pressure is "sensed." Pressure applied to nearby papilla are not as effective to the pressure applied directly over the cell, thus it has a small receptive field as mentioned previously (Nolte 2002).

The Merkel disk receptor, SAI, is non-encapsulated. These receptors are usually found in clusters, often at the center of a papillary ridge. The Merkel ending, a disk-shaped expansion of the terminal of a sensory fiber, inserts into the base of a Merkel cell to create this receptor. One fiber may branch to connect to many of these cells (Nolte 2002). Compressing strain from the skin is passed to the sensory nerve due to the fact that the cell encloses a semi-rigid structure (Kandel, Schwartz et al. 2000). This receptor is found in both hairy and glaborous skin.

The Ruffini ending, SAII, is found in the dermis, subcutaneous, and other connective tissue sites. It functions as a skin stretch receptor. Strands of collagenous connective tissue cross a thin, cigar-shaped capsule. The sensory fiber enters and branches, thus interspersing between the collagenous strands. Thus when the skin is stretched, tension is applied to one or both ends of the cell and squeezes the sensory fiber terminals between the strands. Because of the property of the strands (collagen is not very elastic) the deformation can be held for a long time thus creating the slowly adapting response (Nolte 2002). This receptor helps to detect the shape of grasped objects (Kandel, Schwartz et al. 2000).

The final glaborous skin mechanoreceptor is the Pacinian corpuscle, PC, also shown in Figure 2-6. These receptors are very widespread and found subcutaneously. The onion-like structure, due to the many concentric layers, of this encapsulated cell contribute to its rapidly adapting response. Between the thin layers of epithelial cells are fluid-filled spaces. In the center of the cell is the nerve ending. Because of the mechanical structure of this receptor and the elasticity of the layers, only fast acting forces are transmitted through the layers of the cell to reach the nerve ending. Any

sustained forces simply deform each successive layer slightly less than the previous one and as a result do not reach the nerve ending in the center of the receptor. Because of their speed in detecting changes they have been linked to vibration detection (Nolte 2002).

In addition to the four mechanoreceptors found in glaborous skin, there are a series of additional receptors found in hairy skin, but due the fact that the focus of this thesis is the hand, a glaborous skin region, the reader is encouraged to see (Kandel, Schwartz et al. 2000 Ch 22; Nolte 2002 Ch 9) for a further description of these sensors.

The number and type of mechanoreceptors in the skin vary throughout the body. As a result the ability to discriminate different properties of the stimulus varies as well. This organization can be determined through the use of psychophysical tests of spatial perception such as the two-point limen and the error of localization test (Cholewiak and Collins 1991). In the two-point limen test a subject is presented with either one or two points pressed into the skin. The experimenter then instructs the subject to determine whether he or she feels a single point or a set of two distinct points. The distance between the points when the subject first perceives them as two distinct locations is recorded. This measurement, shown in Figure 2-8 as a solid line, correlates well with receptor density. It is important to note though that, with practice, subjects show an improvement on this task (Cholewiak and Collins 1991) The error of localization test, indicated by dots in Figure 2-8, presents a subject with an initial stimulus, a touch presented at a specific point on the body. Then at some time later, a second stimulus is presented either at the same location or a different one. The subject is asked to indicate whether the second touch was in the same location or a different one. Again the spacing between points when a single location becomes two locations is the variable being measured (Cholewiak and Collins 1991). It is important to note that this test involves some form of spatial memory. The differences between the two tests as shown in the figure are indicative of the fact that other variables, such as the difference in neural activity invoked by each test, can have an effect on the results.

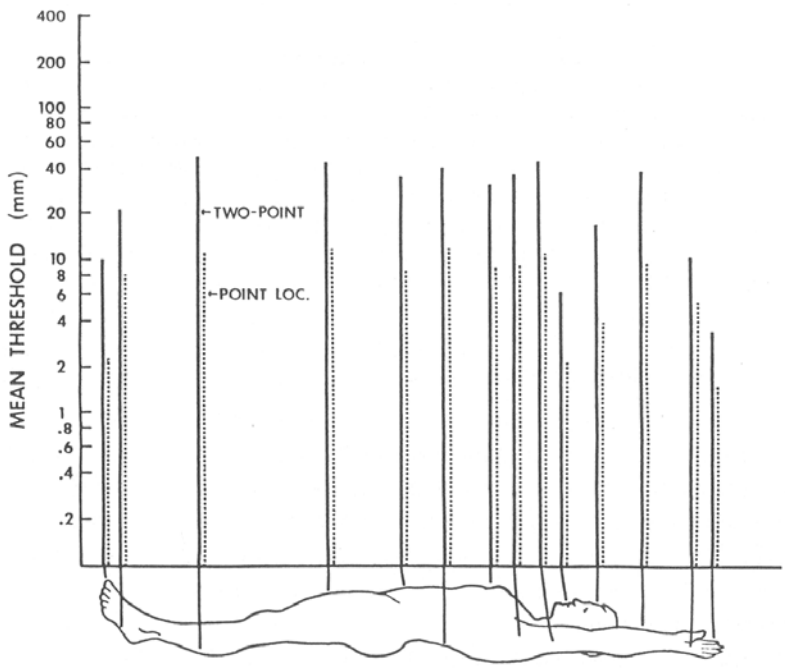

Figure 2-8. Measures of Spatial Acuity on Different Body Sites (Cholewiak and Collins 1991 pg 52). The solid lines indicate the spacing between points in the two-point limen at which the two points are perceived as being separate. The dotted lines correspond to the results of the error localization test

Even with the differences between the two tests, there are general trends which are shown in the data. First, there is a wide difference between the spatial perception of the fingertips, as small as 2 mm on the pad, and the back, as large as 70 mm (Sekuler and Blake 2002). Second, there is a general trend of finer spatial perception, increased receptor density, as one moves from the trunk of the body to the extremities. In many ways this organization makes sense, as a greater spatial perception is required in the fingertips and hand for manipulation of objects than in the arm or back. This spatial resolution also reflects the types of mechanoreceptors present. In the fingertips, there are an abundance of Meissner corpuscles and Merkel disks. These small receptive fields, or punctate, receptors allow for very fine spatial resolution in the fingertips because the diameters of these receptors are smaller than the ridges of the fingerprints in glabrous skin.

In addition to spatial perception, touch has a temporal aspect as well. Studies of the temporal properties of touch have compared touch to the senses of hearing and vision (Pohja 1996). It was found that the limit at which tactile stimuli can be perceived as two separate events if spaced in time was 5ms or more. Any lower temporal difference and the two stimuli will be perceived as one. This was slower than hearing, 0.1 ms, but faster than vision, 25 ms (Pohja 1996). If a sequence of events are presented, it was found that 20 ms was required by all three senses to determine the order in which the stimuli were presented (Pohja 1996).

A much more in-depth discussion of other psychophysical studies to determine the limits of tactile perception appears in (Cholewiak and Collins 1991) In the next section, the ways the mechanoreceptors can combine to encode different stimuli will be presented and the "alphabet" will begin to be discussed.

2.5 Properties of the Stimulus Encoded at the Periphery

As discussed in Section 2.4, the four main types of mechanoreceptors found in glaborous skin respond to stimuli differently. It is as a result of these differences that researchers have shown that certain properties of the stimulus can be encoded at the level of the receptors themselves. In many ways one can think of each mechanoreceptor as part of an alphabet for object detection.

One major area of research involves the encoding of texture and roughness. In the majority of these studies a stimulus is stroked across the finger pad of a monkey and responses from the nerve are recorded. Some examples of stimuli presented have been dot patterns (Johnson and Lamb 1981; Lamb 1983; Connor, Hsiao et al. 1990; Johnson, Phillips et al. 1991; Connor and Johnson 1992; Johnson and Hsiao 1992; Johnson and Hsiao 1994), raised letters (Vega-Bermudez, Johnson et al. 1991), and grooved surfaces (Lederman 1974). The responses to Braille of the four mechanoreceptors of glabrous skin appear in Figure 2-9.

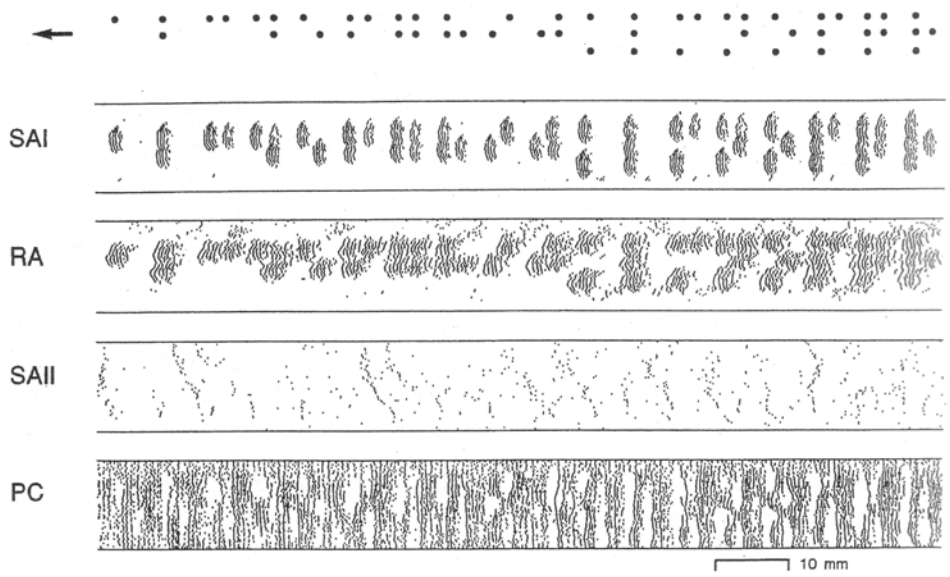

Figure 2-9. Response of Single Human Mechanoreceptors to Scanned Braille Characters from (Johnson and Hsiao 1992, pg 229). At top is the original Braille stimulus, a pattern of embossed dots 0.43 mm high. Below are the responses of the four mechanoreceptors, SAI – Merkel disc receptor, RA – Meissner's corpuscle, SAII Ruffini endings, and PC – Pacinian corpuscle. Each dot corresponds to one action potential.

In the above figure, responses from a single afferent fiber were recorded, and the plot was created by scanning the finger pad across a row of dots, then moving the row vertically up and repeating until the whole Braille pattern was scanned. From this figure, it

becomes clear that the candidates for the encoding of form/texture appear to be primarily the SAI afferents with the possibility of some encoding by RA afferents (Johnson and Hsiao 1992).

Another area of research involves the encoding of shape (LaMotte and Srinivasan 1993) and curvature (LaMotte and Srinivasan 1987; LaMotte and Srinivasan 1987; Srinivasan and LaMotte 1987) by the mechanoreceptors in the periphery. In one set of experiments, a series of cylinders of varying diameter from 1/32 to ½ of an inch were placed into the distal finger pad of an anesthetized monkey (LaMotte and Srinivasan 1993). The responses of SAI, i.e., Merkel disc, and RA, i.e., Meissner corpuscle, fibers were recorded from single mechanoreceptive peripheral nerve fibers. A summary of their findings appears in Figure 2-10, the SA fiber, and Figure 2-11, the RA fiber.

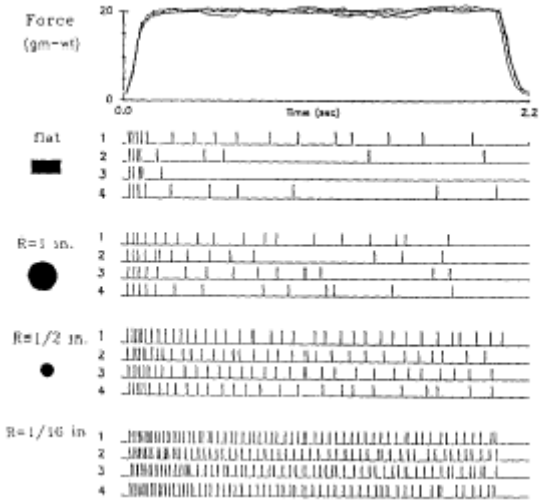

Figure 2-10. Responses of an SA Fiber to a Flat Plate and to Selected Cylindrical Bars of Different Radii of Curvature Indented in the Skin from (LaMotte and Srinivasan 1993, pg 45). The vertical tick marks show an action potential.

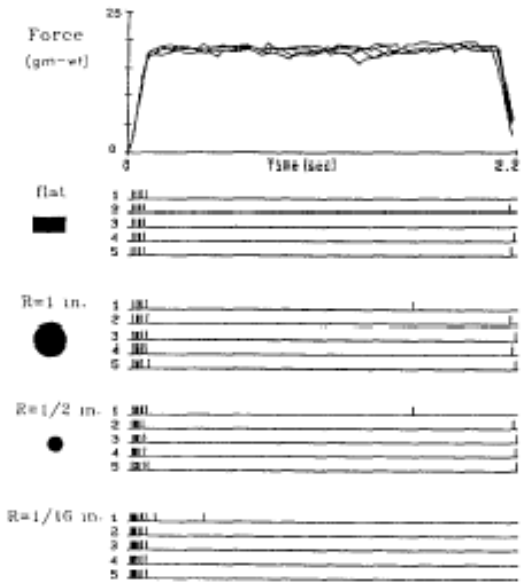

Figure 2-11. The Response of an RA Fiber to a Flat Plate and to Selected Cylindrical Bars of Different Radii of Curvature Indented into the Skin from (LaMotte and Srinivasan 1993, pg 46). The vertical bars indicate an action potential.

As can be seen from the above figures, the SA fibers first had an initial higher discharge rate during the indentation of the probe. Once the probe was indented, the firing rate of the SA fiber increased as the curvature, the reciprocal of the radius of the cylinder, increased. The response of the RA fiber was initial firing as the probe was indented into the skin, which reflected the motion of the probe, and no or very little firing in steady state. However, curvature did not seem to have a large effect on this firing rate.

These findings can be explained as a result of the number of Merkel disks receptors that fire when a probe of some radius of curvature is indented into the skin. A probe with a small radius has a small surface area and thus will activate only a small number of Merkel disk receptors in a population. But because this force is concentrated on a small number of these receptors, the firing rate will be high since each receptor receives a large portion of the force. However, as the diameter increases, the area, i.e., the number of Merkel disks activated, increases as well. But now the response of each individual Merkel disk is lower because the force is distributed across more receptors in the population (Kandel, Schwartz et al. 2000). Thus one can infer that the firing rate of an individual receptor can be related to the pressure, the total force divided by the surface area, it feels.

These are only two examples from studies that observe the responses of single fibers in the periphery. Other work in the realm of vibration has shown that the oscillations of a sinusoidal signal presented to skin will be reflected in a pulse code in which the mechanoreceptor fires an action potential at a rate of one spike per cycle of the sinusoidal wave (Kandel, Schwartz et al. 2000). It has been shown that the three mechanoreceptors which show this response are “tuned” to different frequencies – the Merkel disc receptors respond best between 5-15 Hz, the Meissner’s corpuscles prefer the

range of 20-50 Hz, and the Pacinian corpuscles are active for 60-400 Hz (Kandel, Schwartz et al. 2000). These results presented deal only with the realm of touch. Other similar types of peripheral encoding can be seen in temperature, pain, and proprioception as well. Thus it becomes clear that much information is encoded by the receptors at the periphery, and the "alphabet" of somatic sensation begins here. In the next section, the path a signal travels from receptor to the somatosensory cortex for higher level processing will be traced.

2.6 Pathway from Receptor to Cortex

As was previously mentioned in Sections 2.4 and 2.5, a single nerve fiber will receive input from a cluster of Merkel disc receptors or Meissner's corpuscles. In contrast, the mechanoreceptors with a larger receptive field such as the Pacinian corpuscle and Ruffini ending will be connected to a single nerve fiber. Regardless of what type the somatic receptor is, all somatosensory information, except for the face and part of the head, is carried by dorsal root ganglion neurons as shown in Figure 2-12. Information from the head and face is carried by the trigeminal sensory neurons, which are similar in both morphology and function to the dorsal root ganglion cells (Kandel, Schwartz et al. 2000).

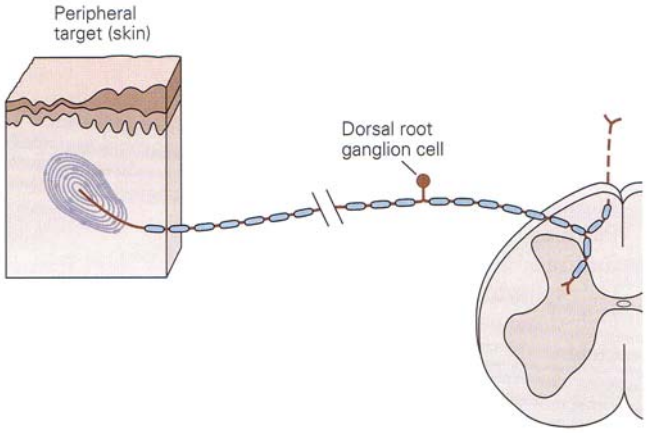

Figure 2-12. The Morphology of a Dorsal Root Ganglion Cell from (Kandel, Schwartz et al. 2000, pg 431).

As shown in the figure, the cell body lies in the ganglion on the dorsal root of a spinal nerve cell (Kandel, Schwartz et al. 2000, pg 431). Unlike most of the other cell types, this cell has two axons. One axon branches out to the receptor while the other connects to the spinal cord. Thus along this cell physical touch information transduced by the receptor travels from the peripheral nervous system (PNS) to the central nervous system (CNS) entering at the dorsal horn of one layer of spinal cord.

There are four types of peripheral nerve fibers through which somatic information can travel. Each type varies in diameter and in whether it is myelinated or unmyelinated as shown in Figure 2-13.

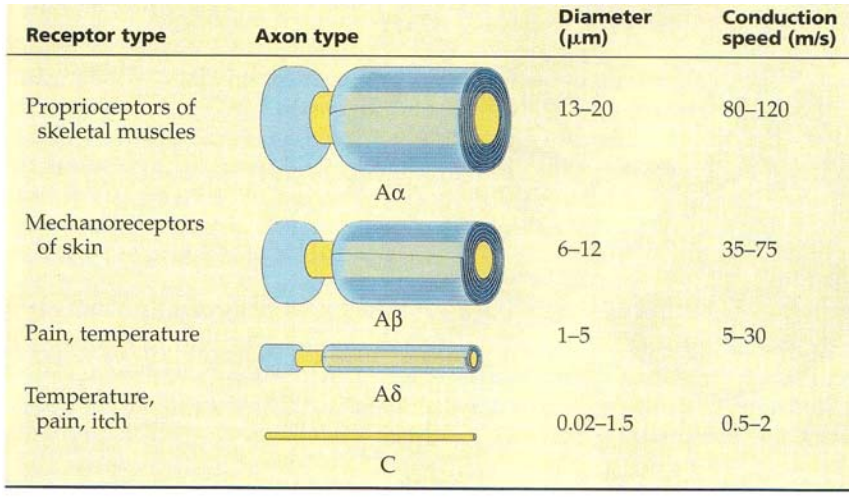

Figure 2-13. Types of Peripheral Nerve Fibers through which Somatic Information can Travel from (Rosenzweig, Breedlove et al. 2002, pg 237)

Both the diameter and the myelination of the fiber affect the conduction speed of the information. A larger diameter of the axon will increase the conduction rate. The myelin sheath, indicated in the figure by the larger diameter tubes surrounding the smaller diameter nerve fibers in the top three fibers, is made up of fat cells and acts as an insulator to the axon thus increasing the speed of conduction. The conduction of an action potential along a nerve fiber has been mathematically modeled; for a further discussion of this see chapter 6 in (Dayan and Abbott 2001). All the mechanoreceptive axons are A-alpha,-beta except for the hair down receptor which is A-delta (Kandel, Schwartz et al. 2000, pg 432).

There is an organizational level as to how the sensory information from each type of somatic receptor enters into the central nervous system through the spinal cord. The spinal cord is divided into a series of layers as shown in Figure 2-14. Each section has nerves that correspond to a specific section of the body.

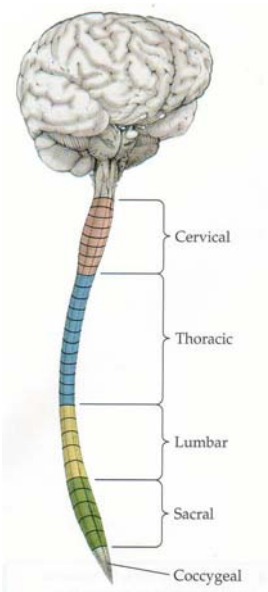

Figure 2-14. The Segments of the Spinal Cord from (Rosenzweig, Breedlove et al. 2002, pg 232)

There are 8 cervical (neck), 12 thoracic (trunk), 5 lumbar (lower back), 5 sacral (pelvic), and 1 coccygeal (bottom) sections (Rosenzweig, Breedlove et al. 2002, pg 39). The way in which regions of skin on the body are innervated by spinal nerves also shows a similar map to the division of the spinal cord. Each region of skin innervated by a specific spinal root is called a dermatome. The dermatome map of the body is shown in Figure 2-15.

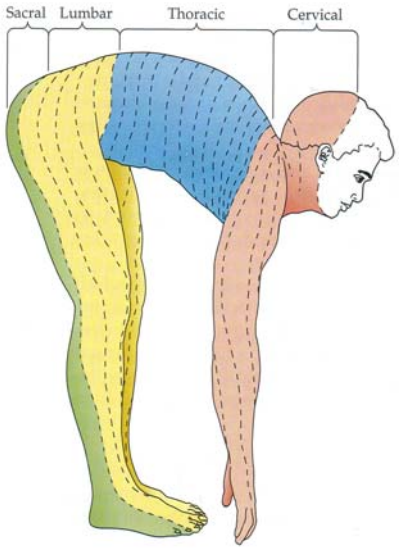

Figure 2-15. The Dermatome Map of the Human Body from (Rosenzweig, Breedlove et al. 2002, pg 232).

The reason for the 4-legged posture shown in the figure is due to the convention described previously in Section 2.1. From a comparison between Figure 2-14 and Figure 2-15, the regions of the skin and the sections of spinal map very closely to one another. The region of the face that is not marked corresponds to the skin that is innervated by the trigeminal sensory neurons that do not connect to the spinal cord but rather connect directly to the brain. Patients with spinal cord injuries will lose sensation in all regions below their injury in the dermatome map, due to the fact that sensory information from those regions of skin cannot make it up the spinal cord and into the brain.

In reality, there is not a clear division between the dermatomes as shown in Figure 2-15. The dermatomes actually overlap as shown in Figure 2-16.

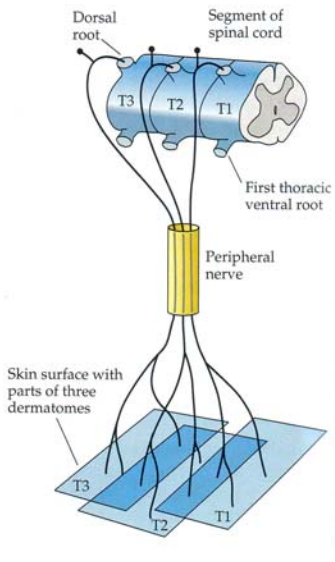

Figure 2-16. The Overlap of Dermatomes from (Rosenzweig, Breedlove et al. 2002, pg 232).

This overlap helps in higher level processing as will be discussed in the next section.

Once inside the spinal cord, there are two paths which somatic information can take on its path to the brain. The first pathway, the dorsal column-medial lemniscal system, is the primary path for touch and proprioception information. The second pathway, the anterolateral system, is the primary pathway for pain and temperature sensation. Both pathways are shown in Figure 2-17. Because the focus of this thesis is touch and not pain and temperature, the reader is encouraged to see Chapter 22 in (Kandel, Schwartz et al. 2000) and Chapter 10 in (Nolte 2002) for a further discussion of this system.

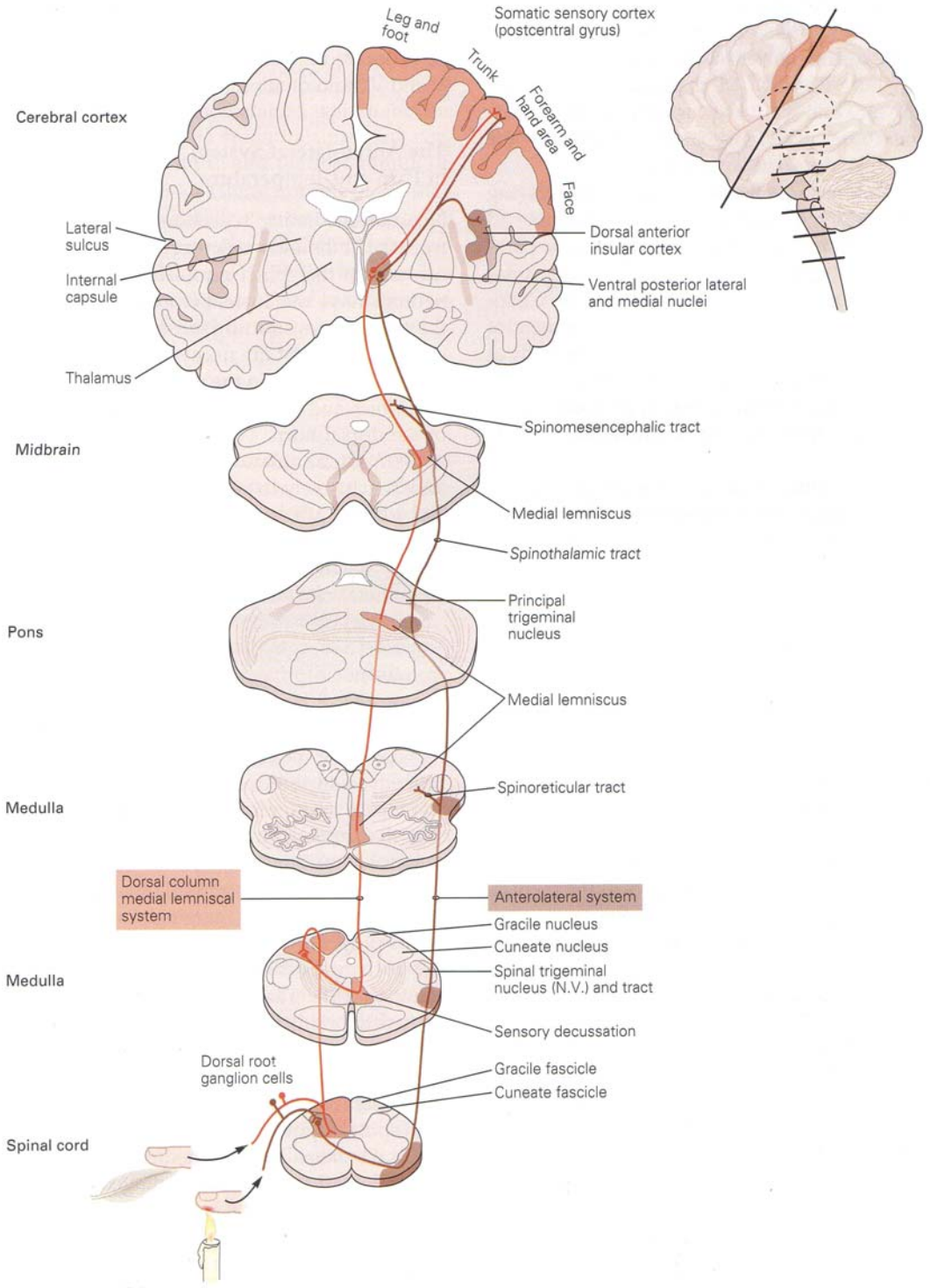

Figure 2-17. The Dorsal Column Medial Lemniscal and Anterolateral Systems from (Kandel, Schwartz et al. 2000, pg 447).

While it appears from the figure that there is a single route in which a specific type of sensory information will travel to the thalamus, this is really not the case. Most sensory information will travel by more than one route (Nolte 2002). But for the sake of simplicity in this discussion, the focus will be on the single primary pathway for touch.

Upon entry into the spinal cord, there is segregation into medial or lateral division based on type of fiber in this pathway. The large diameter, myelinated fibers are contained in the medial division while the smaller, finely myelinated or unmyelinated fibers are contained in the lateral division (Nolte 2002). In addition to this segregation by fiber type, there is an additional segregation based on entry level. Fibers which enter caudal to T6, i.e., to the left of the 6th Thoracic section in Figure 2-15, are grouped in a bundle called the fasciculus gracilis. Those fibers rostral to T6 are grouped in another bundle referred to as the fasciculus cuneatus (Nolte 2002). Each successive layer of fibers adds laterally to the columns already present. Thus a somatotopic map is developed at the level of the spinal cord in which fibers corresponding to the sacral dermatomes are more medial and cervical layer fibers are most lateral (Nolte 2002). Another division occurs based on the type of information. Proprioceptive axons are more ventral than the axons of tactile receptors that are more dorsal in the dorsal column nuclei. In the gracile and cuneate nuclei, the proprioceptive fibers terminate more rostrally than the tactile axons (Kandel, Schwartz et al. 2000).

At the brainstem (the medulla), these primary afferents synapse for the first time in the nucleus gracilis for those fibers grouped in the fasciculus gracilis and the nucleus cuneatus for those fibers bundled in the fasciculus cuneatus. It is here, as shown in Figure 2-17, that sensory decussation occurs – the fibers cross the midline and form the medial lemniscus. Below this point fibers from the right side of the body traveled up the right side of the spinal cord. Above this point, regions in the left side of the brain that deal with somatic sensation correspond to the sensory receptors in the right side of the body. This reversal is seen in other modalities as well. The medial lemniscus continues through the brain and finally synapses in the ventral posterolateral nucles (VPL) of the thalamus. From here, the third-order fibers continue on into the postcentral gyrus, otherwise known as to primary somatosensory cortex (Nolte 2002).

At this point before moving onto the somatosensory cortex, a discussion of spinal reflexes, specifically those that pertain to tactile information seems appropriate. Reflexes are involuntary, stereotyped responses to sensory inputs (Nolte 2002, pg 234). All reflexes are contained to the level of the spinal cord and as such do not require higher forms of processing. In most cases, the reflex loop consists of a sensory neuron which synapses onto an interneuron which in turn synapses onto a motor neuron which results in a response. A diagram of a reflex arc based on touch is shown in

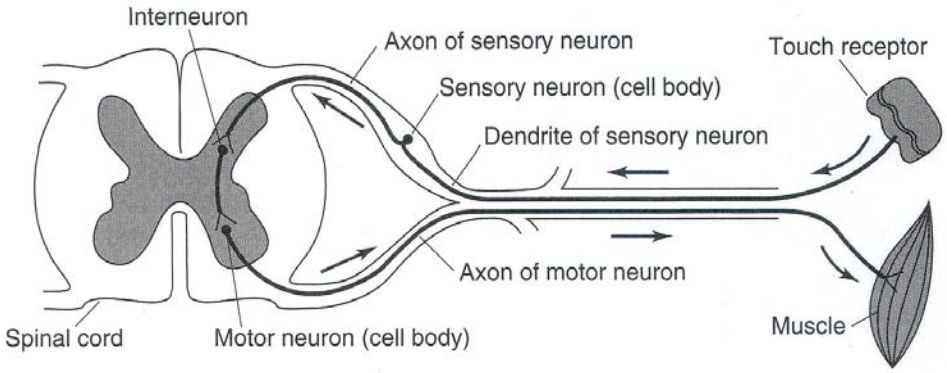

Figure 2-18. The Reflex Arc from (Sekuler and Blake 2002, pg 519).

Because the entire system occurs within the level of the spinal cord, usually with only a single interneuron, the response can be very fast. More complicated reflexes also involve coordination between limbs, such as with crossed effects, in which an opposite limb must counteract the motion. For example, when you step on a tack and pull one leg away suddenly the opposite leg counteracts and prevents you from falling down (Nolte 2002). A further discussion of reflexes can be found in Chapter 10 of (Nolte 2002) and Chapter 36 of (Kandel, Schwartz et al. 2000).

The entire path from mechanoreceptor to primary somatosensory cortex consists of only 3 synapses. The first occurs when the axon of the dorsal root ganglion cell synapses at either the gracile or cuneate nucleus in the medulla just prior to decussation. The second synapse occurs when the medial lemniscus synapses at the VPL. The final synapse occurs when a fiber from the VPL synapses at the postcentral gyrus. At each level of the CNS, the somatotopic map is preserved. In the next section, the processing and organization of the somatosensory cortex will be discussed.

2.7 The Somatosensory Cortex

The somatosensory cortex can be thought of as having three major divisions – the primary somatosensory cortex (SI), the secondary somatosensory cortex (SII), and the posterior parietal cortex (Kandel, Schwartz et al. 2000). Figure 2-19 illustrates these divisions in relation to the rest of the brain.

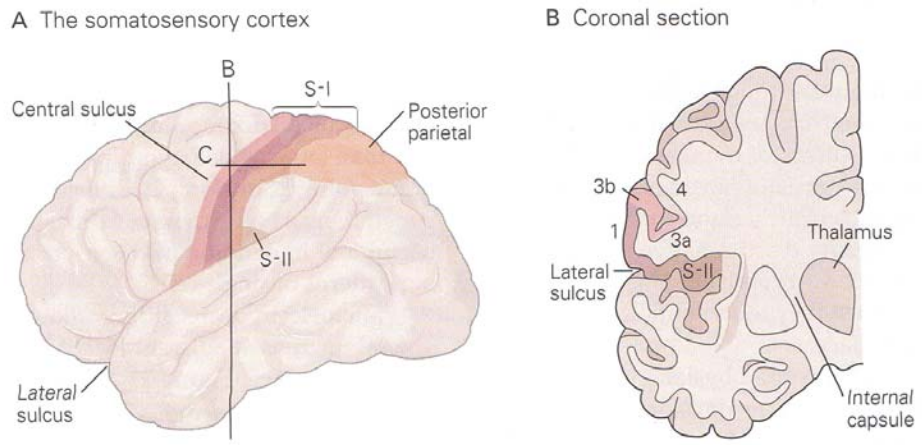

Figure 2-19. The 3 Divisions of the Somatosensory Cortex from (Kandel, Schwartz et al. 2000, pg 453).

The primary somatosensory cortex (SI) consists of Brodmann's areas 3a, 3b, 1, and 2. Touch information is sent to areas 3b and 1, while proprioception is sent to areas 3a and 2. The majority of fibers ascending from the VPL in the thalamus terminate in 3a and 3b, while a small percentage terminate in areas 1 and 2. Areas 1 and 2 also receive information from areas 3a and 3b. It is also possible for processing to occur both serially and in parallel due to the nature of the interconnections between the regions as shown in Figure 2-20 (Kandel, Schwartz et al. 2000).

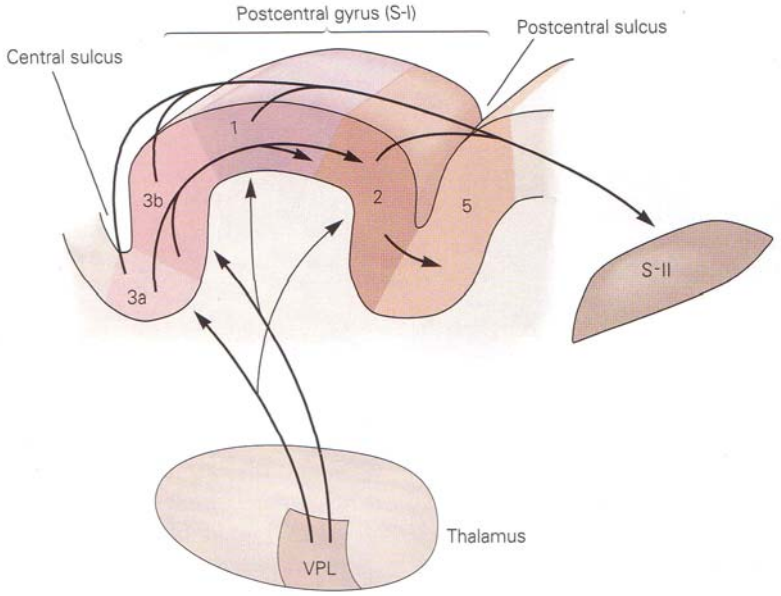

Figure 2-20. The Flow of Information through the Primary Somatosensory Cortex from (Kandel, Schwartz et al. 2000, pg 453).

The secondary somatosensory cortex (SII) receives input from the primary somatosensory cortex and projects to the insular cortex, which then passes information to

the temporal lobe for tactile memory (Kandel, Schwartz et al. 2000). The posterior parietal cortex consists of Brodmann's areas 5 and 7. In this region, both sides of the brain are connected through the corpus collosum, the bundle of axons which cross from one hemisphere to the other shown in Figure 2-3. Thus this is the first point in which somatic information from both sides of the body is integrated. The posterior parietal cortex receives input from SI as well as the pulvinar and projects to the motor areas of the frontal lobe, and thus is an important part in both sensory initiation and the guidance of movement (Kandel, Schwartz et al. 2000, pg 453). Proprioceptive and tactile information, as well information from the two hands are integrated in Area 5. Visual, tactile, and proprioceptive inputs are integrated to combine visual and stereognosis (the detection of the shape of objects grasped in the hand) information together in area 7 (Kandel, Schwartz et al. 2000).

The somatotopic map continues in each region of the primary somatosensory cortex (3a, 3b, 1, and 2). However, as can be shown in Figure 2-21, this map does not reflect the body surface but rather the number of receptors in each region.

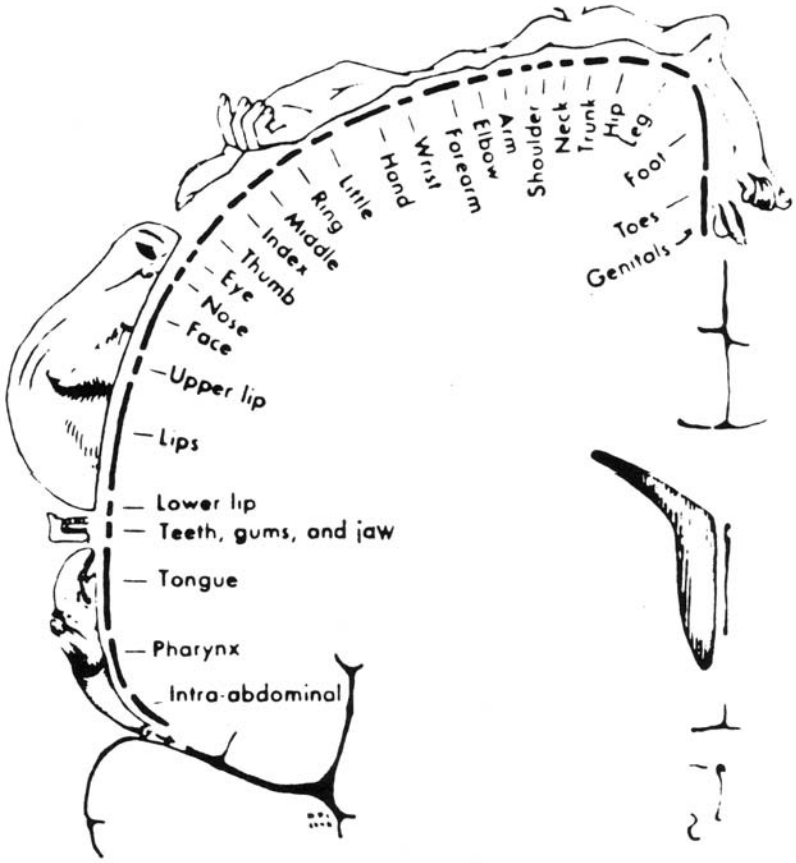

Figure 2-21. The Somatotopic Map of the Primary Somatosensory Cortex from (Penfield and Rasmussen 1950/1978).

Regions such as the fingers, lips, and tongue, which have a high density of receptors, are devoted to a larger area of cortex than regions such as the trunk which have a much lower density. This map has also be referred to as the Homunculus, or "little man," which is

shown in Figure 2-22. In this image, the size of each body region reflects the number of receptors present in that location.

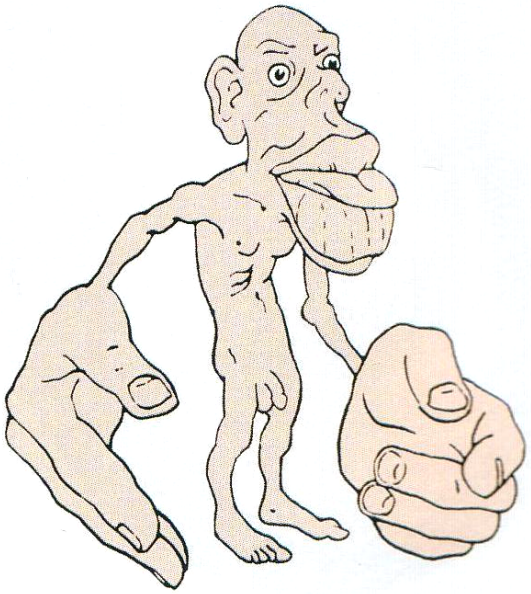

Figure 2-22. The Homunculus from (Rosenzweig, Breedlove et al. 2002, pg 233).

Another further division occurs in the cortical columns. The cortex consists of six layers, with each layer corresponding to a specific communication or processing pathway. A section from area 3b is shown in Figure 2-23.

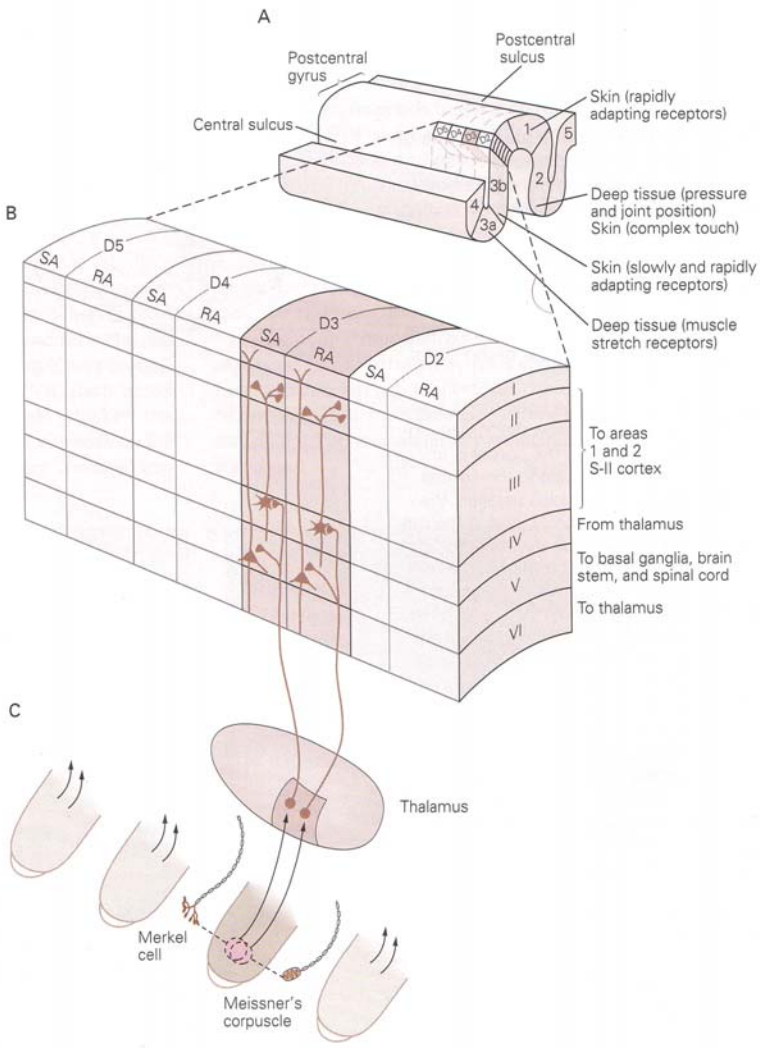

Figure 2-23. Cortical Columns in the Primary Somatosensory Cortex from (Kandel, Schwartz et al. 2000, pg 459). In A, the location of the section of Area 3b chosen for detail in B is shown. B shows the columnal organization. C shows the input, overlapping receptive fields from RA and SA receptors in the fingertip.

Input to the cortex from the thalamus enters through cortical layer IV. Layers V and VI are used for communication to other regions of the CNS. Layers II and III are used for communication to areas 1, 2, and SII. Each column is first organized based on the somatotopic map; columns of cortex correspond to specific regions of the body. A second organization occurs within each column, as in the case of Area 3b, into inputs from rapidly adapting and slowly adapting receptors.

Cortical neurons also have receptive fields, but unlike those of the dorsal root ganglion cells in the periphery a cortical neuron will receive input from a large number of mechanoreceptive fibers, due to the relay nuclei like the dorsal column nuclei and thalamic nuclei which send projections to further relay nuclei and inhibitory interneurons thus grouping the responses of many individual receptors (Kandel, Schwartz et al. 2000).

Even though the receptive field for a cortical neuron is much larger than that of an individual receptor, it is capable of fine discrimination. Thus higher level processing can be performed on this larger number of cells.

The center of the receptive field has a region of maximum sensitivity. As a stimulus moves closer to the center of a receptive field, the response increases. As a stimulus moves toward the periphery from the center of the stimulus, the response becomes weaker until finally the cortical neuron will not fire. In addition to this preferred location of stimulation for each cortical neuron, a region of inhibition surrounds the receptive field. This inhibitory surround allows for finer acuity as shown in Figure 2-24.

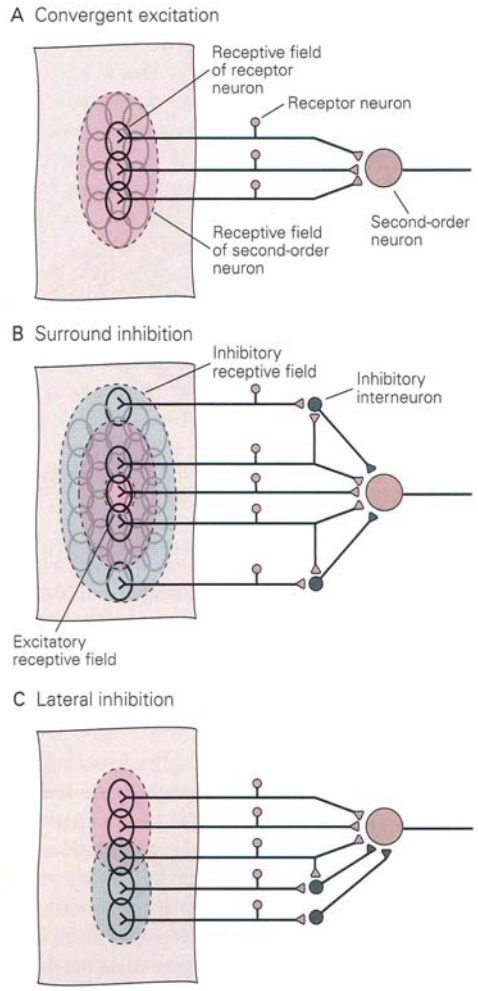

Figure 2-24. Combinations of Lower Order Neurons to Form Higher Order Neurons from (Kandel, Schwartz et al. 2000, pg 463).

Lateral inhibition helps with feature detection as it can be used to help discriminate edges.

As information from lower level cortical regions, such as 3a and 3b, is projected to higher-level cortical regions, such as 1, 2, 5, and 7, the size of the receptive field

increases, but the processing becomes more complex as shown in Figure 2-25. The receptive fields of lower cortical areas combine into the fields of the higher levels as shown below – a single region on one fingertip in Area 3b is combined with those of the other fingertips in Area 1 then further combined into the finger pads in Area 2, and finally the two hands are integrated in Area 5.

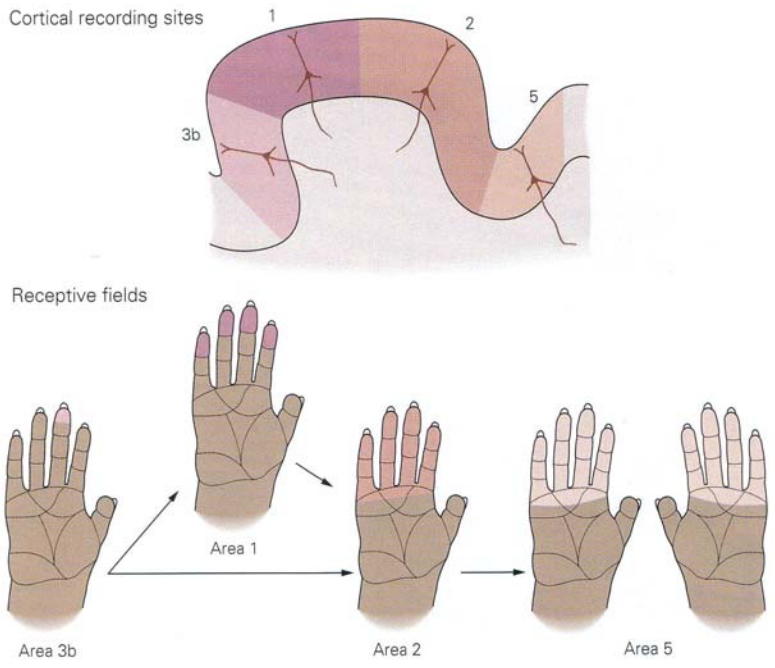

Figure 2-25. The Increase in Receptive Field Size in Higher Cortical Areas from (Kandel, Schwartz et al. 2000, pg 455).

The higher-level cortical regions have more complex neurons. For example, there are motion-sensitive (Areas 3b, 1, and 2), direction-sensitive (Areas 1 and 2), and orientation-sensitive neurons (Area 2) (Hyvarinen and Poranen 1978; Kandel, Schwartz et al. 2000). Motion-sensitive neurons do not respond to skin indentation but rather prefer motion in any direction, as shown in Figure 2-26.

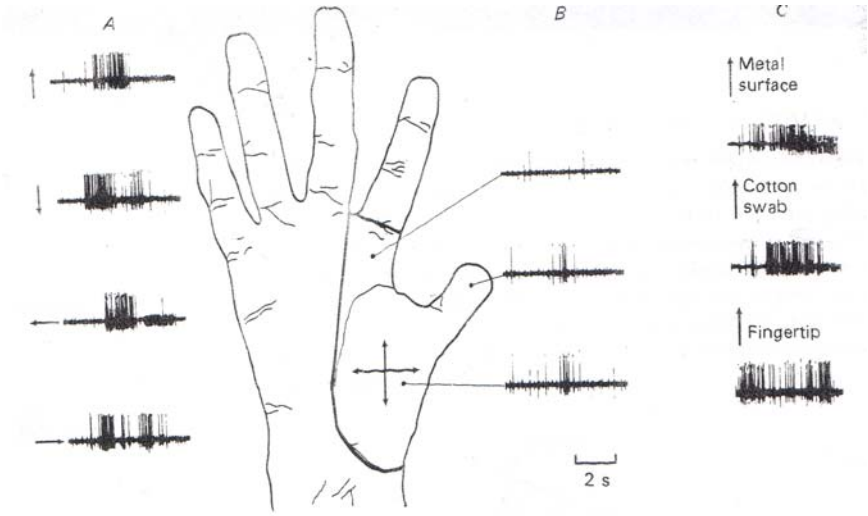

Figure 2-26. Response of a Motion-Sensitive Neuron in Area 1 from (Hyvarinen and Poranen 1978, pg 526). The dark lines on the hand indicate the size of the receptive field. A shows the response of the motion-sensitive neuron to motion in four orthogonal directions. B shows the lack of response to punctate stimuli at each of the 3 indicated locations. C shows that a similar response was produced for distally moving stimuli regardless of type.

Orientation-sensitive neurons are capable of determining the angle of an object placed on the skin as shown in Figure 2-27.

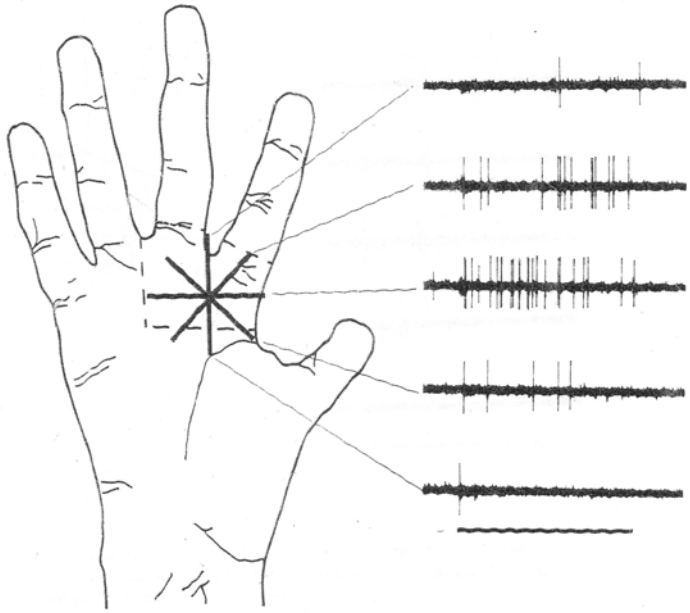

Figure 2-27. The Response of an Orientation-Sensitive Neuron in Area 2 from (Hyvarinen and Poranen 1978, pg 531). The Receptive field is indicated by the dotted lines. The solid lines indicate the orientation of a 0.7 mm wide metal bar indented into the skin. The best performance was seen at an orientation perpendicular to the axis of the hand.

Direction-sensitive neurons, shown in Figure 2-28, are capable of determining the direction of the object and fire when an object is moved across the skin in a preferred direction and are silent otherwise.

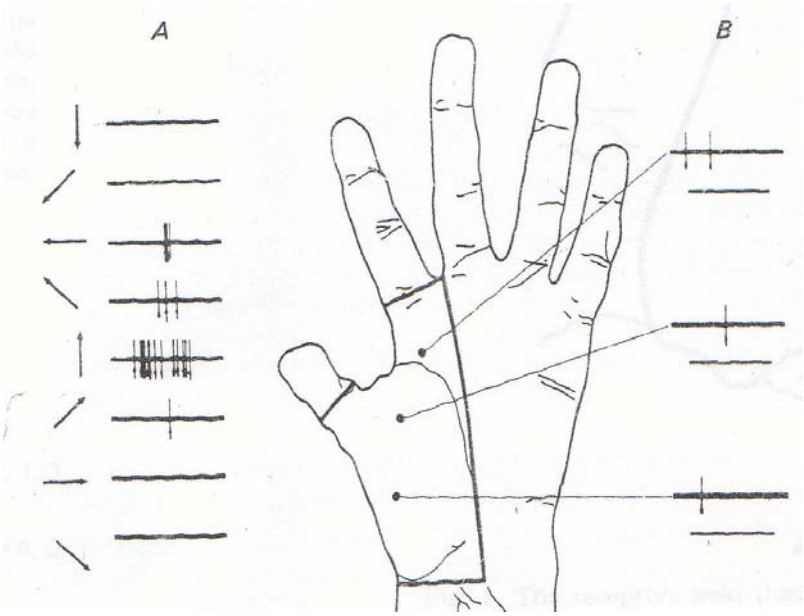

Figure 2-28. Response of a Direction Sensitive Neuron in Area 1 from (Hyvarinen and Poranen 1978, pg 526). The outlined region on the palm corresponds to the receptive field of this cell. A shows the response of the neuron to moving punctate stimuli in the indicated direction. B shows the response of punctate stimuli indented into the skin at each indicated point.

One possible way a direction-sensitive neuron can be assembled from a collection of lower level relay neurons is shown in Figure 2-29. By the spatial orientation and lateral inhibition of these relay neurons, direction can be inferred from the response. Thus a bar moving through a region of excitation then inhibition, or vice versa, will imply movement in one direction. However, movement that passes through both excitatory and inhibitory regions simultaneously will not show a direction sensitivity.

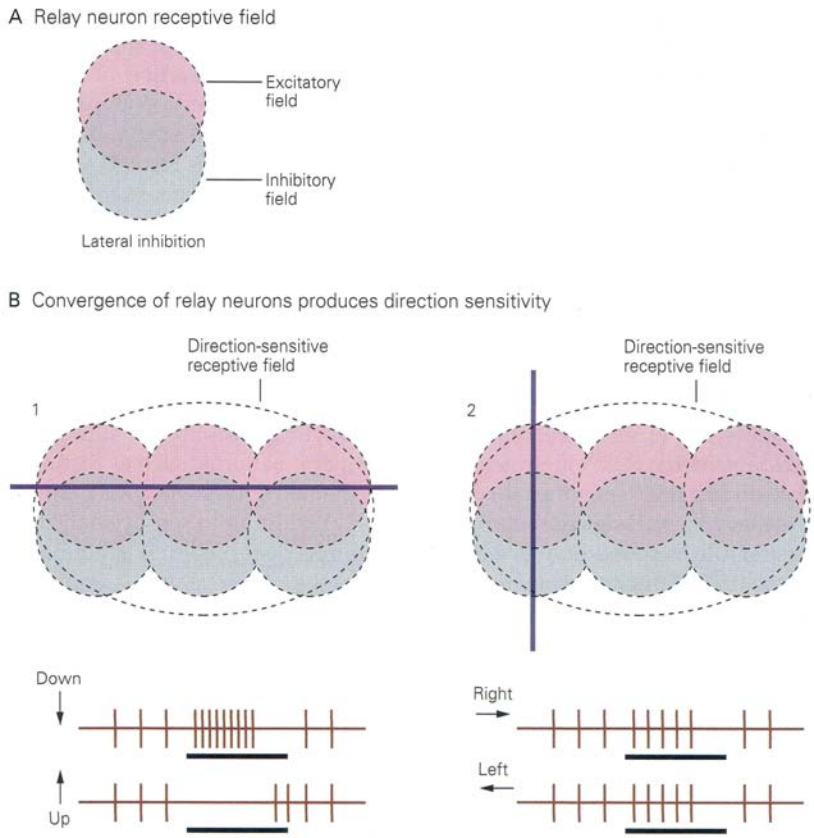

Figure 2-29. Creation of a Direction-Sensitive Neuron from the Spatial Arrangement of Presynaptic Inputs (Kandel, Schwartz et al. 2000, pg 467). A shows the lateral inhibition of a relay neuron's receptive field. B shows how groupings of these relay nuclei can be combined to produce a direction-sensitive cortical neuron. In B1, the bar moves perpendicular to the excitatory and inhibitory fields, thus a downward movement will first cross a region of excitation and then inhibition as shown in the down spike train. In the up spike train, the bar first moves through a region of inhibition then excitation. If a bar moves parallel as shown in B2, there will not be a difference in response as a function of direction since both excitation and inhibition regions are activated simultaneously.

In addition, other cells and regions of the somatosensory cortex as well as other modalities of the somatic senses show a similar construction of higher order cortical neurons based on the combination of lower order neurons. Thus it becomes that the "words" and "sentences" of perception through touch are formed by a combination of the alphabet of lower level processing.

2.8 Other Findings from Studies of Humans

In addition to the cell recordings in both the PNS and CNS, a series of other studies have been conducted which also shed light on the idea of an alphabet of somatic perception.

The detection of softness or hardness has been a realm of very little research. One study assessed the perception of softness in humans (Srinivasan and LaMotte 1995). In this study, rubber samples and compliant spring cells, which had a rigid surface, were presented to human subjects in a series of experiments, with three general conditions. In the first condition, the subjects had both their kinesthetic and tactile sensory information available, i.e., this was the case of "active touch." In the second condition, the cutaneous information was removed through the use of local anesthesia on the finger pad, but kinesthetic information remained intact in this altered form of "active touch". The final condition was passive touch, in which the stimulus was pushed into the finger pad under computer control; thus only cutaneous information was present.

While the subjects were able to discriminate the softness of the rubber samples using "active touch;" the discrimination of the compliance of the spring cells was poorer and required more applied force to do so. When cutaneous information was removed during the second condition, kinesthetic information alone was not enough to discriminate between the rubber samples or the spring cells. Under passive touch, in which the kinesthetic information was removed, subjects were capable of discriminating between the rubber samples, but not the spring cells. Thus for objects with rigid surfaces both kinesthetic and cutaneous information is required. Objects with deformable surfaces can be encoded by tactile information alone.

Another study used multi-dimensional scaling to group objects along three different axes (Hollins, Faldowski et al. 1993). In this study, a series of 17 objects, including wood, sandpaper, and velvet, were first placed beneath the index finger, then scanned across the fingertip from proximal to distal, and finally removed. Subjects were allowed to assign the object a rating along 5 different scales, each pertaining to the object's texture. From the analysis of this experiment, the 3 dimensions were roughness-smoothness, hardness-softness, and elasticity or "springiness."

2.9 Argument for the Somatic Alphabet

Thus as has been shown throughout this section, there clearly is not one single type of sensor and not one single type of processing but rather a very complex organization of simple sensors. By combining the responses of the various sensors in the somatosensory cortex, as if letters in an alphabet, objects can be sensed and stimuli can be perceived. Thus the approach one should take in designing a somatic system for a robot is not to try to create a single "somatic" sensor which is capable of reproducing all the properties of the various receptors in the skin, but rather to employ a distributed sensing, or an "alphabet" approach in which a series of sensors each with a different set of properties are combined to create the sense of touch. In such a system, a single sensor can be filtered or analyzed in different ways. For example, a single sensor that detects pressure can be differentiated to not only act like a slowly adapting receptor encoding the

static pressure, but also be differentiated to signal changes and thus act like a rapidly adapting receptor.

This thesis begins to explore this type of approach by initially constraining the problem to the mechanoreceptors of the hand. A series of commercial force-sensing resistors are combined in clusters on the palm, back of hand, side, and fingertips under a layer of synthetic silicone skin. The goal is to use this platform as a test bed to explore how one might build a synthetic somatic system from the single receptor level to higher-order processing of populations of these receptors. Throughout the process, the somatic system is used as inspiration.

3. Touch in Robotics

3.1 Introduction

When the word "robot" is mentioned, the terms "soft," "organic," and "fleshy" rarely come to mind. Our images of robots from the realm of either research, entertainment, or industry usually consist of a large machine made of metal or other hard materials designed to perform some type of task. Often times it is the function of the robot that dictates its form. For example, the large welding robots of the automotive industry look similar to each other, regardless of what company designed them. How can a skin be designed for a robot? Why is a sense of touch, in its full somatic meaning, useful for robots? These questions will be addressed in this chapter.

In this chapter, the goal of a "sensitive skin" which can fully cover the entire surface of a robot will be outlined and the potential design challenges will be discussed. Next a current survey of the types of sensing technologies available which have applications as somatic sensors, i.e., the letters of the alphabet, will be discussed. Current implementations of tactile sensing in both fingers and hands will then be discussed. Finally, the chapter will conclude with a discussion of how a fuller sense of touch can be employed in robotics in light of the "somatic alphabet" and the issues discussed in the previous chapter.

3.2 "Sensitive Skin": Moving Beyond the Robotic Gripper

The majority of the types of somatic sensors used in robotics today are proprioceptive, i.e., potentiometers encoding position and/or encoders which detect velocity. These sensors are often used as part of feedback loops in control systems. If a sense of touch is employed, it may be as simple as a bump sensor on a mobile robot used to prevent the robot from driving into a wall or to avoid other obstacles (Everett 1995). More complicated tactile sensors, detecting slip or pressure for example, may be implemented but often are placed only on the hands or grippers as will be discussed later in this section. Often what region of the robot is sensed corresponds to the task the robot must perform.

In June of 2001, in the first issue of the IEEE Sensors Journal, an article entitled "Sensitive Skin" appeared (Lumelsky, Shur et al. 2001). In this abstract of this article, the authors write:

> "Sensitive skin is a large-area, flexible array of sensors with data processing capabilities, which can be used to cover the entire surface of a machine or even a part of the human body. Depending on the skin electronics, it endows its carrier with an ability to sense its surroundings via the skin's proximity, touch, pressure, temperature, chemical/biological, or other sensors. Sensitive skin devices will make possible the use of unsupervised machines operating in unstructured, unpredictable surroundings—among people, among many obstacles, outdoors on a crowded street, undersea, or on faraway planets. Sensitive skin will make machines "cautious" and thus friendly to their

> environment. This will allow us to build machine helpers for the disabled and elderly, bring sensing to human prosthetics, and widen the scale of machines' use in service industry…" (Lumelsky, Shur et al. 2001, pg 41).

The goal of a "sensitive skin" for robotics implies covering the entire surface area of the robot with a collection of sensors. In a similar idea to alphabet of somatic perception, discussed in Chapter 2, a wide variety of sensors should be used. Such a design poses a series of design challenges which must be considered.

The first is the notion of flexibility. If the skin and the sensing system of the robot are to be the same entity, all of the wiring, sensing elements, and local processing, in addition to the material of the skin, itself must be able to bend around joints, conform to curvature, and stretch while still providing accurate sensor readings. One approach as to how this challenge may be met comes from the realm of conductive fabric sensors (DeRossi, Carpi et al. 2002; Sergio, Manaresi et al. 2002). Another idea is to eliminate the wiring entirely through the use of inductive coupling (Hakozaki, Hatori et al. 2001) or optics (Yamada, Goto et al. 2002). The approach taken in this thesis is to decouple the skin from the sensor. Thus a silicone skin, which will be described in Chapter 7, covers the sensors which are rigidly mounted to the hand.

Another design challenge is the integration of processing elements into the skin. Some initial work has been done in this realm, combining both sensing and processing elements, for both a shear-stress sensor (Xu, Tai et al. 2002) and a fingerprint detector (Shigematsu, Morimura et al. 1999). How the skin processes information from a large number of sensors poses a similar problem to those researching wireless sensor networks, mainly how can a network of distributed sensing and processing elements communicate information to each other. Some approaches to this problem are the research being conducted at Intel Research Berkeley with "Smart Dust" and similar systems (Warneke, Last et al. 2001; Madden, Franklin et al. 2002; Mainwaring, Polastre et al. 2002) and at the MIT Media Lab with the "Pushpin Computing" (Lifton, Seetharam et al. 2002).

As robots become a part of daily life, giving them a "sensitive skin" will be necessary. Such a sensory system will promote social interaction between the robot and the humans who share its workspace, as the sense of touch could be another way in which training of the robot is conducted.

3.3 Tactile Sensing in Robotics: A Survey of Approaches

As discussed in the previous section, a "sensitive skin" employs a wide variety of sensors. In this section, a survey of the various types of sensors which could be employed in light of the discussion of the somatic senses in Chapter 2 will be provided. The next section will give some examples of how some of these sensors have been integrated in robotic fingers and hands.

The four main types of modalities of somatic sensation, as shown in Table 2-1, are touch, temperature, pain, and limb proprioception. Pain, for simplicity, can be thought of as an extreme case of both a type of touch sensor and a type of temperature sensor in which activation of that sensor above a threshold may cause damage to the robot. The only exception one may think of to this grouping would be in the case of

damage to the robot through a "cut," i.e., the case in which the physical structure of the robot is pierced or damaged by an external force. While a tactile sensor may signal the impact that caused the piercing or damage, it would not convey the "throbbing pain" indicative of damage. Thus the four modalities can be reduced to three.

Each type of modality can be encoded by a wide variety of electronic sensors. Due to the focus of this thesis on the realm of touch, the reader is encouraged to see (Fraden 1996, Ch 16) for a discussion of temperature sensors and (Everett 1995, Ch. 2; Fraden 1996, Ch 5 and 7; Jones, Seiger et al. 1999, Ch 5) for a discussion of proprioceptive sensors.

In the realm of touch, there are a wide variety of tactile sensors which can be used in robotics. Some sensors have been designed to detect slip, the relative movement of an object in relation to the sensor (Son, Monteverde et al. 1994; Yamada, Maeno et al. 2002). These sensors act in similar ways to the rapidly adapting mechanoreceptors described in Chapter 2. Other sensors detect static pressure profiles, such as the Tekscan Smart Skin (Papakostas, Lima et al. 2002). This piezoresistive sensor system is capable of detecting an area between 100 and 10^7 square millimeters with a resolution between 0.1 and 10 mm.

Capacitive sensors have been employed both in a table top version, DiamondTouch from MERL (Leigh and Dietz) and in the hands and fingers of the UTAH/MIT Hand (Johnston, Zhang et al. 1996). Other sensor systems have used piezo-electric resonance (Krishna and Rajanna 2002). The design of the tactile sensor described in (Haris and Asim 2001) closely resembles the anatomy of the skin. Stretch receptors could potentially be built in a similar manner to those described by (DeRossi, Carpi et al. 2002). A further discussion of other types of tactile sensors can be found in (Rosheim 1994, ch 6; Fraden 1996, ch 8 and 9; Crowder 1998)

3.4 Sensitive Robotic Fingers and Hands

Employing a sense of touch in a robotic manipulator can help with grasping or detection. Sensor systems have been implemented in either a single finger of a robotic hand or the entirety. Figure 3-1 shows three different implementations of tactile sensing on a robotic fingertip.

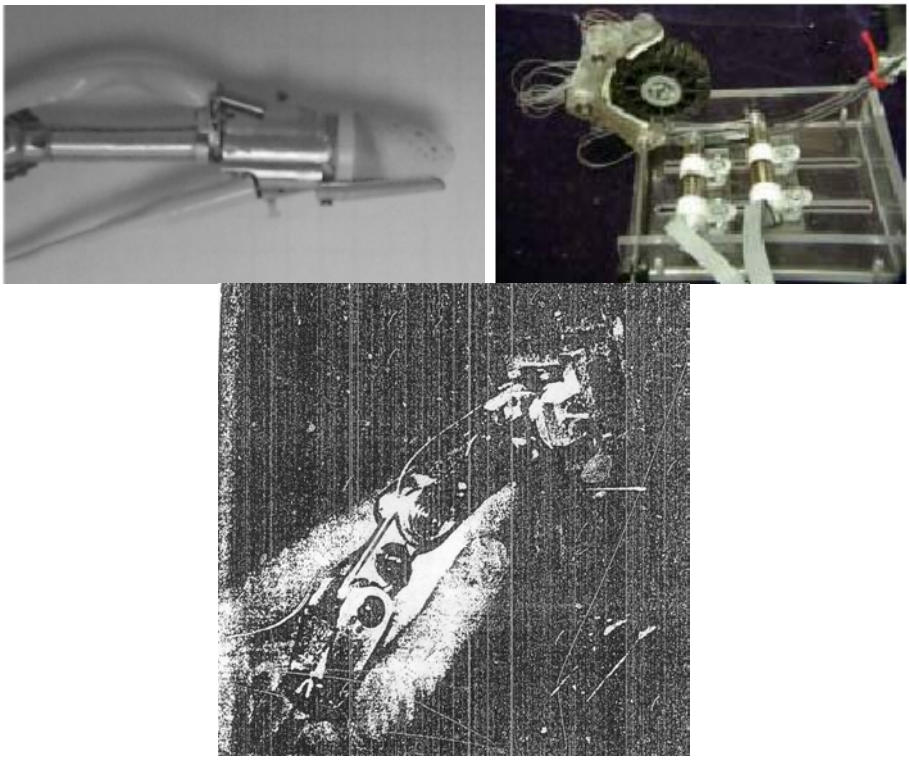

Figure 3-1. Three Different Robotic Fingertips with Tactile Sensing. In the upper left is the deformable membrane finger (Hristu, Ferrier et al. 2000), in the upper right is the multi-point finger (Banks unknown year), and at bottom is the finger from (Hillis 1981).

The deformable membrane finger (Hristu, Ferrier et al. 2000) shown at upper right in Figure 3-1 is unique in that it consists of a fluid-filled membrane on the fingertip. Thus this allows for the objects with which the finger comes into contact, to actually indent into the finger. A camera views a series of dot patterns through a transparent window as shown in Figure 3-2, and the indentation is reconstructed using a visual algorithm with the altered dot pattern shown in Figure 3-3 as an input.

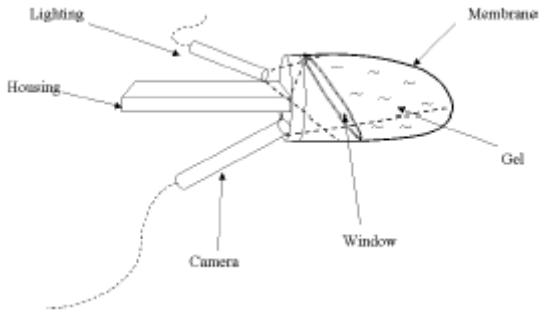

Figure 3-2. Schematic of the Deformable Finger Tactile Sensor from (Hristu, Ferrier et al. 2000)

Figure 3-3. Camera View of Membrane: (a) undeformed (b) in contact with object (Hristu, Ferrier et al. 2000).

This membrane reconstruction is capable of being completed at speeds of up to 15 Hz on a dual Pentium 400 MHz computer with a 5 x 5 grid array of dots (Hristu, Ferrier et al. 2000). While a very novel approach that features a good degree of sensing, the bulkiness of the camera and light cables as well as the cost per fingertip due to the necessity of a camera for each finger may limit the uses of this sensor.

The finger developed by (Banks unknown year) is also an optical system. Unlike the previous finger, in which deformation was inferred by a single sensor (camera), this finger used an array of optical transducers in which the forces applied to the foam substrate were detected by changes in light intensity. This design does allow for more flexibility in the design, as the sensing system can be applied to any rigid surface and thus expand from finger to hand to entire body. However, the feel of foam is not very lifelike and thus may break the illusion of life, previously discussed in Chapter 1, if someone were to touch the robot.

Conductive rubber was the basis of the sensing system employed by Hillis in his Master's Thesis (Hillis 1981) shown in Figure 3-1. The design of the sensor is shown in Figure 3-4.

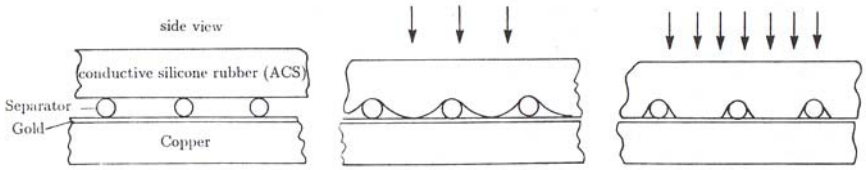

Figure 3-4. Design of Conductive Rubber Pressure Sensor used by (Hillis 1981). Image is from (Grupen, Henderson et al. 1989, pg 43).

Hundreds of pressure sensors were within the space of a fingertip in his design and each was capable of detecting between a range of 1 to 100 grams. A control loop was employed in the finger through which touch was used to help assess properties the properties of the object and then test these hypotheses. In the context of the limited computing resources in 1981 when his thesis was written, a LISP machine and 5 Z80 processors, the results are some of the first that show how active touch sensing can be employed

Other tactile systems have been employed on entire hands as shown in Figure 3-5.

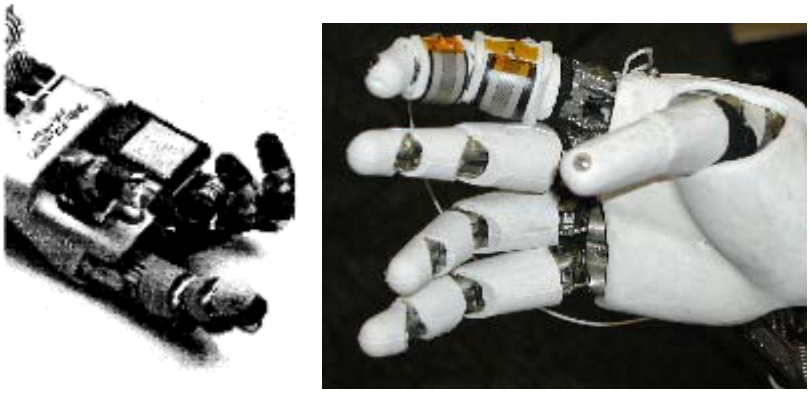

Figure 3-5. Robotic Hands with Tactile Sensing. At left is the UTAH/MIT Dexterous Hand with Tactile Sensing Suite attached (Johnston, Zhang et al. 1996). At right is the Robonaut hand with tactile sensor attached to one finger (NASA website 2001).

The tactile sensing suite employed on the UTAH/MIT Dexterous hand is a commercial system available through Sarcos Inc (Salt Lake City, Utah). As shown in Figure 3-6 the system consists of curved sections for each finger and a flat sensor for the palm.

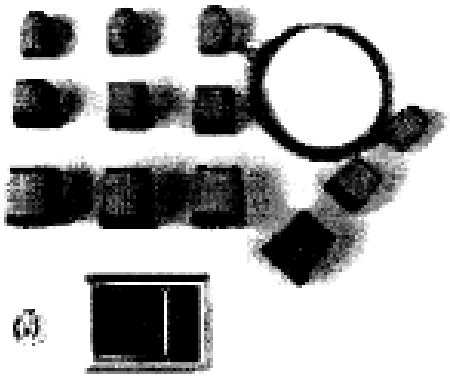

Figure 3-6. The Tactile Sensor Suite Shown as Individual Sensing Components (Johnston, Zhang et al. 1996).

Each sensor element or tactel is spaced on 2.77mm centers (Johnston, Zhang et al. 1996) with the palm sensor consisting of 64 sensors, the first finger link containing 76 sensors, the second containing 76, and finally the fingertip containing 56. A close up of a similar fingertip sensor also developed by Sarcos is shown in Figure 3-7.

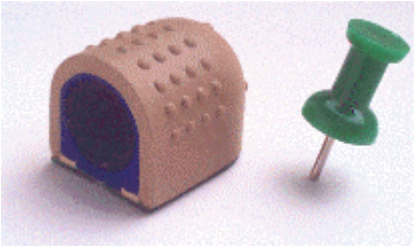

Figure 3-7. Tactile Sensors close-up.(University of Utah School of Computing Website)

The electronics which drive each sensor array are located in close proximity to each finger sensor, and an intermediate board on the back of the hand receives serial communication from each sensor and transmits this to an interface card on a VME bus (Johnston, Zhang et al. 1996). A further discussion of the results of a series of tests employed on these sensors appears in (Johnston, Zhang et al. 1996).

Robonaut is an attempt to model a "human-like robot with human-like capabilities" and, as such, a human-like model of autonomous grasping capabilities are being employed (NASA website 2001). In their approach, they are experimenting with commercial sensors as well as the development of their own sensors to allow for Robonaut to rely heavily on the feedback from tactile sensors to help with the grasp of the robot's hand. The current approach uses Force Sensing Resistors, FSRs, which are also employed in this thesis.

Other robotic hands that grip feature force/torque feedback at the joints of the fingers such as the DLR hand, which is used for teleoperation, and the Motion Control Hand, which is an actuated prosthetic hand (Menzel and D'Aluisio 2000). However, these types of sensors much more closely fit into the realm of limb proprioception and as such are beyond the scope of the initial work of this thesis which is focused on the sense of touch.

3.5 How the "Alphabet" Framework Could Be Applied to Robotics

As was shown in this chapter, there currently exist a wide variety of available sensors, many of which could be implemented as part of a somatic alphabet framework. The greater the sensing capability, both in resolution and in number of modalities, the larger number of percepts can be formed. For example the roughness of an object could be encoded through tactile or vibratory sensors. This and other information could be useful to help a robot perform a task by "feeling" the handle of a tool as it picks it up.

Touch can also be employed as part of a control loop. If both tactile feedback and force feedback are combined, a better controller results (Johnston, Zhang et al. 1996). Tactile information can be used to help to trace the contours of an object and further understand its shape.

Touch and vision could also be combined to allow the robot to gain a greater understanding of its world. This combination could also help to invoke a "curiousness" in the robot, for example if the robot senses it has been touched, it could direct its vision

system to that location on the body. The two senses could also work together to perform coordinated gestures such as the popular child's game of patty cake.

Thus there currently exists much need in the field of robotics for a sense of touch.

4. Overview of the Design

4.1 Leonardo, a Sociable Robot

The goal of the Robotic Life Group at the MIT Media Lab is to build capable and appealing robot creatures inspired from the science of animal and human behavior which are engaging to humans and as such encourage social interaction between humans and robots. Leonardo, see Figure 4-1, was created through a collaboration with Stan Winston Studio, the four-time academy award winning special effects studio responsible for such characters as "Teddy" in A.I. and the animatronic dinosaurs of Jurassic Park.

Figure 4-1. Leonardo. Photo copyright Sam Ogden. Leonardo character design copyright Stan Winston Studio

As can be seen from Figure 4-1, Leonardo was designed to look like a creature. Unlike traditional humanoid robots, which usually are made of metal, have a hard exterior, and low facial movement, Leonardo was designed to have an organic look and feel. In addition to its furry exterior and silicone face, over 60 degrees of freedom allow for a very lifelike range of movement with an emphasis on expression and communication. Currently, Leonardo is the most expressive robot in the world today (Robotic Life Group 2003).

In addition to serving as a research platform for lifelike, organic movement, Leonardo also is a test bed for work in sociable robots. A sociable robot is defined in Professor Cynthia Breazeal's *Designing Sociable Robots* (Breazeal 2002, pg 1) as:

> "… a sociable robot is able to communicate and interact with us, understand and even relate to us, in a personal way. It should be able to understand us and itself in social terms. We, in turn, should be able to understand it in the same social terms – to be able to relate to it and to empathize with it. Such a robot must be able to adapt and learn throughout its lifetime, incorporating shared experiences with other individuals into its understanding of self, of others, and of the relationships they share. In short, a sociable robot is socially intelligent in a human-like way, and interacting with it is like interacting with another person."

Leonardo, to truly be a sociable robot, must be able to interact with people as if it were another living creature itself. Thus it must be capable of displaying some intentions and the ability to learn. It must have a set of behaviors. It must be able to express emotion. It must be able to react to the world around it in a convincing way. One of the ways in which Leonardo will be able to react and interact to the world around is through a sense of touch, not only on the hands, but truly over its entire body. This is the ultimate goal for the initial work described in this thesis.

4.2 Design Constraints and Challenges

It was very important to try to work within the design of Stan Winston Studio in constructing the tactile sensing system for Leonardo. The mechanical design of Leonardo's hand is shown in Figure 4-2.

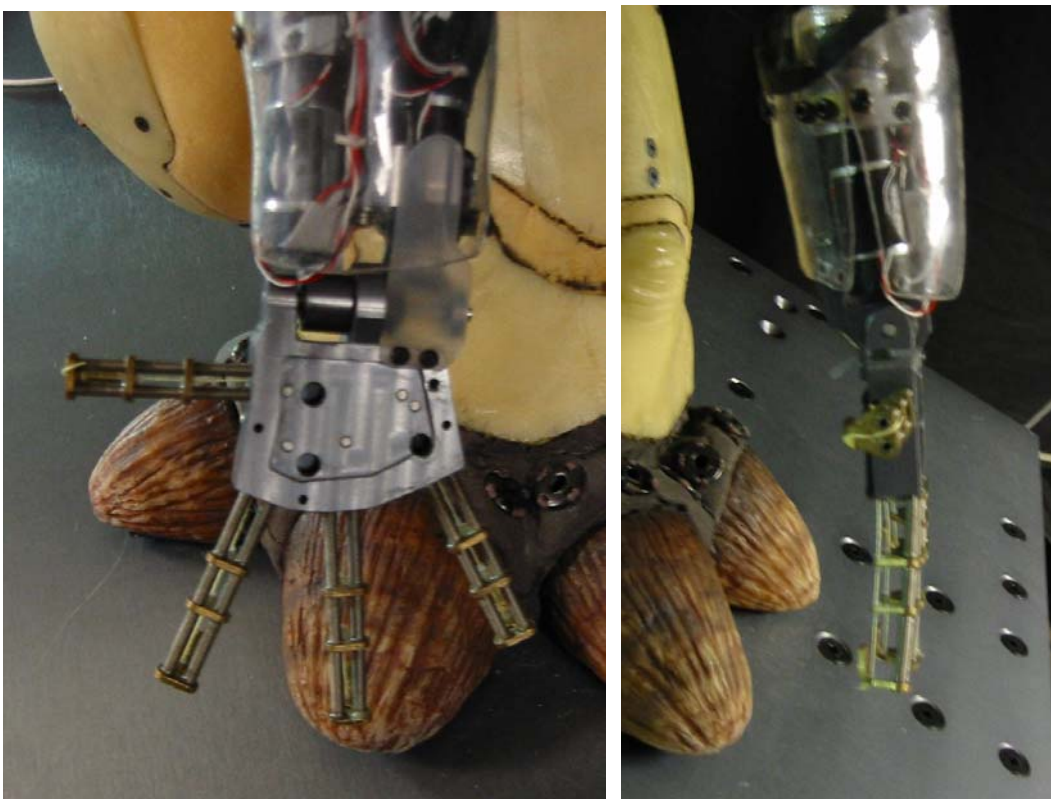

Figure 4-2. Mechanical Design of Leonardo's Hand copyright Stan Winston Studio. At left is shown the back of the hand. At right is shown the side view.

Leonardo's hand design is very different from those of other robotic hands of which a sample are shown in Figure 4-3.

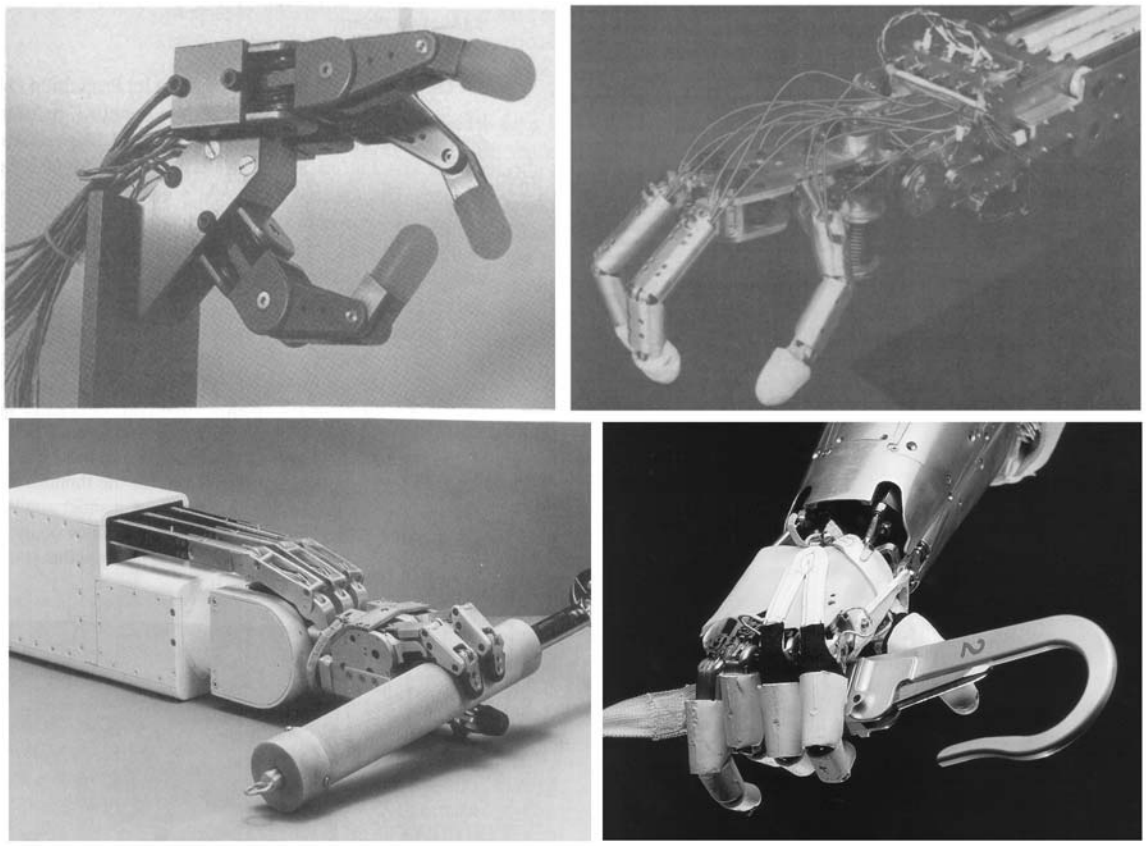

Figure 4-3. Images of Robotic Hands. Clockwise from top left: Stanford/JPL Hand (Salisbury hand) (Rosheim 1994), Hitachi Hand (Rosheim 1994), Jameson Hand (Rosheim 1994), Robonaut Hand (Menzel and D'Aluisio 2000)

First, unlike most of the other hands, Leonardo's hand features coupled fingers. Currently, one motor operates all 4 fingers creating a grasping motion. Thus it provides a very limited platform for dexterous manipulation. An additional problem is that the fingers are very compliant due to the use of springs as shown in Figure 4-2. Thus any force applied to the finger will cause it to bend. The reason for this compliance was to protect the fingers from damage in the event the hand was accidentally driven into an object or if someone had grabbed Leonardo's fingers as he started to move his arm. Interestingly enough, these potential problems which contributed to the compliant design are some of the same problems which a sense of touch may actually prevent. Any tactile system designed for Leonardo's hands must take into account these design challenges.

4.3 The "Pixel" Platform

Because of the difficulty of an entire research group developing on a single platform, in this case the Leonardo robot, Stan Winston Studio created a series of test platforms called "pixels" prior to the creation of Leonardo. Instead of using the Maxon motors incorporated in the design of Leonardo, these "pixels" used high-end hobby

servos. In addition to a set of eyes and ears, a single arm was created that mirrored the degrees of freedom in the actual arm of Leonardo. This arm, show in Figure 4-4, featured a much smaller hand than would be finally employed for Leonardo. The arm "pixel" was chosen as the platform to begin development of a tactile sensing system for Leonardo as it would allow for control of the movement of the arm and provide a preliminary test bed to explore how motion and tactile sensing could be combined together.

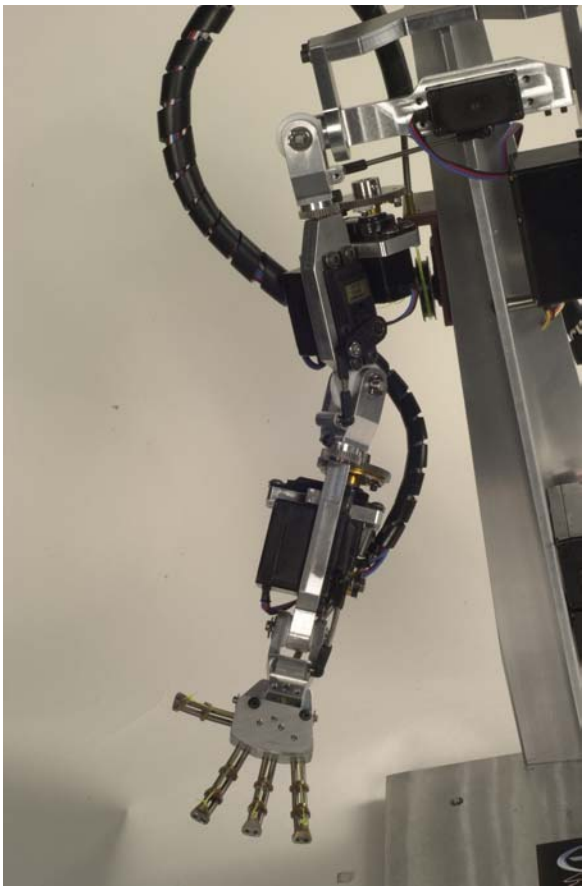

Figure 4-4. The Arm "Pixel" Platform. Photo and design copyright Stan Winston Studio.

5. Electromechanical Design of the New "Pixel" Hand

5.1 Modifications of the "Pixel" Hand

As described in Section 4.3, the "pixel" arm was chosen as the development platform for research into providing a sense of touch to Leonardo's hands. However, the hand that was originally included in the "pixel" design was much smaller than Leonardo's hand as shown in Figure 5-1.

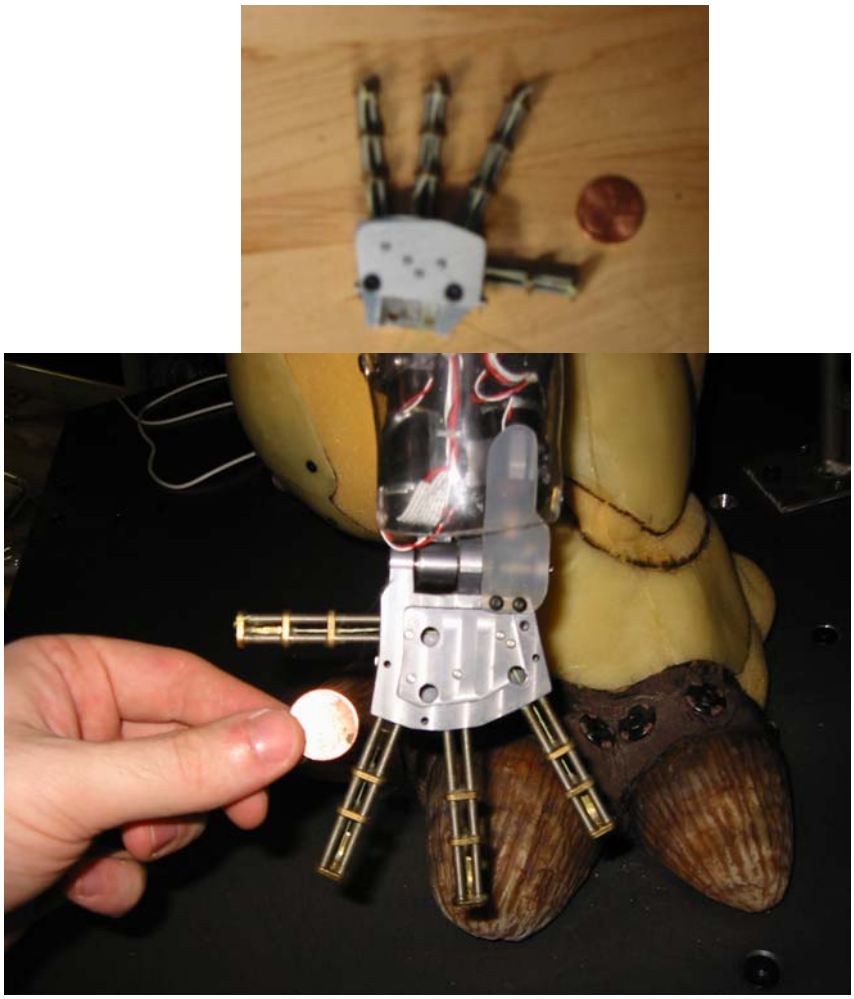

Figure 5-1. Comparison of "Pixel" Hand (top) to Leonardo's Hand (bottom). In each image, a penny is used for scale. Both designs are copyright Stan Winston Studio.

Thus it was clear that a new hand needed to be designed to closer approximate the size of Leonardo's hand.

The original design of both the "pixel" hand and Leonardo's hand featured a Kevlar cable which was used to pull each finger closed. These four cables passed through a series of steel dowel pins which were used to guide the cable from the base of

the fingers, down the middle of the hand at the base, and finally through a hole in the middle of the wrist which would run the cable through housing to the motor. Figure 5-2 shows the cable routing in the "pixel" hand.

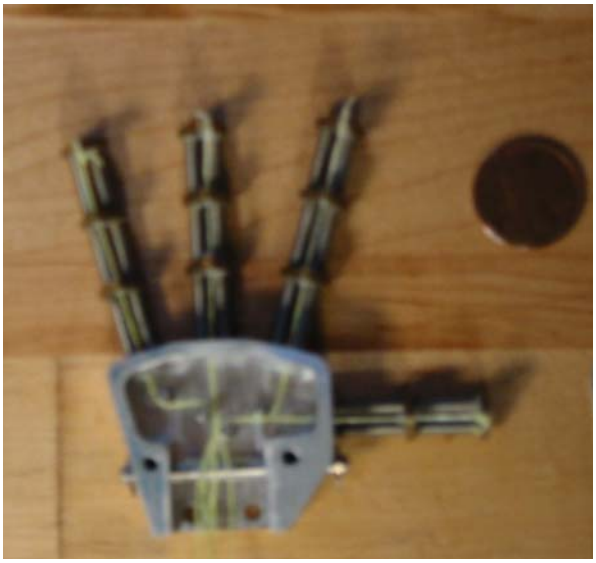

Figure 5-2. The Routing of the Kevlar Cable in the "Pixel" Hand. A penny is shown in the image for scale. The design of the "pixel" hand is copyright Stan Winston Studio.

An aluminum cover protected the cables in the palm from being damaged.

Any sensors mounted on the fingertips or hand would ultimately have to have their electrical wires pass through the middle of the hand. Running electrical wires on the surface of the hands could not only result in damage to the wires or sensors but could also result in interference with the sensors. Also with an original estimate of over 40 sensors, having a clean wiring scheme became necessary. Thus it became clear that the new design of the hand must incorporate a way to separate the mechanical cables from the electrical cables to prevent damage. The approach chosen was a dual layer approach, as shown in Figure 5-3.

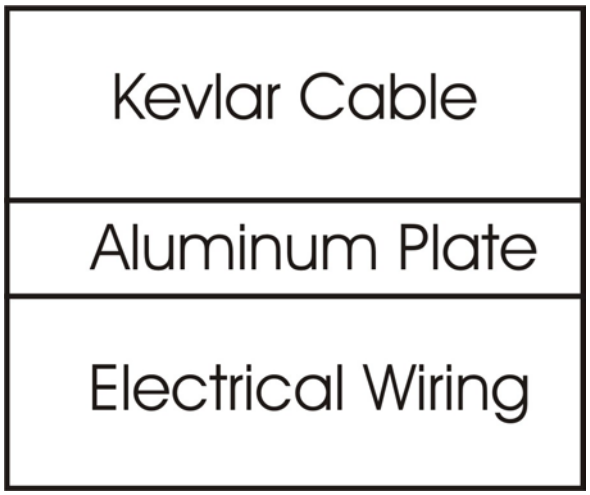

Figure 5-3. Dual Layer Design for the New "Pixel" Hand. An aluminum plate would separate the electrical wiring running below the Kevlar mechanical cable

In this approach electrical wiring would be primarily concentrated at the base of the hand. Conveniently, it was determined that springs used in the fingers could be used to route small diameter electrical cables from the fingertips to the middle of the hand. The springs would terminate in the front of the hand, and all wires from the fingertip sensors could be cleanly run out through the back of the hand. Any sensors mounted on the back or the sides of the hand would have wires which would pass through this layer as well. The only challenge would be to cleanly run any cables from the palm of the hand, which would be above the Kevlar layer, through the Kevlar layer and into the electrical wiring layer. Above the aluminum divider plate, the Kevlar cable would be run in a similar manner to how it had been run previously.

As was previously discussed in Chapter 2, the fingertips are one of the most densely populated tactile sensing regions on the body. Thus it would be crucial that each finger in the new "pixel" hand have some form of tactile sensing. The original design of the "pixel" fingertips ended with a brass vertebrae, to which the Kevlar cable was tied. Thus it was clear that a set of fingertips must be designed upon which the sensors could be mounted.

5.2 Sensors, Wiring, and Circuit Boards

The tactile sensors chosen for the new "pixel" hand were Interlink's force sensing resistors (FSRs) model #400 (Interlink Electronics product literature.). A further discussion of the sensor performance and circuits used appears in Chapter 6. Figure 5-4 shows the dimensions of the sensor.

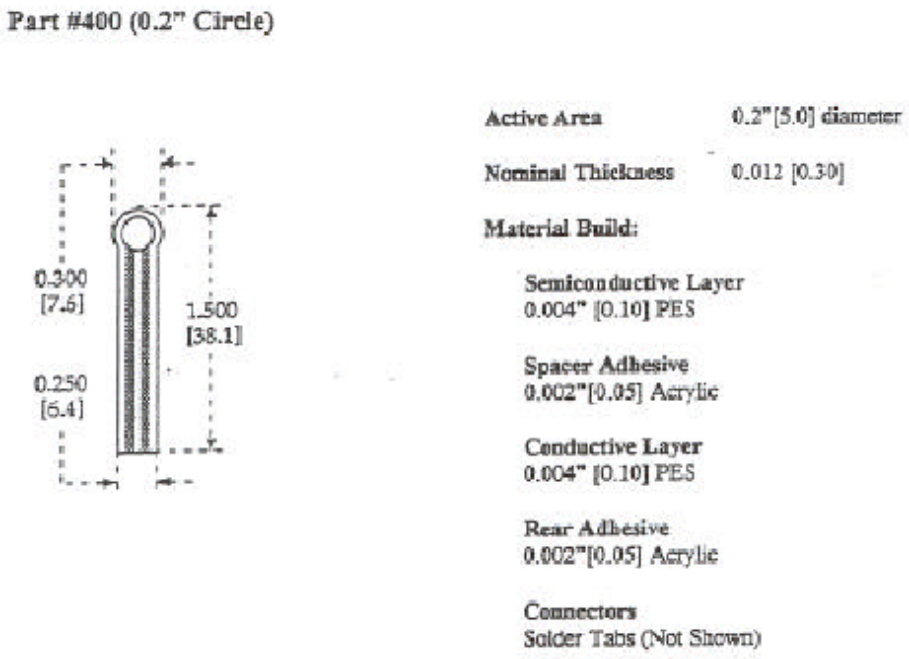

Figure 5-4. Dimensions of the Interlink Model #400 FSR. (Interlink Electronics product literature.)

The long lead length of the sensor posed a problem since at the end of the 1.5 inch long sensor were a set of solder tabs, that extended an additional 0.15" inches making the total length of the sensor 1.515" inches long. With a sensing diameter of 0.2" there would have to be overlap of sensor leads and sensors in creating an array of FSRs. Beyond the overlap, the long leads posed another problem – it was inevitable that most of the leads would overhang the actual hand and fingertips, thus increasing the likelihood of sensor damage and interference in motion of the fingers.

To counter the problems faced by the long lead length initial tests were conducted to see if the sensor lead length could be reduced. The solder tabs used in the interlink sensors are a product of Tyco Electronics, part number 88997-2, obtained through Hawk Electronics, www.hawkusa.com. Because of the normal manufacturing process for flat flex cables, the intended use for the solder tabs, the tabs are sold on a large spool and a hand crimper does not exist. An electric crimper was available, but a cost of thousands of dollars prohibited purchase. Thus a method of hand crimping was developed through trial and error using 4 different tools. The four tools are shown in Figure 5- 5.

Figure 5- 5. The Four Hand Tools Used to Crimp the Solder Tabs to the Cut FSRs

While there was some small change in resistance by reducing the lead length of the FSRs, on the order of a few ohms, it was negligible in light of the resistance change of the sensor. With careful crimping, no other changes in performance were seen with the alteration of the lead length. The final length of the FSR was reduced to 0.75" +/- 0.02". Reducing the lead length alone allowed for a greater than half reduction in length of the sensor. Figure 5-6 shows a comparison of the unmodified and modified FSR.

Figure 5-6. The Modified (bottom) and Unmodified (top) FSR. A penny is shown in the photo for scale.

The size of the modified sensor dictated the number of sensors which could be placed on the hand. A solid model was created of the hand to assist in determining the total number of sensors. Figure 5-7 shows two views of the solid model of the new hand which was used to assist in the placement of sensors.

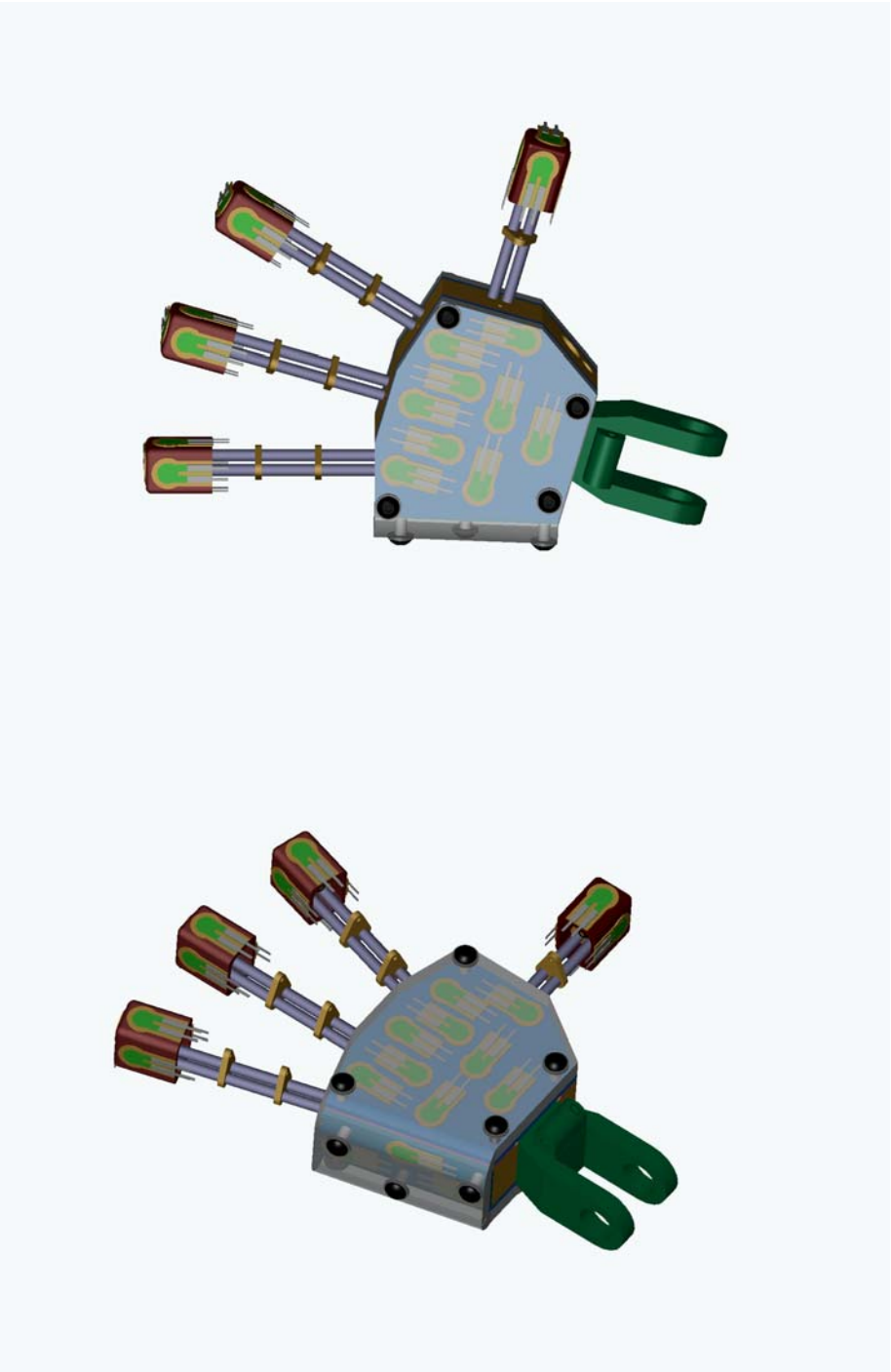

Figure 5-7. Two Views of the Original Solid Model Used for Sensor Placement. The palm in both images is shown. Later it was determined that an additional sensor could be placed at the base of the palm and the back of the hand making a total of 10 sensors on each side.

As discussed in Section 5.2, sensors were to be placed on each of the four fingertips, as well as the side, back, and palm of the hand. The final number of sensors is shown broken down by region in Table 5-1.

Table 5-1. The Number of Sensors per Region.

Region	Number of Sensors
Palm	10
Side	3
Back of Hand	10
Pinky Finger	5
Middle Finger	5
Index Finger	5
Thumb	5
Total	43

Each sensor requires two wires, thus with 43 sensors, a total of 86 wires are needed. This number can be drastically reduced if all sensors share a common ground. Thus the total number of wires required is 44. A discussion of the voltage divider circuit used appears in Chapter 6.

All of the 44 wires would enter the hand through two cables, entering through the rear of the hand and strain relieved through use of a 4-40 set screw to prevent damage. The first cable, 37 conductor 28 gauge from Cooner Wire model CW6424 www.coonerwire.com, would carry a common ground and connect to the majority of the sensors. The second cable, 10 conductor 28 gauge also from Cooner Wire model CW3614 would connect primarily to the remaining 7 sensors. Each cable was chosen for its high flexibility and shielding.

A printed circuit board was designed for mounting the sensors on the palm, back of the hand, and side. The purpose of these circuit boards were many fold. First, it would allow for accurate and repeatable placement of each sensor because circular traces on the board would mark the locations of each FSR. Second, it would minimize the amount of hand wiring since all connections, including the common ground amongst the sensors, could be wired together through traces on the board. Third, it allowed for easy replacement if a sensor were to be damaged, simply unsolder and pull the sensor of the board. Finally, through use of a connector it would allow for easy assembly and disassembly not only for repairs but also for improvements in the design of the boards.

Figure 5-8, Figure 5-9, and Figure 5-10 show the Protel design of side, palm, and back of hand boards respectively. In all 3 figures, the color blue corresponds to traces on the bottom of the board, the color red corresponds to traces on the top of the board, the color purple corresponds to the keep out layer, and the color yellow corresponds to solder mask. Each board was dimensioned using the solid model of Figure 5-7 as a guide.

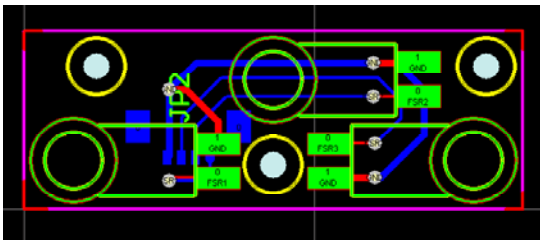

Figure 5-8. Protel Screen Shot of the Design of the Side Circuit Board. Note, the green color indicates that the silkscreen of each sensor violates a design rule in the manufacture of the boards. However, because the boards were created without a silkscreen, this violation can be ignored.

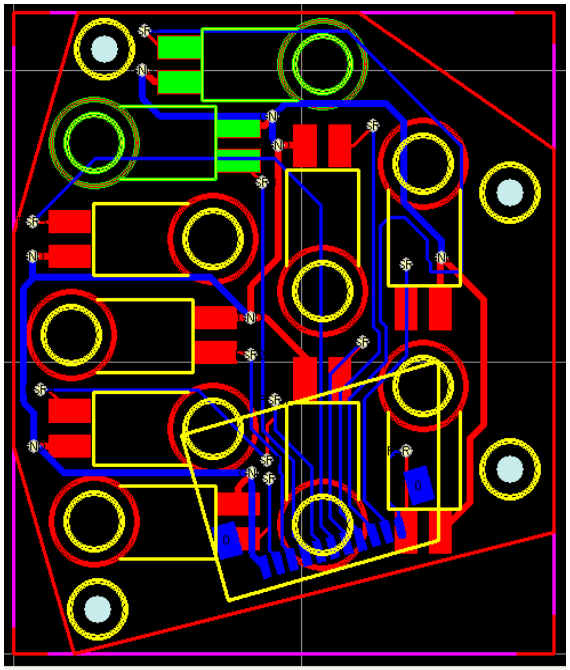

Figure 5-9. Protel Screen Shot of the Palm Circuit Board Design. Note, the green color indicates that the silkscreen of the two sensors violate a design rule in the manufacturing of the boards. However, because the boards were created without a silkscreen, this violation can be ignored.

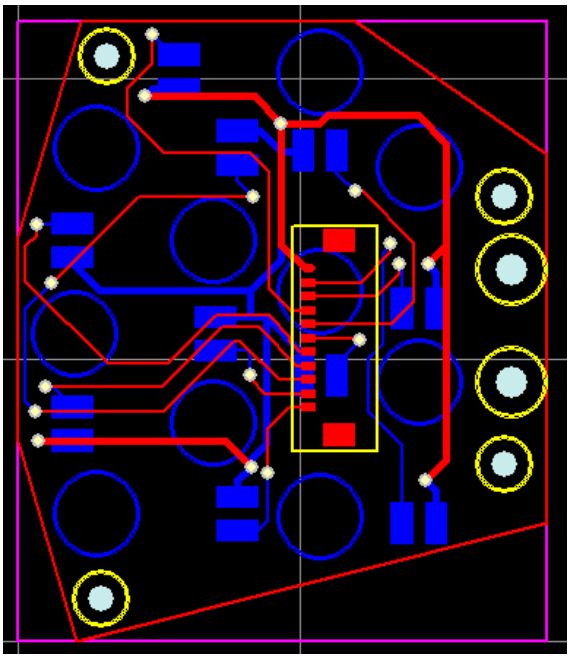

Figure 5-10. Protel Screen Shot of the Back of Hand Circuit Board Design.

A comparison of Figure 5-9 and Figure 5-10 shows that the placement of sensors on each board is the mirror image of each other. The major difference is the orientation of the connectors (indicated on each board by the pad with the row of 11 similar rectangles placed in a row). On the back of the hand board, the connector is placed in the center. On the palm board the connector is placed close to one side to allow for the electrical wires from the board to pass through the mechanical Kevlar cable layer as was discussed in Section 5.1.

The yellow rectangle or trapezoidal keep out layer in each figure corresponds to the slot in the mechanical design of the hand through which the connector would pass through. It was used as a point of reference for connector placement. The yellow circles surrounding the drill holes were used as a guide for screw placement to prevent sensors from being placed too close to a screw head. Finally, the red lines surrounding all the sensors in Figure 5-9 and Figure 5-10 indicate the trim lines for the circuit. Because of rapid production service employed by Alberta Printed Circuits, the circuit board manufacturers, only rectangular shaped boards could be produced. A laser cut template made out of ¼ inch acrylic was used as a guide to trim and sand each of the boards to the desired shape.

Figure 5-11, Figure 5-12, and Figure 5-13 show the final boards, trimmed to the correct size with the sensors mounted

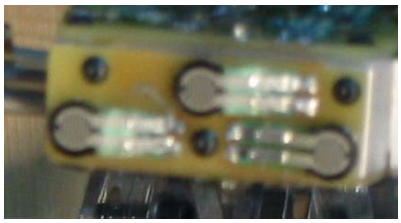

Figure 5-11. Final Side Sensor Board with Sensors Mounted

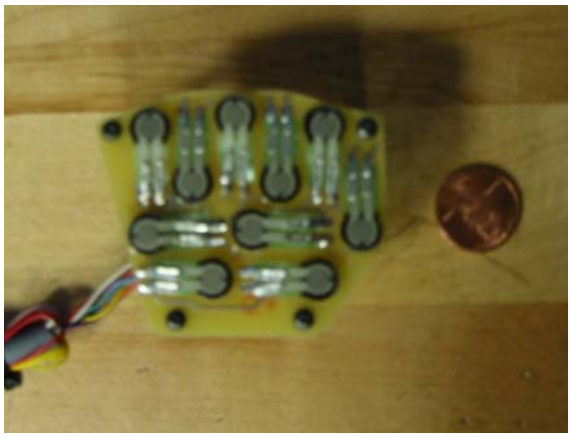

Figure 5-12. Final Palm Sensor Board with Sensors Mounted

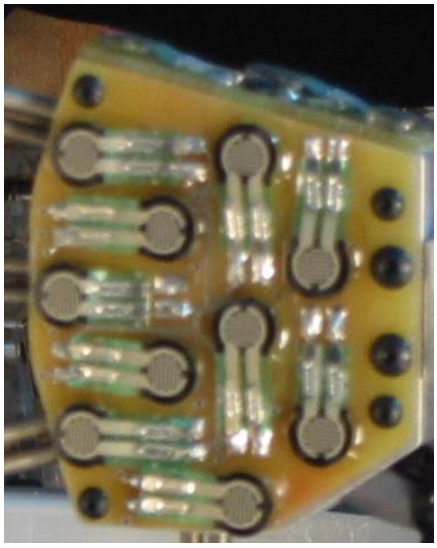

Figure 5-13. Final Palm Sensor Board with Sensors Mounted

An initial design of the sensor boards affixed the sensors directly to the surface of the boards. However, this posed a problem since now the high points of boards were not the FSRs but rather the solder joints connecting each sensor to the board. Thus, with such a

high density of sensors on the surfaces of each board, each sensor cannot receive a good reading since it is buried underneath the neighboring solder joints. To correct this small laser cut acrylic spacers, 0.3" diameter 1/16" thick, were epoxied to the surface of the circuit boards. The sensors were then epoxied to these spacers and the flexible lead was gently bent and soldered to the surface of the board. In all cases, the epoxy used was Devcon 14270 5-minute epoxy. Cyanoacrylate adhesives could not be used because they would degrade the sensor substrate and lead to cracking (Interlink Electronics product literature.). Figure 5-14 shows a graphical description of the problem and the solution.

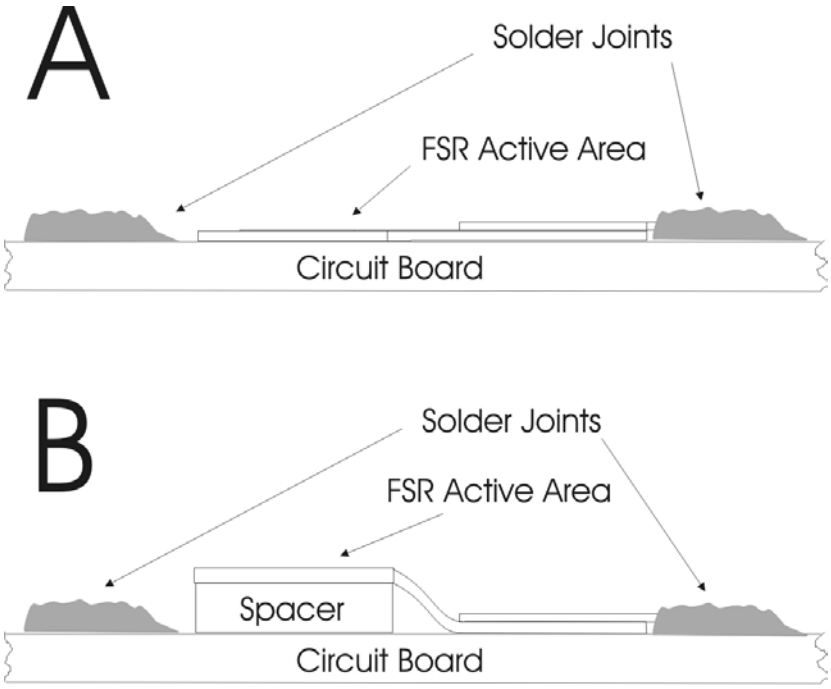

Figure 5-14. The Graphical Depiction of the Spacer Problem and solution. Figure A shows the problem, the sensor active area is buried below the solder joints. Note, the solder joints directly in front and behind the sensor are not shown in this diagram. Figure B shows that with the inclusion of the spacer the active area of the senor now becomes the high point of the sensor.

Due to the small size of the hand and the number of conductors needed in each connector, a very limited selection of connectors was available. The connectors chosen were the Molex Micro-Miniature 1.25mm connectors obtained through Digikey, www.digikey.com. For the side board, a four-pin straight surface mount connector was used. Both the palm and the back of the hand boards used an eleven-pin connector with the palm board using a surface mount while the back of hand used the right angle version. In each case the additional pin on the connector was used for a common ground among the sensors.

The fingertips had 5 sensors per finger as shown in Table 5-1. Each sensor was mounted to an aluminum fingertip, the design of which will be discussed in Section 5.3, in a similar method described earlier, but no spacer was used. Because only one sensor

would be used per face and the solder joints would actually be at the base of the fingertip, it was determined that a spacer was not necessary. The FSR mounted on the tip of each finger was of original lead length. It was first epoxied to the tip, then epoxied down the side of the fingertip. The sensor for the back of the fingertip was then epoxied over this lead. Figure 5-15 shows a photo of the mounted sensors.

Figure 5-15. The Mounted Fingertip FSRs.

As can be showed in Figure 5-15, small holes were drilled through the sides of each fingertip. A ground wire and signal wire, both Daburn 30 gauge single conductor wire 2671/30, pass through each hole. The wires connecting to the top of the fingertip sensor do not pass through these holes, but rather travel up the backside of the lead and solder to the solder tabs. In all cases shrink tubing was used to protecting the connections of the wires to the solder tabs, and in the case of the top sensor lead, provided added strength and protection to both the lead and the wire pair. Each ground wire leading to each sensor was connected to the ground wire running up into the fingertip from the hand, thus a bundle of 5 wires became one.

All the wires that enter into the fingertips from the hand travel up through the center of the springs in the fingers in groups of three. In order to cleanly connect the wires from the fingertips to the Cooner Wires that lead out from the hand to the A/D board, a circuit board was designed. This board would further reduce the number of wires needed as it would allow the ground wires from each of the three sensor boards as well as each finger to be connected to the common ground of the Cooner Wires. The Protel screen shot as well as the actual circuit board are shown in figure 5-15.

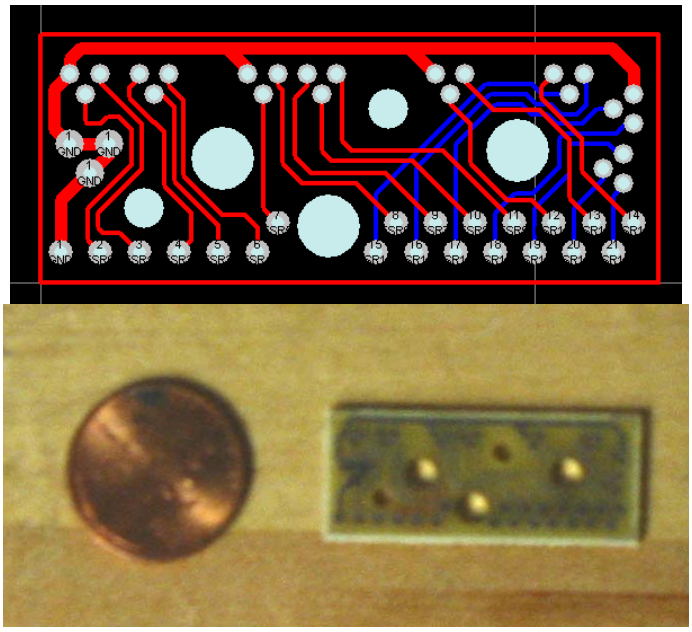

Figure 5-16. The Protel Screen Shot and Actual Mid-Plane Circuit Board. In the screen shot (top) red indicates traces on the top of the circuit board and blue indicated traces on the bottom of the circuit board. A penny is placed next to the actual circuit board to provide a sense of scale.

The 3 larger holes are for passage of the steel dowel pins used in the mechanical cable routing. The two smaller holes are for #1-72 socket head cap screws used to mount the circuit board to the hand. The rows of through-holes on the bottom of the board are where 21 of the 37 conductors of the Cooner Wire CW6424 cable connect. The eight groups of similarly sized 3 through-holes are where each of the bundles of 3 Daburn wires from the fingertips connect to the board. The final triad of through-holes is where a ground lead from each of the three sensor circuit boards, palm, side, and back of hand, connect to the board.

Figure 5-17 shows the path from sensor signal to A/D board. In many ways this bundling of cables together is similar to how the axons of the mechanoreceptors are bundled together as they enter into the spinal cord at the dorsal root, as discussed in Chapter 2. A further discussion of this similarity will occur in the next chapter.

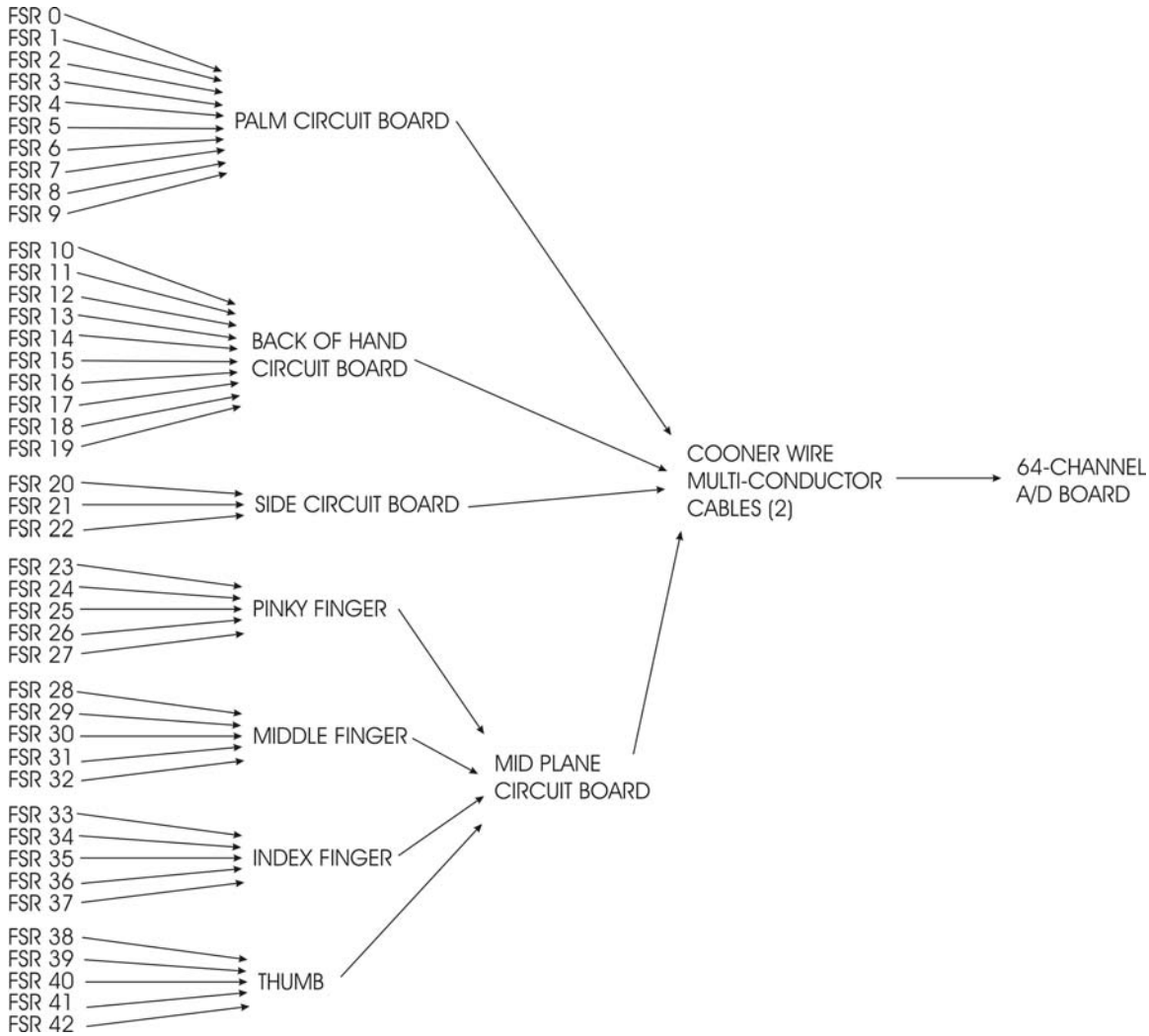

Figure 5-17. Wiring Diagram for FSR Signal from Sensor to A/D Board.

5.3 Mechanical Design of the New "Pixel" Hand

As was previously discussed in Section 5.1, it was clear that a new hand had to be designed to both allow for the dual layer design and to increase the surface area of the hand for increased sensor density. It was also important to stay as close to the original design as possible because there were many similarities between the original "pixel" hand and the hand of Leonardo, as mentioned previously in Chapter 4. Thus the new "pixel" hand would be based on the original part drawings of Stan Winston Studio but the palm and back of hand areas would be scaled by 1.5 times to increase the surface area. In this section each of the mechanical components will be described in detail as well as how the entire assembly fits together to create the final hand.

The hand consists of a series of 6 different types of machined parts. For ease of discussion, each type will be discussed moving from the fingertips back into the hand.

The first type are the 6061 aluminum fingers which were not based upon any previous designs of Stan Winston Studio. Figure 5-18 shows both the solid model as well as the finished part. It is important to note that the addition of holes through which the electrical wires that connect to the sensors on the fingertips followed the original design and thus are not indicated on the solid model. Also, the rounded corners were designed so as to prevent tearing of the silicone skin which would later cover the fingertips. A further discussion of Silicone rubber and its application to this project appears in chapter 7.

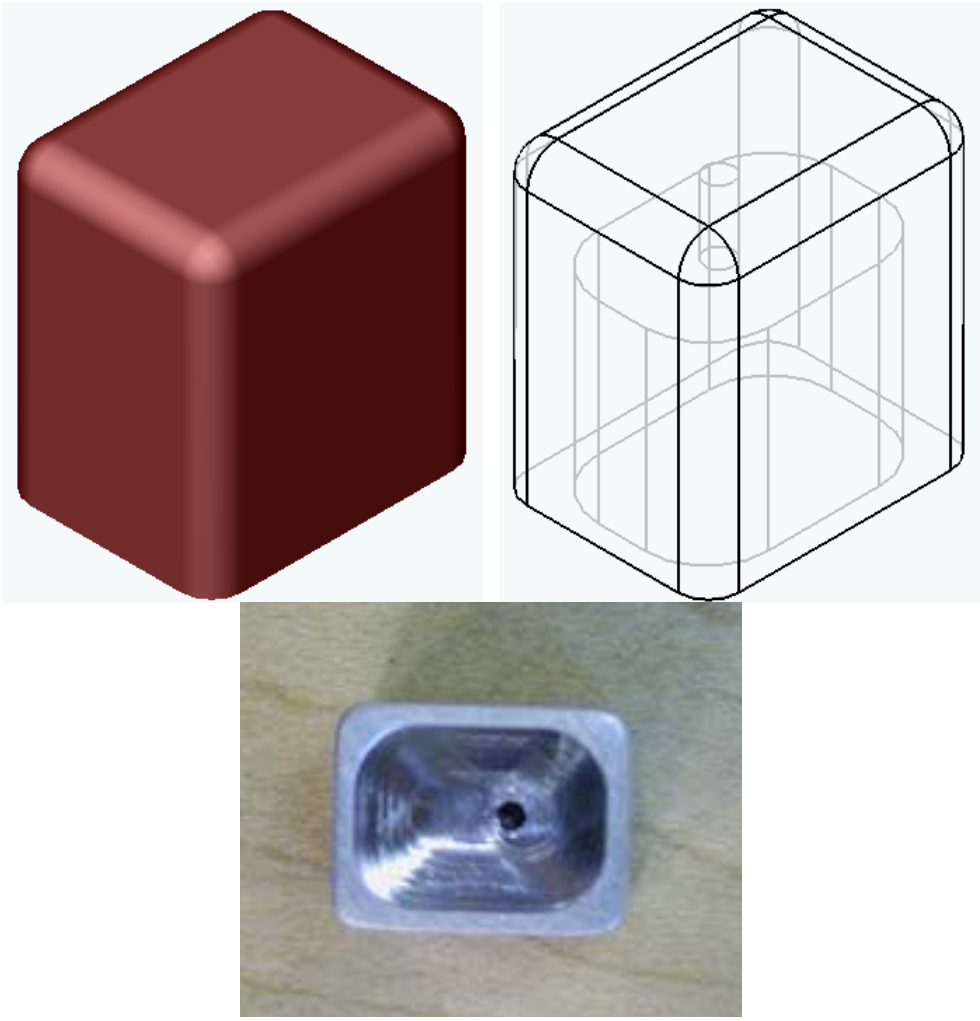

Figure 5-18. The Fingertips. The solid model appears both as a solid (left) and as a wire-frame (right). The actual part, shown from the bottom, is below the solid models. Photo courtesy of Jeff Lieberman.

The second and third types of machined parts were the two types of finger vertebrae – the unmodified finger vertebrae, identical to the original Stan Winston Studio design, and the modified fingertip vertebrae. Figure 5-19 shows both the solid model as well as the final machined part of each type. Each type was made of brass.

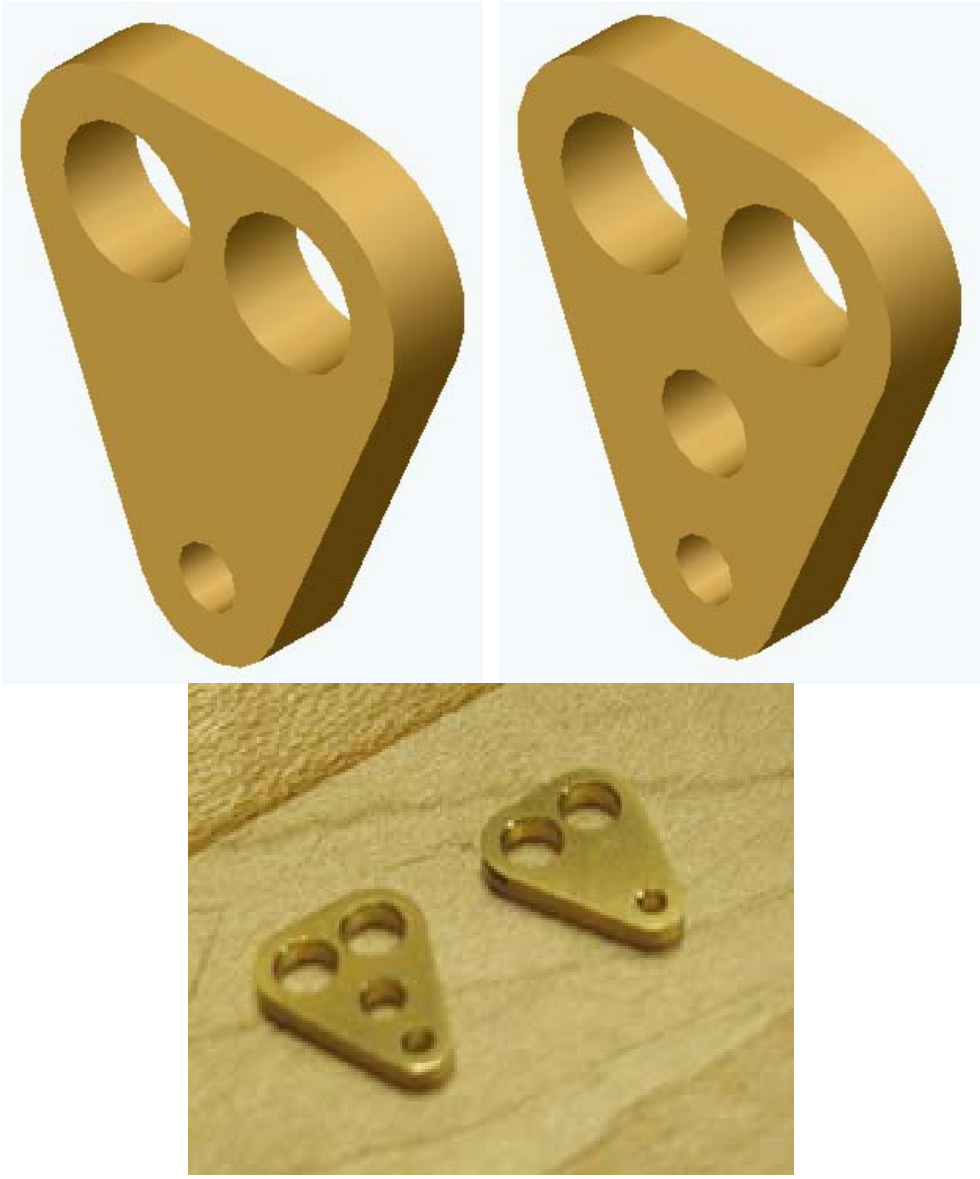

Figure 5-19. Two Types of Fingertip Vertebrae. The Finger Vertebrae (upper left) is identical to the original Stan Winston Studio design. The Fingertip Vertebrae (upper right) features the addition of a #1-72 close fit hole. The lower photo shows the final machined parts. Photo courtesy of Jeff Lieberman.

As shown by a comparison of the two designs, both are identical except for the inclusion of the #1-72 close fit hole which is used for mounting the fingertip shown in Figure 5-18 to the finger. The larger diameter holes are where the springs pass through and are soldered. The smaller diameter hole is Teflon lined to reduce friction and the Kevlar cable is passed through it. Each of the three long fingers (pinky, middle, and index) is composed of 2 finger vertebrae and 1 fingertip vertebrae on the end, while the thumb is composed of one of each type. The design of the spring fingers is exactly the same as in the original Stan Winston Studio design seen in Figure 4-2 and Figure 4-4.

Figure 5-20 shows a completed finger with fingertip attached both as a solid model as well as the completed design.

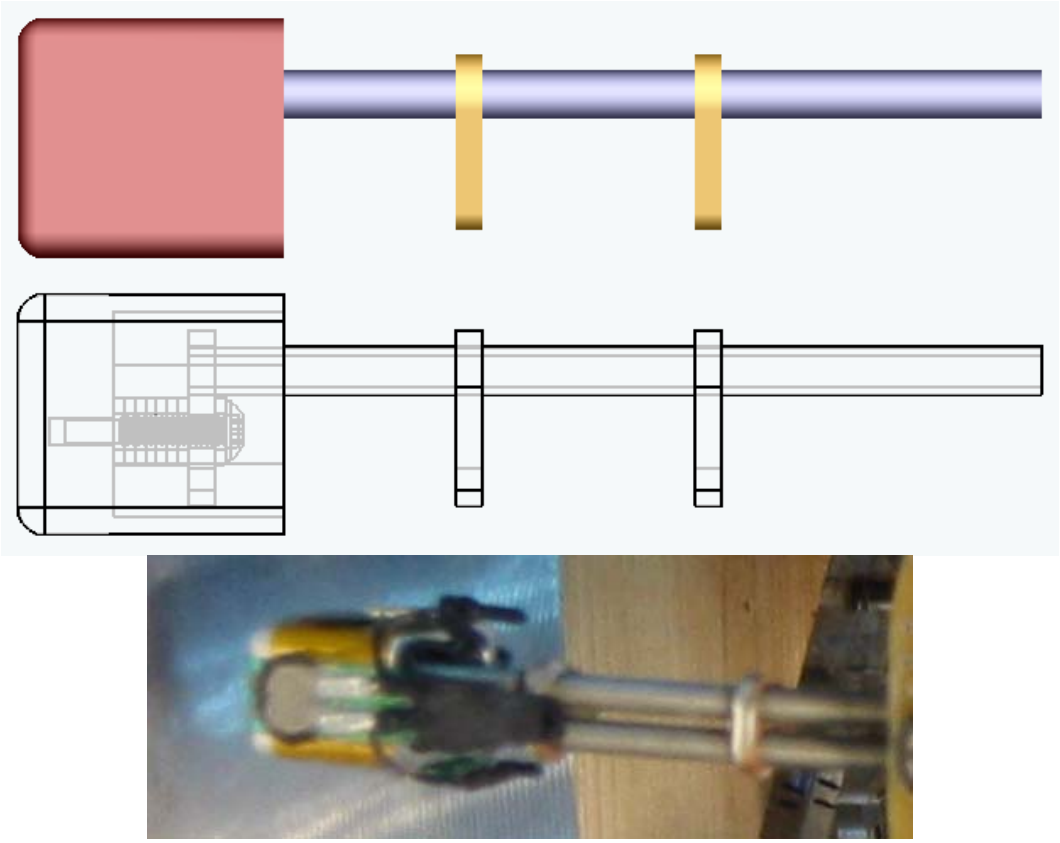

Figure 5-20. The Assembled Finger. The solid model appears on the top as a solid, and in the middle as a wire frame. The finished finger, with sensors attached appears in the bottom of the figure.

The washers used to suspend the fingertip above the fingertip vertebrae can be seen in the wire frame version in the center of the figure. The final design uses four #1 washers. The reason for the clearance is to allow for the electrical wires traveling up the center of the finger springs to wrap up and around the fingertip vertebrae to connect to the FSRs at the base of the fingertip as shown in Figure 5-21.

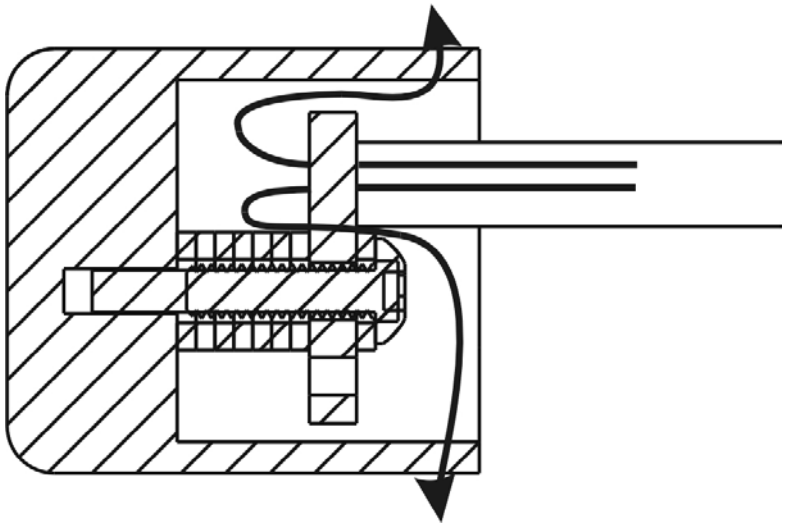

Figure 5-21. The Wiring Path in the Fingertip. The black arrows indicate the possible paths a wire can take.

The most complex part of the design was the hand. All components, both electrical and mechanical, had to pass through it or connect to it. Figure 5-22 through Figure 5- 25 show different views of this part, both as a solid model as well as the finished machined part. The hand was made of 6061 aluminum.

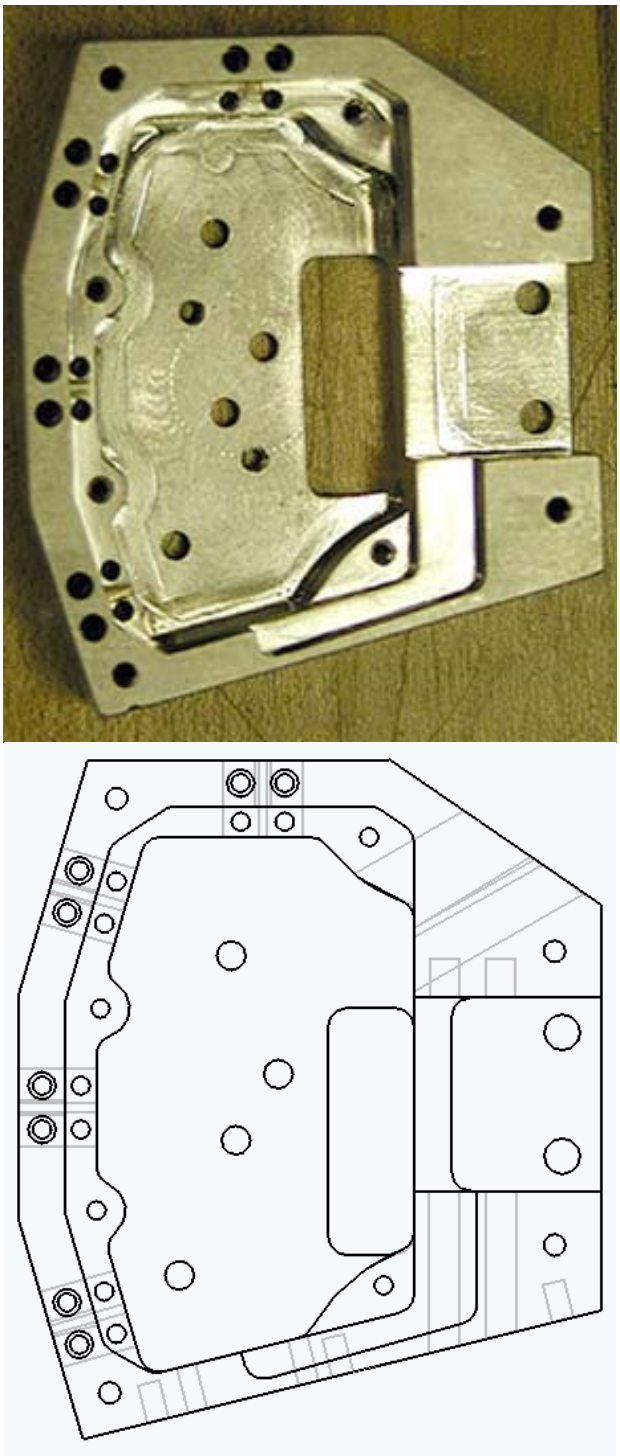

Figure 5-22. Top View of Hand. The actual part is shown at top. Photo by Jeff Lieberman The solid model is shown at the bottom in wire frame format.

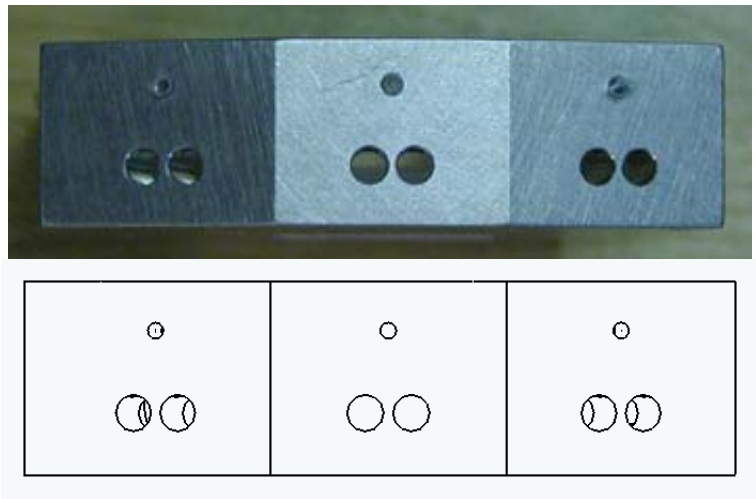

Figure 5-23. Front View of the Hand. The actual part is shown on Top
Photo by Jeff Lieberman and the solid model is shown below.

In Figure 5-23, Teflon liners are placed on the inside of the smaller holes and the Kevlar cables are routed through as they run into the fingers. The springs that comprise the fingers are inserted through the larger holes and clamped with two #2 set screws per spring.

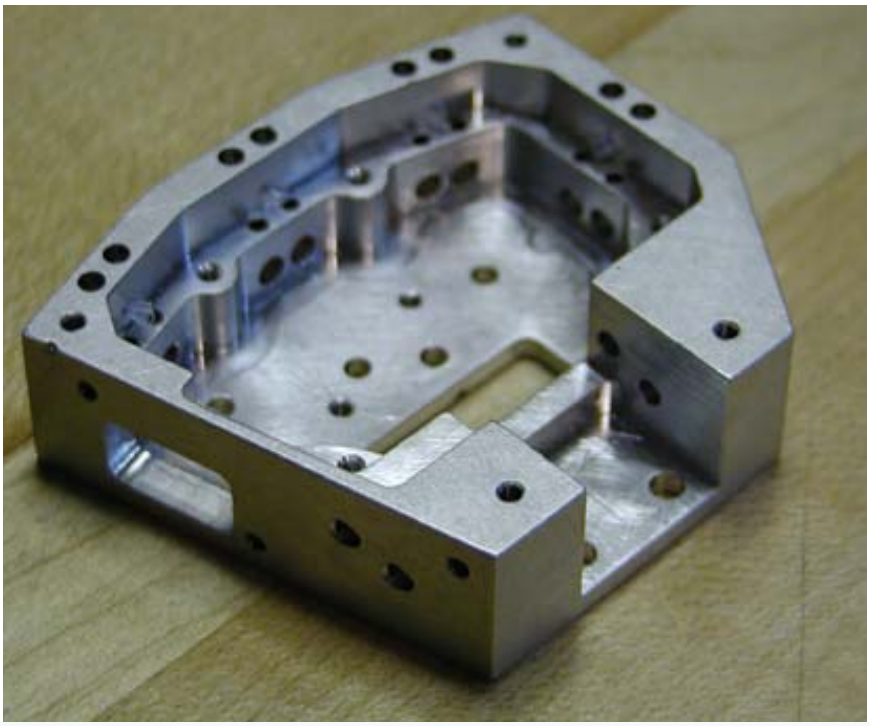

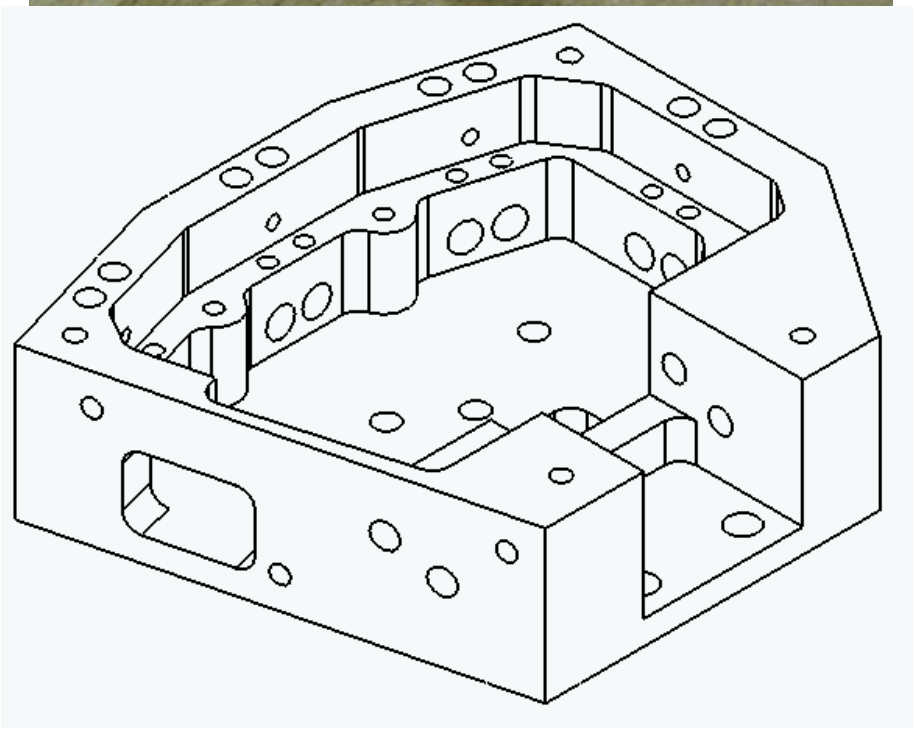

Figure 5-24. Isometric View of Hand Part. The actual part appears at top. Photo by Jeff Lieberman. A wire version of the solid model appears below.

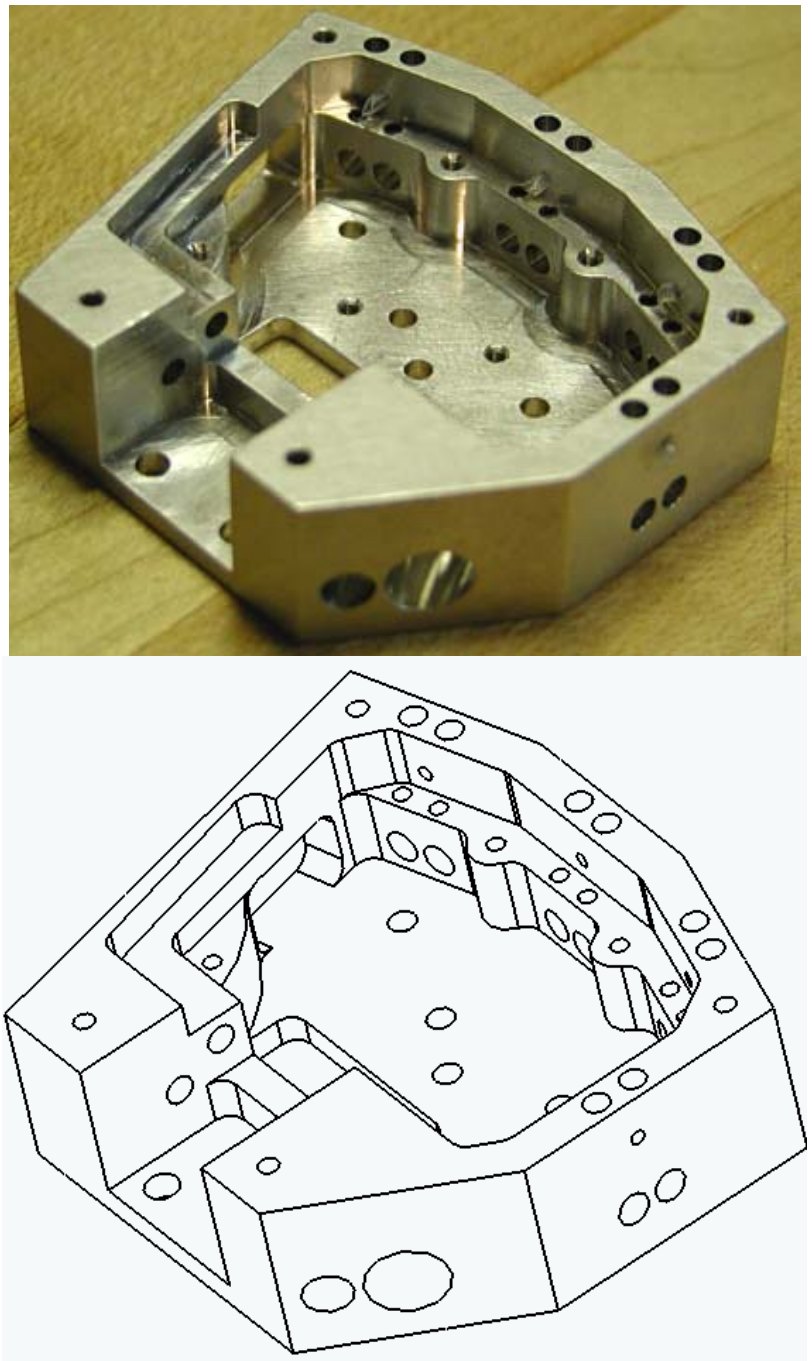

Figure 5- 25. Another View of the Hand Part. The actual part appears at top. Photo courtesy of Jeff Lieberman. The solid model appears below.

The Mid-Plane plate which divides the electrical layer from the mechanical as discussed in Section 5.1 appears in Figure 5-26. The plate was made of 1/32" 6061 Aluminum.

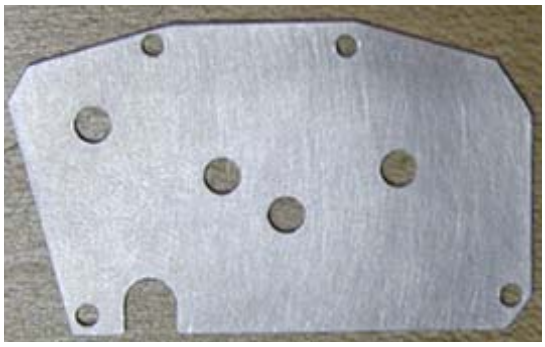

Figure 5-26. The Mid-Plane Plate. Photo courtesy of Jeff Lieberman.

Four #1-72 socket head cap screws pass through the four smallest holes to secure the plate to the hand. The four larger holes are oversized and fit over the 3/32" steel dowel pins used for cable routing. The semi-circular hole at the bottom of the plate is for the wires of the connector for the palm circuit board. Figure 5-27 shows how the mid-plane plate sits in the hand.

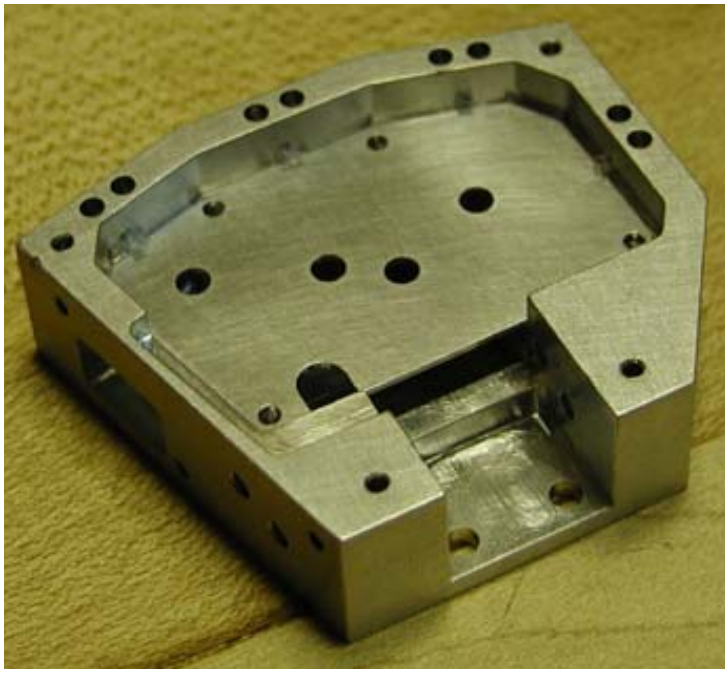

Figure 5-27. The Mid-Plane Plate in the Hand. Photo courtesy of Jeff Lieberman.

The final machined part was the top plate, made of 1/32" thick 6061 aluminum. This plate, shown in Figure 5-28, was a modified version of the original "pixel" plate and the Leonardo plate both designed by Stan Winston Studios

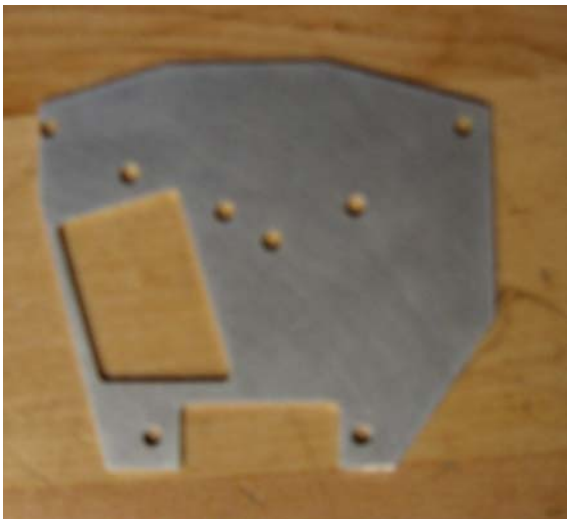

Figure 5-28. The Top Plate.

The smaller holes are clearance holes for #2-56 button head cap screws which mount the palm circuit board to the hand. The slot at the bottom of the plate is clearance for attachment of the hand to the wrist. The slot at the left of the plate is removed to allow the connector from the palm circuit board to pass through. The larger holes, also featured in the original design, are press-fit for the 3/32" steel dowels pins which help increase the mechanical stability of the palm circuit board. Unlike each of the previous plates, the top plate for the new hand was designed to cover the entire hand as shown in Figure 5-29.

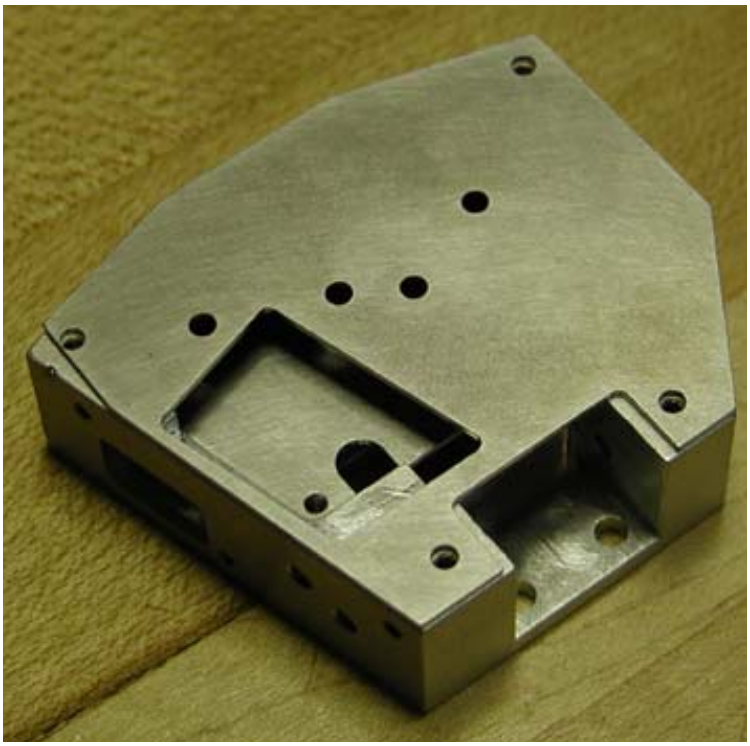

Figure 5-29. Top Plate on Top of Hand with Mid-Plane Plate. Photo courtesy of Jeff Lieberman.

5.4 Assembly of Components

While there is much modularity in the design of the new "pixel" hand insofar as how the components can be assembled or removed for repair or improvement, there are certain steps which must occur before others, as has already been alluded to in previous sections. First, once the fingers have been assembled as described in Section 5.3 they are installed into the hand and clamped with the #2 set screws as shown in Figure 5-30. Note, the aluminum fingertips are not installed on the fingers at this stage of the assembly.

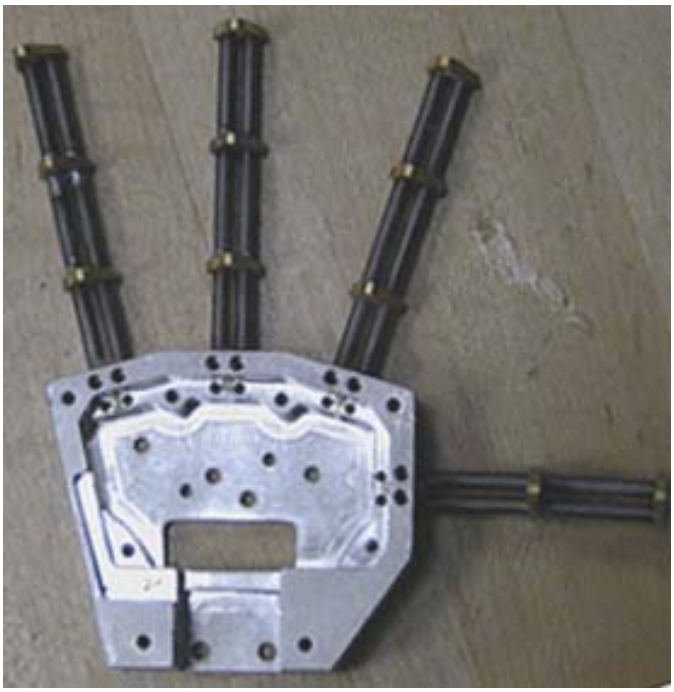

Figure 5-30. Hand with Fingers. Photo courtesy of Jeff Lieberman

Next, the 3/32" dowel pins are press fit into the hand, both through the side of the hand as well as through the top. These will guide the Kevlar cable from the base of the fingers through the hand and finally out the back of the hand into the cable housing leading to the servo motor. The mid-plane circuit board, with cables attached, is then secured in place at the bottom of the hand with #1-72 socket head cap screws. The Daburn cables from the mid-plane board are then strung through the springs in groups of 3 as was previously discussed in Section 5.3 as shown in Figure 5-31.

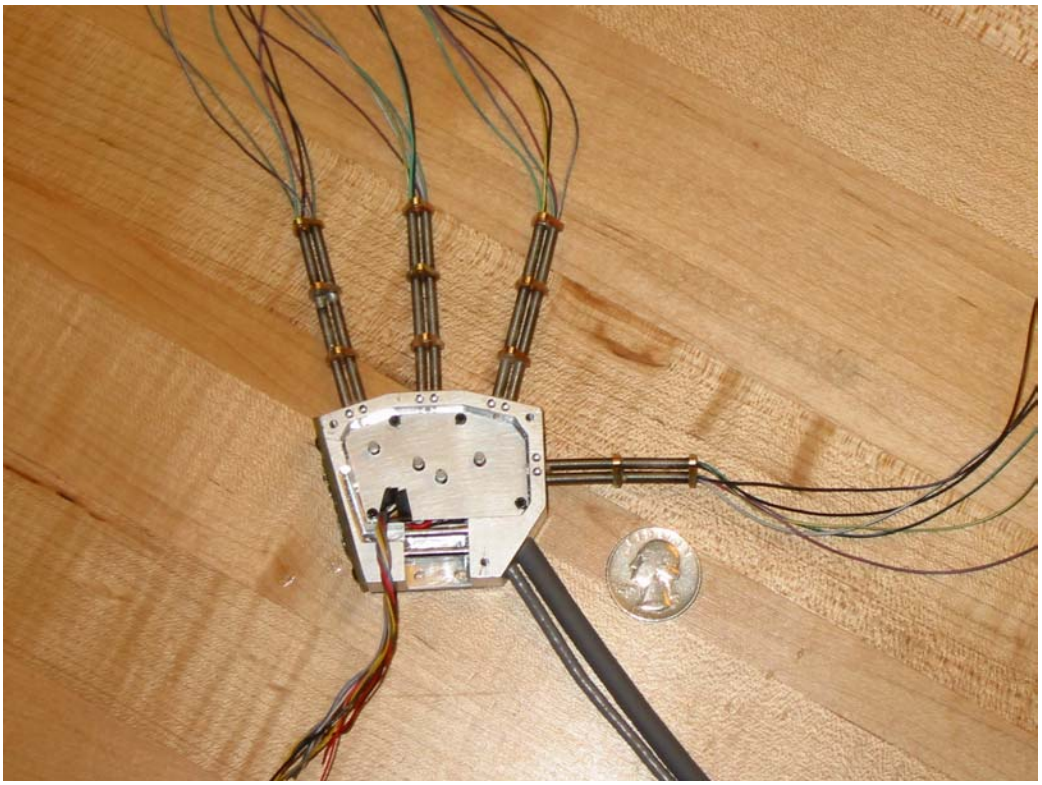

Figure 5-31. Mid-Plane Circuit Board Mounted in Hand. A quarter is placed in the photo to provide a sense of scale.

The three sensor circuit boards, the palm, back of hand, and side boards, are then installed. Each finger is then attached to the hand, and electrical wires as routed through the fingertips and soldered to each FSR as discussed previously in this chapter. The Kevlar cable is run through the cable housing and attached to the pulley of the servo which controls the grip. Than hand is placed onto the wrist and two #4 BHCS are used to secure the hand in place. The final assembled hand prior to placement of the silicone skin is shown in Figure 5-32 through Figure 5-36.

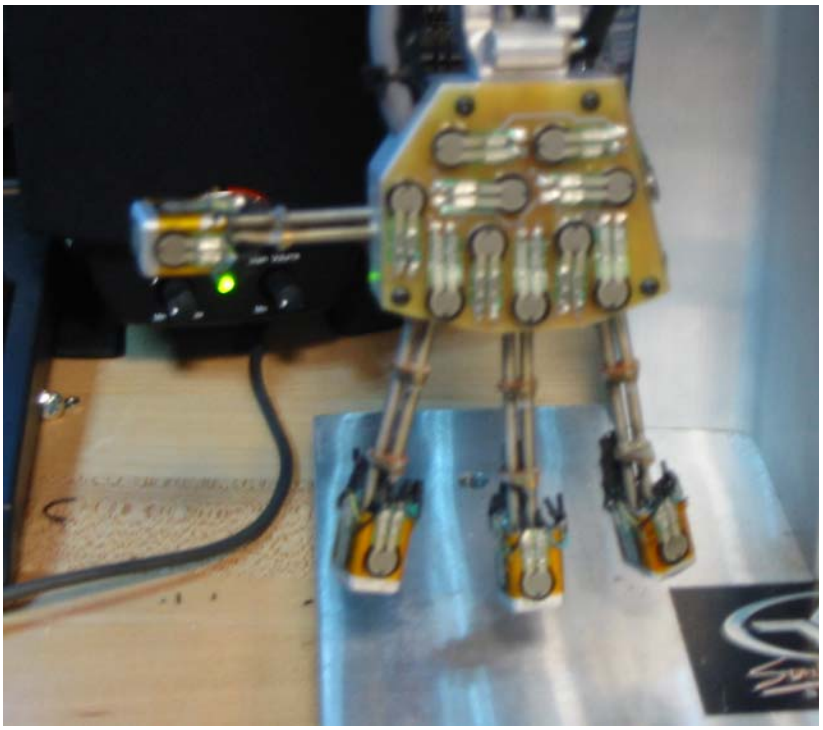

Figure 5-32. The Assembled Hand – Palm View

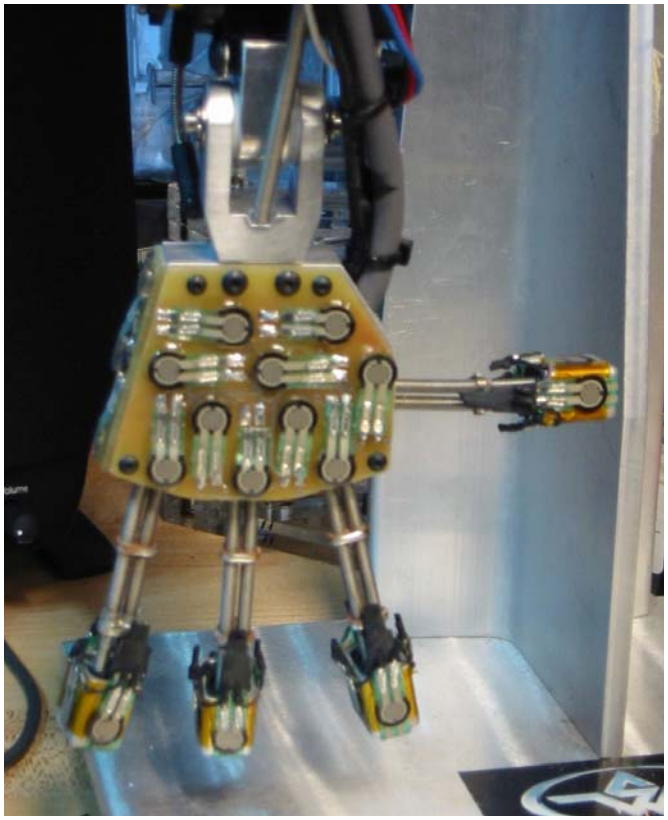

Figure 5-33. The Assembled Hand – Back of Hand View

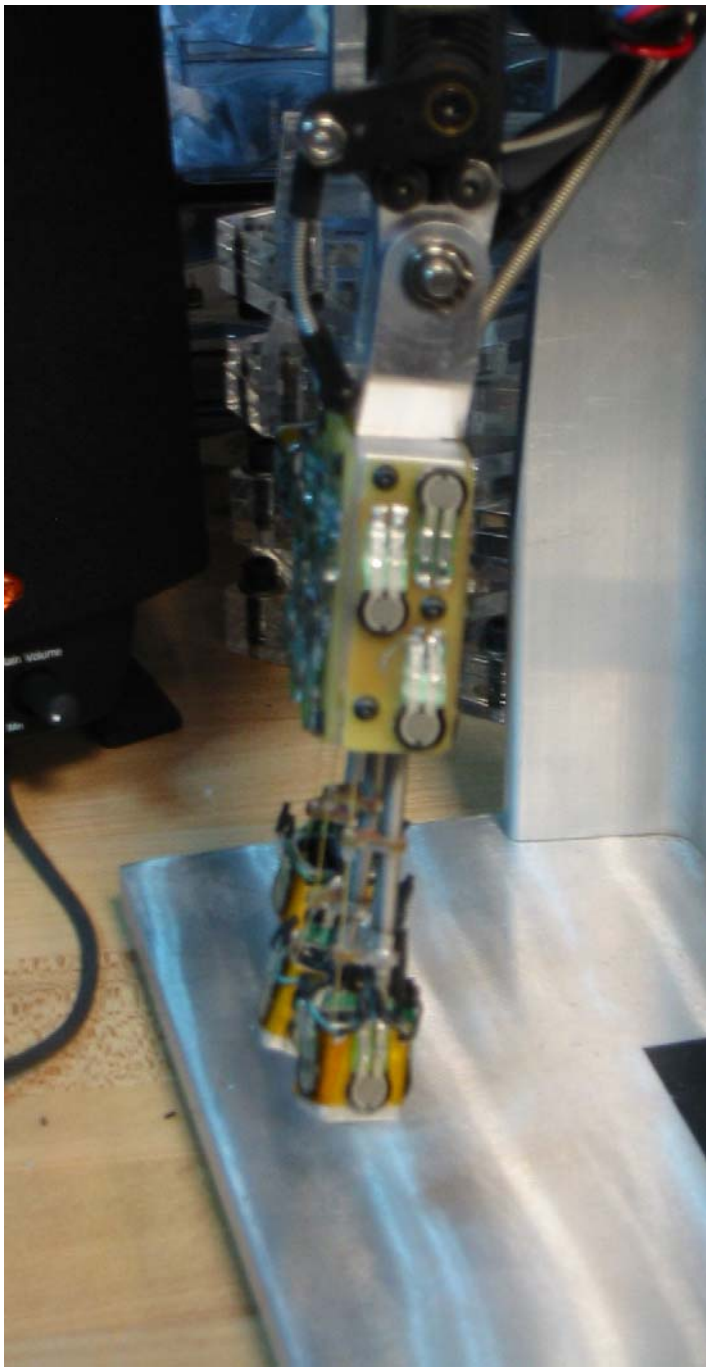

Figure 5-34. The Assembled Hand – Side View

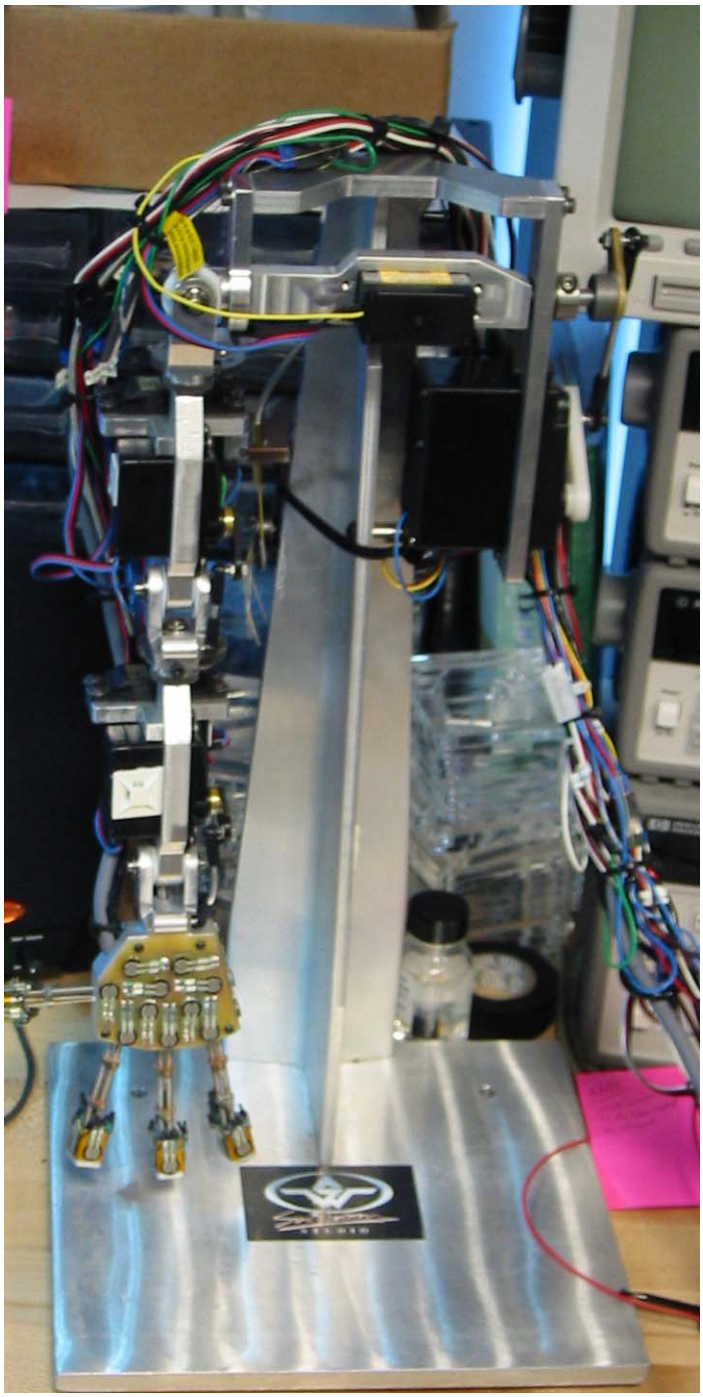

Figure 5-35. The Assembled Hand and Arm

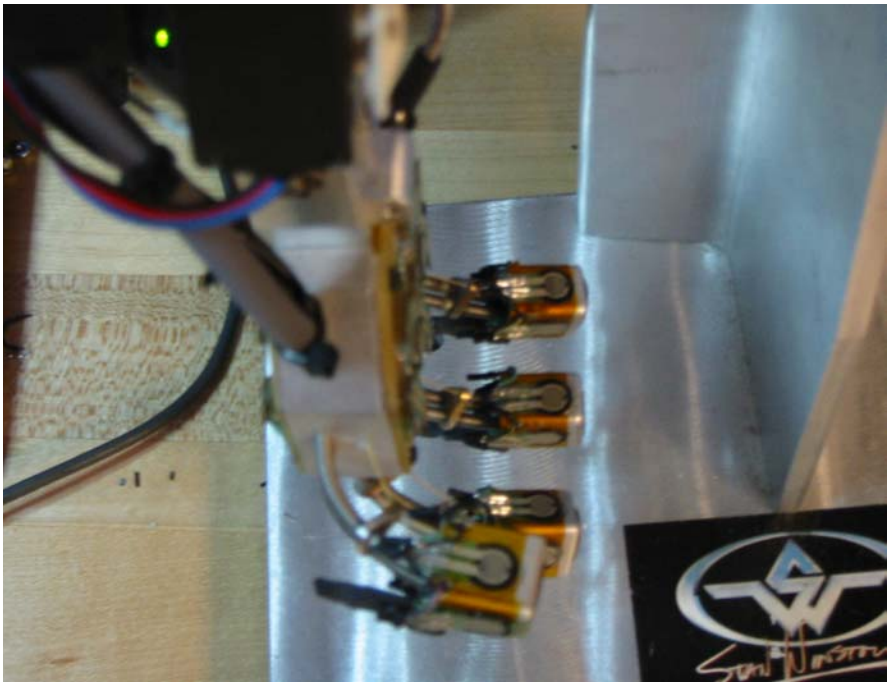

Figure 5-36. The Assembled Hand - Grip

6. Electronics

6.1 Overview of the Electronic System

There are two pathways between the "pixel" arm and the computer as shown in Figure 6-1.

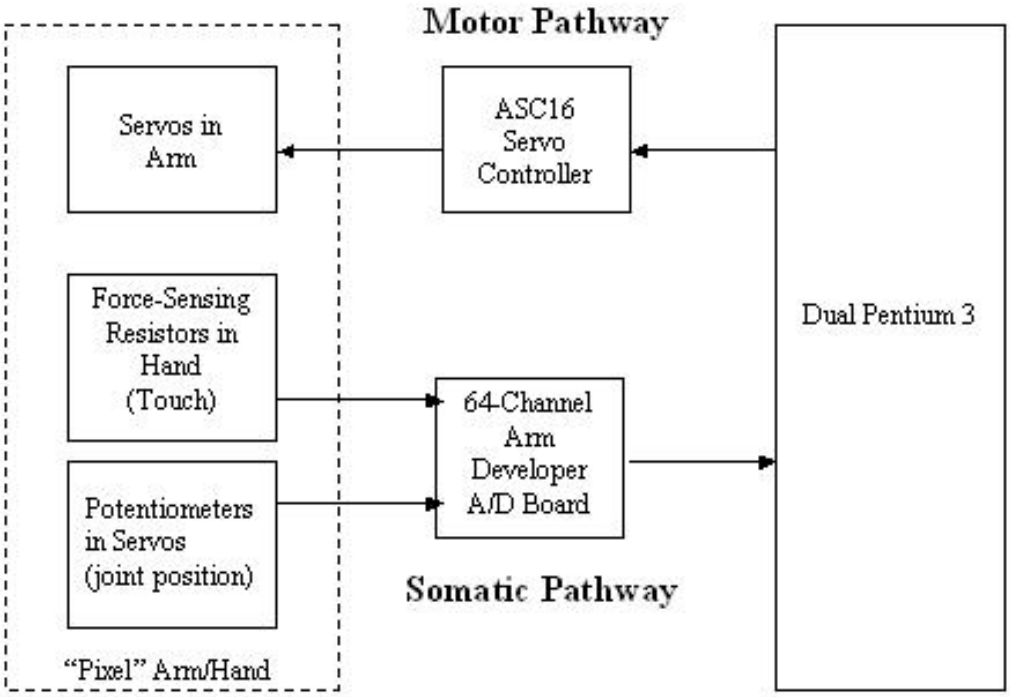

Figure 6-1. Diagram of Electronic Pathways

In the input pathway (the somatic pathway), sensor information from the Interlink FSRs as well as positional information from the potentiometers in the servos of the arm enter the 64-Channel A/D board, are processed, and then passed through the serial port into the computer. In the output pathway (the motor pathway) motor commands are sent via serial from the computer to the ASC16 Servo Controller Board, which in turn causes the arm to move.

This arrangement of somatic and motor information shares many similarities to that of the spinal cord of the Central Nervous System, as discussed in Chapter 2. For illustrative purposes, the spinal cord is shown with motor and sensory neurons in Figure 6-2

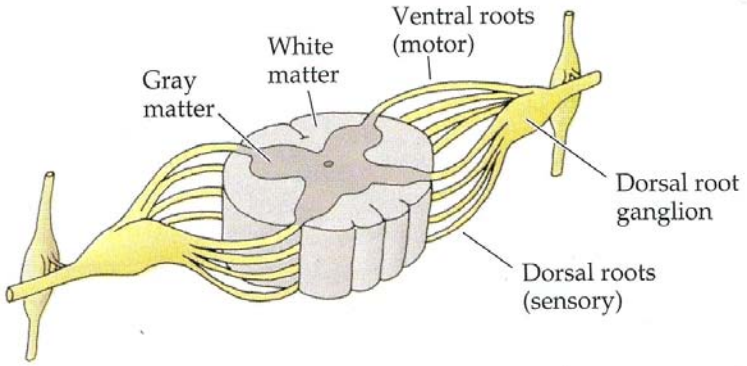

Figure 6-2. A Section of the Spinal Cord Showing Dorsal Roots (Sensory) and Ventral Roots (Motor) from (Rosenzweig, Breedlove et al. 2002, pg 39)

One can imagine a series of paired sensory processing and motor control circuit boards comprising a "robotic spinal cord" with pairs of boards at each level mapping to different regions of the body. It may even be possible to use the local processing and communication on each board to allow for reflex loops at this level of the system.

In this chapter a full discussion of the selection of sensors as well as circuit design of the Arm Developer circuit board will be provided. Finally the selection of the ASC16 servo controller will be discussed at the end of this chapter.

6.2 Sensor Selection and Performance

As discussed in Chapter 3, there are a wide variety of potential sensing options. However, the specific design constraints of cost (since there is the potential for a large number of discrete sensors), responsiveness, low physical profile, small size, and sensitivity led to the choice of the interlink force-sensing resistors for this application. A force-sensing resistor is a polymer thick film (PTF) device which decreases in resistance as the force applied to the active area of the sensor increases. (Interlink Electronics product literature.)

The physical principle of how the sensor works is simple as shown in Figure 6-3. The top layer of the sensor contains a flexible substrate with a printed semiconductor. The bottom layer contains a flexible substrate with electrodes arranged in a finger-like pattern. The middle layer features a spacer. When force is applied to the top of the sensor, the semiconductor is pressed through the opening in the middle layer and connects the electrodes of the bottom layer increasing the conductance and lowering the resistance of the sensor. As more force is applied, more of the top layer comes in contact with the bottom layer and thus the resistance of the sensor will further decrease. This is very similar to the physical transduction of force of the Merkel disk receptor discussed in Chapter 2.

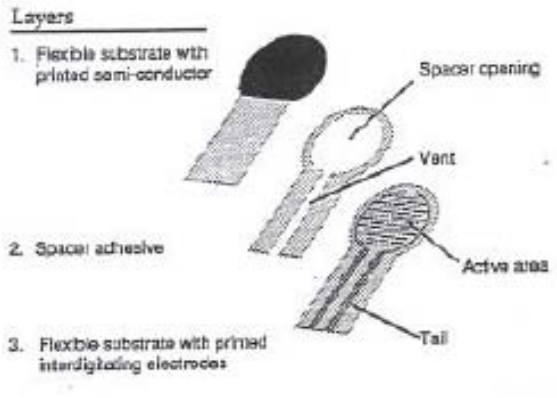

Figure 6-3. Construction of the FSR Sensor (Interlink Electronics product literature.)

The response of the sensor is shown in Figure 6-4.

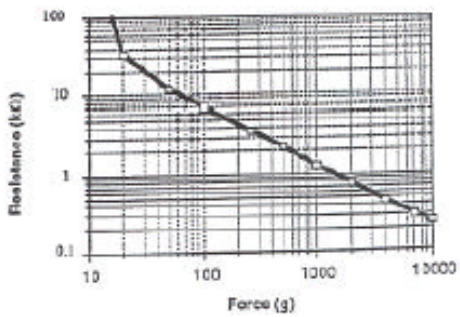

Figure 6-4. The Response of a Model #402 (0.5" diameter circular sensing area) to Applied Loads (Interlink Electronics product literature.) The actuator which applied the loads was made of stainless steel and had a 0.4" hemispherical diameter tip of polyurethane rubber with a value of 60 durometer.

As can be shown clearly from the plot, the sensor exhibits a dual behavior. Initially the sensor functions like a switch until the "turn-on threshold" or "break force" which is shown by the change in slope. At this point (between 10 and 100 kΩ), the resistance changes to below 10 kΩ and a power law response is shown. Many factors will affect where this point occurs such as the size, thickness, substrate, and shape of the actuator and adhesive used. Because the area of the sensor determines the pressure applied, i.e. for the same size actuator under the same applied load, the smaller the active area of the sensor will increase the pressure as shown in Equation 6-1.

$$P = \frac{F}{A}$$

Equation 6-1. The equation for the Pressure as a Function of Applied load (F) and Active Area of the Sensor (A). This equation assumes that the surface area of the actuator is a constant and is larger than the size of the sensor active area. A similar response can be shown for cases in which the actuator area varies and is smaller than the sensor active area. Thus (A) really indicates the area of contact, which is the area of the actuator when actuator is smaller than sensor and the area of the sensor active area when the actuator is larger than the sensor.

Thus the maximum saturation point of an FSR is between 100 and 200 psi dependent on the sensor. Forces can be exerted by spreading the applied load across a larger surface area.

In addition to the interlink sensors which are used as tactile sensors, a sense of proprioception is determined through the alteration of the r/c, radio control, servos in the arm. The potentiometer used for position sensing in the control loop of the servo is used to obtain a sensor of position of each arm for future sensing of the kinematics of the arm to determine the position of the hand and fingers in 3-dimensional space. The goal is to use this information as part of an active touching scheme in which both arm position and tactile sensing information could be integrated later in software to help determine the location of objects as well as some object properties.

A diagram of a potentiometer is shown in Figure 6-5.

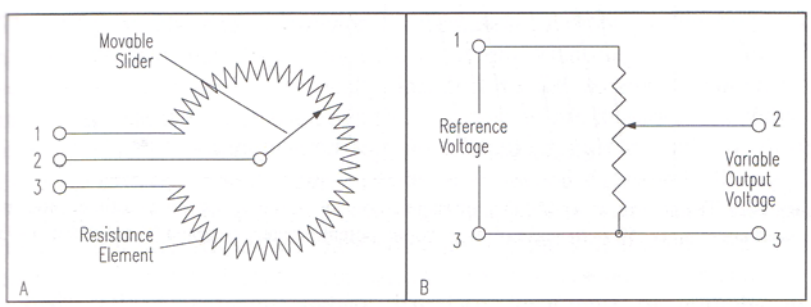

Figure 6-5. How a Potentiometer Encodes Joint Angle from (Everett 1995, pg 37). A shows the physical system in which a moveable slider makes contact with a resistance element. B shows the electrical diagram of the system.

The potentiometer, like the FSR, encodes sensory information by changing resistance. The servo horn is attached to a wiper that moves across a resistance element. As the wiper turns, the amount of output resistance increases or decreases based on the amount of the resistive element below the wiper. Thus this system allows for a low-cost, medium-accuracy joint angle sensor (Everett 1995).

6.3 The Arm Developer 64-Channel A/D Board

The "nerves" carrying information from the FSRs and potentiometers enter into what can be considered the "robotic central nervous system" at the 64-Channel Analog-to-Digital Conversion Board. A photo of the circuit board appears in Figure 6-6.

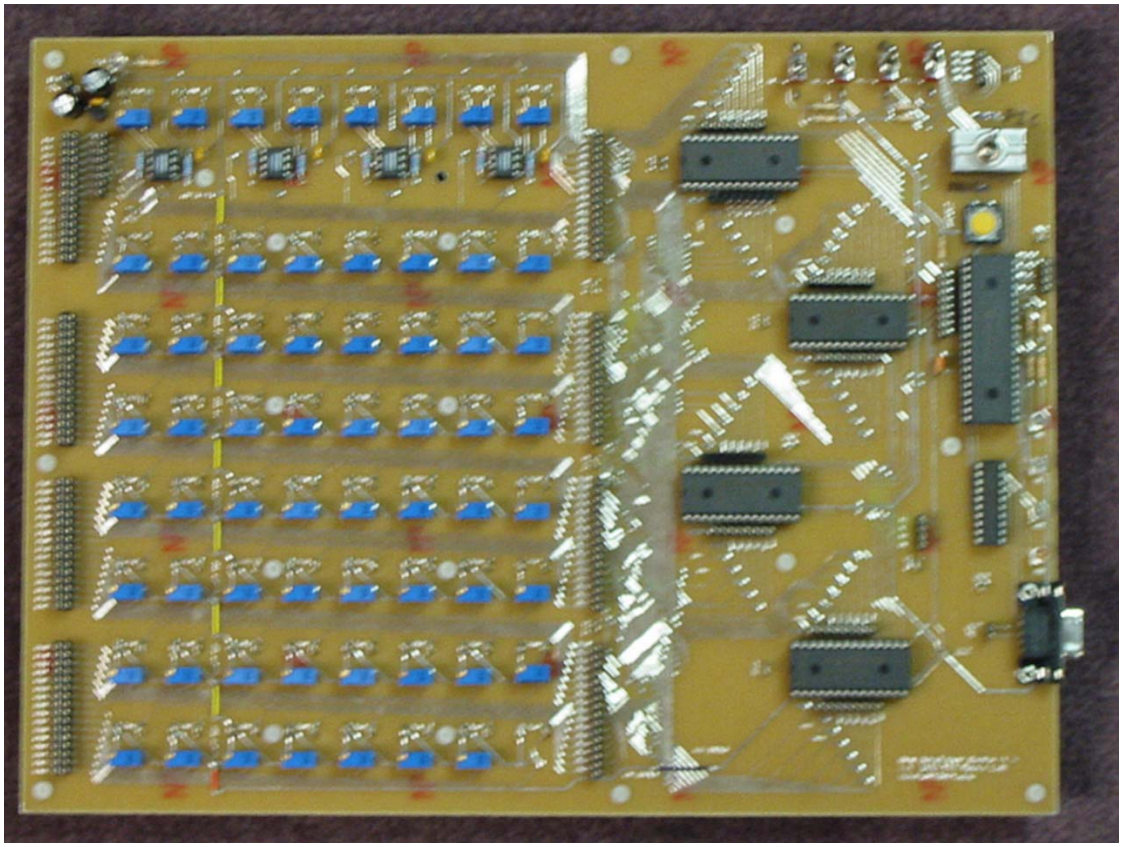

Figure 6-6. The 64-Channel A/D Board.

As mentioned previously, analogies between this circuit board and a layer of the spinal cord can be made. First, an entire section of skin is mapped to one processor. In this case, the hand and fingers correspond to one circuit board. While not exactly the same as the dermatomes described in Chapter 2, in the sense that each dermatome corresponds to a whole band of skin and not a specific body part such as the hand, there do exist similarities. One can imagine the creation of a full-body map of sensation using a series of these analog-to-digital conversion boards with each board mapping to a specific section of skin or body part.

A second similarity is that, while not currently implemented, the possibility of a reflex loop at this level exists. The PIC 16F877 processor could potentially locally process the incoming sensor signals, such as determining if an incoming stimulus was "painful" as in the flex reflex, and then communicate to the motor board to retract the limb. Thus in this design, the PIC acts as the interneuron, shown in Figure 2-18,

connecting the sensory neuron (FSR or other sensor) to the motor neuron (the ASC16 or other servo controller board).

A third similarity is that the PIC 16F877 processor also allows for the potential on the creation of relay nuclei. In the current implementation, sensor signals can be selectively turned on and off. The current design employs this to help with debugging or to allow for a limited range of active sensors. Thus there is the potential for inhibition at this level.

The flow from individual sensor through serial output is shown is Figure 6-7.

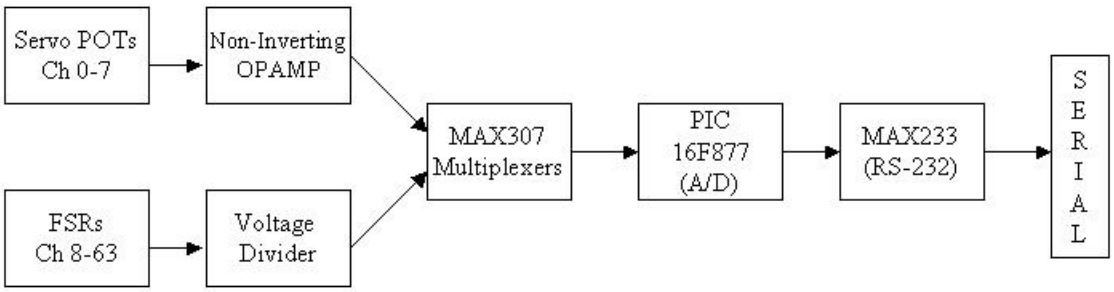

Figure 6-7. The Flow of Information through the 64-Channel A/D Board.

There are two main types of sensory input. Joint angle information (proprioception) from each servo enters the circuit through channels 0-7. The range of the output of the internal potentiometer is less than the desired 0-5V range for maximum resolution. Thus a non-inverting op-amp circuit, shown in Figure 6-8, is used to increase the range.

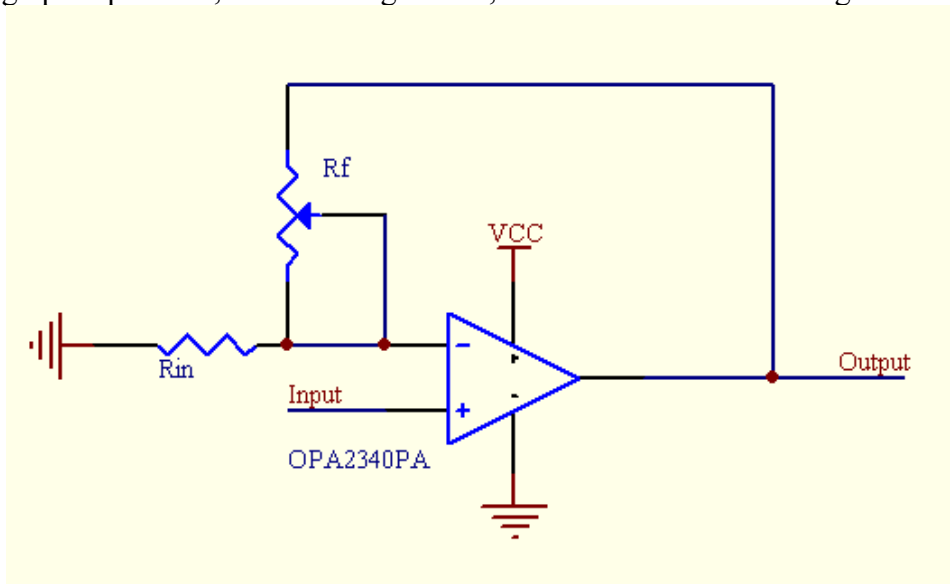

Figure 6-8. The Non-Inverting Op Amp Circuit Used to Increase the Resolution of the Potentiometer.

The OPA2340PA operation amplifier was selected because of its 0 to 5V rail-to-rail and single supply design. The output voltage can be determined using Equation 6-2:

$$V_{out} = \frac{R_{in} + R_f}{R_{in}} V_{in}$$

Equation 6-2. Equation of the Non-inverting Op Amp. V_{out} is the output voltage of the operational amplifier, V_{in} is the input voltage from the potentiometer. R_f and R_i are the resistors as shown in Figure 6-8.

The desired gain is approximately 2, which is dependent on the different potentiometers due to the use of two different types of servos in the design of the arm. Thus to allow for variability in the gain, a 50 kilo-ohm 25-turn potentiometer is used as the feedback resistor.

Tactile information from the FSRs enters the circuit through channels 8-50. A voltage divider circuit is used to convert the resistance change of the sensor into a change in voltage. This circuit is illustrated in Figure 6-9.

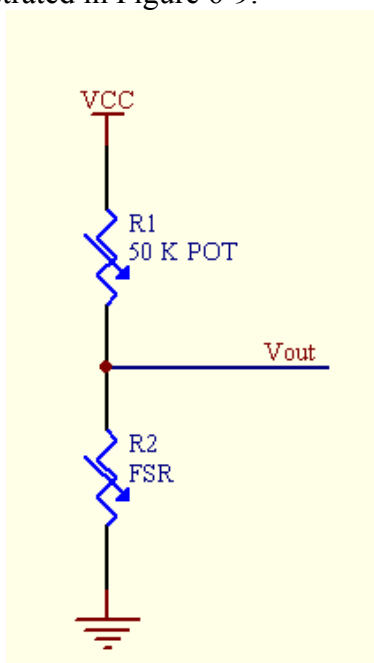

Figure 6-9. Voltage Divider Circuit Used with FSRs.

A 50 kilo-ohm 25-turn potentiometer is used to allow for adjustment of the output of the circuit as it is unknown how the various silicone skins or other factors may affect the sensor performance. The output voltage can be determined using

$$V_{out} = \frac{R_2}{R_1 + R_2} V_{in}$$

Equation 6-3. The Voltage Divider Relationship. V_{in} is the input voltage, in the case of Figure 6-9 it is V_{cc}. V_{out} is the output voltage. R_1 and R_2 are as indicated in Figure 6-9.

Channels 51 through 63 in the Arm Developer Circuit Board are currently open for further sensing capabilities. By design, the potentiometer, R_1 shown in Figure 6-9,

can be removed to allow for future sensors to have a direct pathway to the multiplexer input. Currently for some initial testing a force gauge with analog output has been attached to channel 63, and this information is processed by the PIC as well. Thus both sensor data and test equipment can be encoded by the arm developer simultaneously.

After the initial preprocessing of the sensors as shown in the previous two circuits, the 64 channels are split between 4 MAX307 dual 8-channel analog mutiplexers. This multiplexer was chosen for its single supply operation and high speed.

At the heart of the circuit board is the PIC 16F877 microcontroller. It was chosen for its familiarity as well as its 8 channels of 10-bit A/D conversion and high number of input/output pins. The microcontroller executes in two modes – setup and execution. In the first mode, the user selects which sensor channels are active, and these sensors are stored on the PIC in the form of a lookup table. The "user" can be either a person entering commands through a terminal or a computer communicating through serial. The purpose of this mode is to allow for real-time selection of sensors without having to reprogram the PIC in the cases of adding new channels of sensing or in the case of development when a small selection of sensors are focused upon.

The second mode is the execution of the analog-to-digital conversion and output of this information via serial. The process of conversion is two-fold. First, based upon the table of active sensors, the mutiplexer channel is selected. Second, the analog-to-digital conversion is then conducted also based upon the table of active sensors. After each conversion, the value is sent using a MAX233 RS-232 driver/receiver for serial communication. The baud rate used is 19200.

Many additional features are also employed to help with development and debugging. Channels 0 through 7 have a test point prior to the input of the op-amp as well as directly afterwards. Every potentiometer used with both the op-amps in channels 0 through 7 and the FSR channels features test points which can be used to determine the exact resistance. Every channel features a test point prior to and after the massive re-routing of traces shown just to the right of center in Figure 6-6. The goal of this is to allow for continuity testing to ensure that there is not a manufacturing or design error which would send a channel to the wrong multiplexer. Test points are also placed at each control line to the multiplexer as well as the input to the A/D channels of the PIC and the input and output of the serial communication channels. Finally, a series of switches, shown in the upper right hand corner of Figure 6-6, are employed. The main 4-way switch is used to place the mutilplexer under control of either the PIC or human input. When the main switch is selected for manual multiplexer channel selection, each of the four smaller switches is used to raise one of the four multiplexer selector pins high or low. The purpose of this is to allow the signal leaving the multiplexer to be isolated in the case of debugging or testing.

The PIC code can be found in Appendix A.

6.4 The Motor Control System

Active touch requires both tactile sensing as well as arm and hand movement. Thus it was important for the "pixel" arm to have motor control. Due to the wide variety

of hobby servo motion control cards that exist today it was deemed unnecessary to devote time to the design of a custom motor driver. The card chosen was the Positive Logic Engineering ASC16, 16-axis Advanced Servo Controller obtained from the Robot Store, www.robotstore.com. A picture of the circuit board is shown in Figure 6-10.

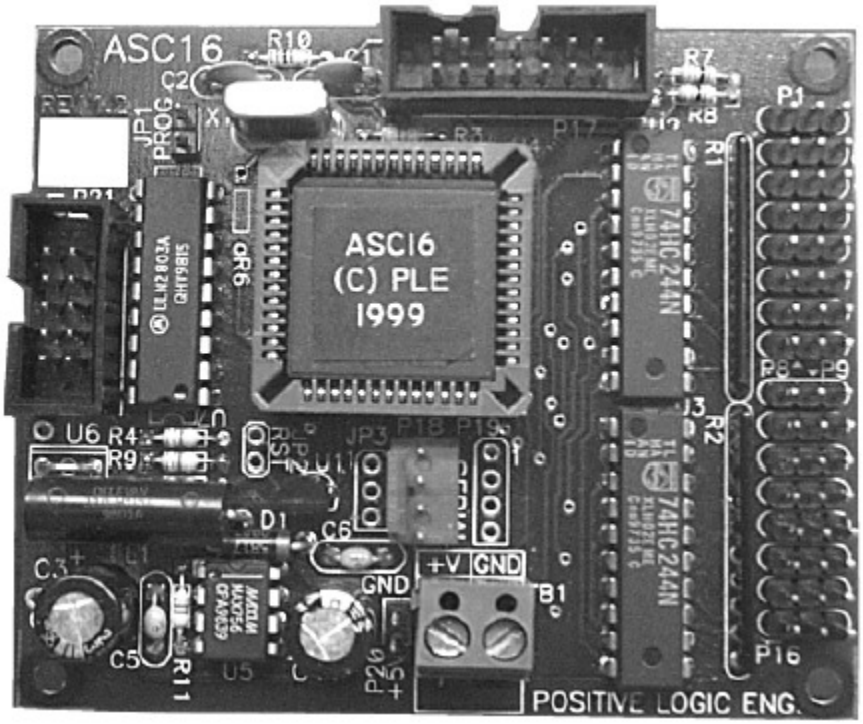

Figure 6-10. Positive Logic Engineering's ASC16 16-Axis Advanced Servo Controller (Positive Logic Engineering 1998).

This card was selected for its wide variety of useful features. It features high-resolution onboard control of position (4000 count), velocity (256 count), and acceleration (256 count). It allows for the instantaneous freezing of motion, which is useful for reflex actions, as will be explained in Chapter 8. It also allowed for starting positions to be stored in on-board memory thus ensuring that the arm always is powered up in the default position. Finally, it features a software package which allows for control of the arm through sliders which is useful in setting the range of motion for each servo.

7. Synthetic Silicone Skin

7.1 Why give a Robot Skin?

As was previously described in Chapter 2, our skin is viscoelastic. But should synthetic skins designed for robots be as well? In their article, (Karason, Srinivasan et al. 1999) answer this question with the following:

> "By definition, tactile sensing is achieved through direct contact with objects, and therefore a 'skin' is necessary to protect the sensors from physical damage. The requirements that the skin should be soft comes from the needs to have (1) regions of contact within which skin surface conforms to the object surface (instead of point or line contact that occurs between two rigid objects), and (2) significant deformation within the medium so that the sensors are activated and have enough resolution. If the substrate material on which the sensors and the skin rest is also soft, then, in addition to the above, better prehension stability can be achieved…Thus, although robotic tactile sensors themselves might differ in their operation…the overall configuration of all the designs is that of mechano-sensitive transducers embedded in a deformable medium." (Karason, Srinivasan et al. 1999, pgs 131-132)

Thus it becomes clear that a "soft skin" is necessary for tactile sensing. But these requirements are based solely on function. If one is to design either a sociable robot or an anthropomorphic robot that attempts to display the illusion of life, the "skin" has other important design constraints as well. It must be flexible and stretch around joints. It must look lifelike and organic. If the robot and human are to interact together through touch, the skin must have an organic feel as well. Thus when the external look and movement of the robot are equal to or greater than its function, a whole new set of design constraints for a "sensitive skin" must be employed.

But what material should this "skin" be made of? To answer this question one should look to the fields of prosthetics and special effects. The field of prosthetic rehabilitation, more than any other field of medicine, knows how important the exterior "skin" is to a patient who has suffered the loss of a limb, or has lost portions of his or her face to cancer or other disease. In the words of Keith F. Thomas, a maxillofacial prosthetist, "the mental trauma associated with severe facial deformity must be immense, as the face is the most important non-verbal means of communication" (Thomas 1994, pg 26). In this field, materials and techniques are used in order to create prostheses that can help patients regain some of their dignity. A few examples of some of these realistic prostheses appear in Figure 7-1.

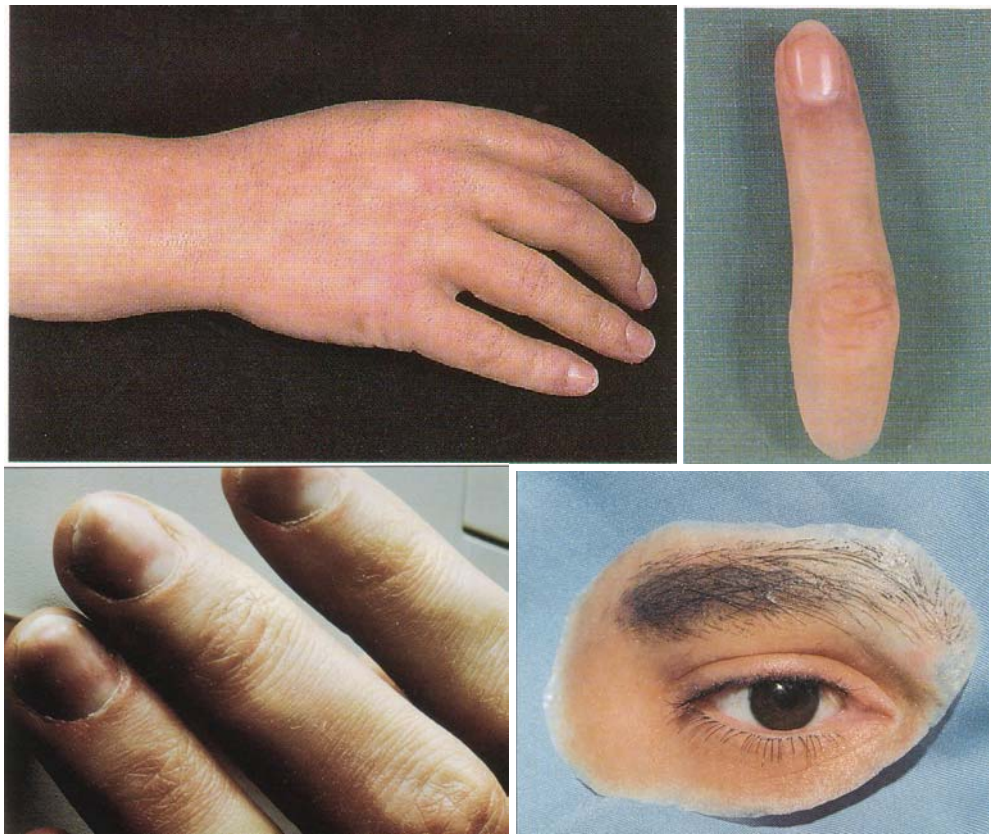

Figure 7-1. Examples of Realistic Prostheses. At top are a silicone rubber hand and fingertip from (Thomas 1994, pg 136). Lower left is a detailed close-up of silicone rubber fingers from (McKinstry 1995, pg 120). Lower right is an ocular prosthesis from (McKinstry 1995, pg 117)

As is clearly evident from these images, each possesses an amazing lifelike quality. The translucency, shown best in the feathered edges of the ocular prosthesis, is key to this quality. In addition, silicone rubber is capable of picking up very minute detail as can be shown in the close-up of the fingers in Figure 7-1. Silicone rubber is "the most popular material to use in this field due to their speed and ease of processing, and their flexibility and durability" (Heller and McKinstry 1995, pg 84).

In many ways the animatronics and special effects industries achieve the illusion of life on a daily basis. Through the puppeteering and design of their creatures, they convince the audience that dinosaurs have come back to life, or that a toy truly can feel. Again, the exterior look of the robot or puppet is intimately related to the audience's perception. It is for this industry that a whole new type of silicone – the special effects silicone has been developed. These silicones are much softer and stretchier than there medical counterparts and are also easier to work with. Even a new series of silicone gel prosthetic appliances is under development, which will allow the actor to further convince the audience that he has aged 40 or 50 years or has transformed into a new fanciful character.

Silicone has also begun to enter the world of robotics as well, but still has a long way to go before it is fully accepted into the field. It has been used as part of an animated face robot as shown in Figure 7-2 (Hara and Kobayashi 1997).

Figure 7-2. Three Different Facial Expressions of Hiroshi Kobayashi's Face Robots from (Aylett 2002, pg 111) At left is shown happiness. Center is anger. At right is sadness.

This past summer, at SIGGRAPH 2002 in San Antonio, the Robotic Life Group presented "Public Anemone," a large interactive installation of robotic theater in which the main robot, the anemone, was outfitted with a silicone skin. The addition of the silicone skin not only protected the robot from the waterfall and pond nearby but also helped to provide an increased illusion of life as can be seen from the images in Figure 7-3.

Figure 7-3. Public Anemone shown at SIGGRAPH 2002 in San Antonio Texas.

In addition to providing an exterior to robots, silicone has also been employed as part of the development of a slip sensor (Yamada, Maeno et al. 2002).

In this chapter, a general overview of silicone will first be provided. Next, the methods and formulas used to create the silicone glove and fingertips for the new "pixel" hand will be described. Finally, the discussion will conclude with a comparison of 4 different types of commercially available special effects silicones and their potential for use in robotics and tactile sensing.

7.2 Types of Silicone

There are two main types of silicone which are used in the special effects industry and have applications in the field of robotics and tactile sensing. The first type is condensation cure, also referred to as "tin cure" or simply "tin". These silicones need both air and moisture in order to cure but will set up against a wide variety of materials (McLaughlin 1999). They are room temperature vulcanizing (RTV), which means that these silicones do not require an oven to cure. Thus tin cure silicones are appropriate for use in robotics or other research as, unlike with foam latex – another popular skin material in the special effects industry, there is no need for the upfront cost of buying a large oven. Tin silicones are available as either a 2-part kit, consisting of the base and the catalyst which when combined will form the rubber, or a 1-part silicone, such as caulk, which will begin to set once it is exposed to the air. There are also two types of 1-part tin silicones. Acetoxy silicones give off acetic acid (vinegar) as they cure (McLaughlin 1999, pg 3). Oxime cure silicones, also known as neutral cure silicones, do not have the strong odor of acetoxy silicones. The most common applications for tin silicones are for mold making and robotic/animatronic skins, due to the fact they will set up against a wide variety of materials.

The second type of silicone cure type is the platinum addition cure, also known as "platinum cure" or simply "platinum." Unlike tin silicones, where there is a negligible amount of shrinkage, platinum silicones show practically no shrinkage and are capable of curing inside of a vacuum. However, these silicones are much more difficult to work with and have usually been employed for use in the field of prosthetics where the environments are very clean. Platinum silicones will not set up in the presence of amines, ammonia, tin, nitrogen oxide, carbon monoxide, sulfur and materials containing sulfur such as some modeling clays (like Roma Plastilina), natural and synthetic rubbers, latex, and foamed latex (McLaughlin 1999, pg 4). These silicones are available as RTV or HTC (High Temperature Cure). High Temperature Cure platinum silicones will not cure unless heat is applied to them, but they will cure at a much faster rate – some in a matter of minutes. All platinums are sold in 2-part kits – base and catalyst. Due to the high purity of these silicones, they are often used for medical applications and many of them have FDA approval. Some of these silicones are also optically clear. It is important to note that while tin silicones will cure in a platinum mold, a platinum silicone will not cure in a tin mold.

Silicones of either type can be colored using a wide variety of methods. Because of the translucency of silicone, it is possible to emulate the layers of skin in a three-dimensional painting fashion. For a further description of ways of coloring silicone see (Thomas 1994, ch 10; McLaughlin 1999). It is also possible to change the properties of the rubber with the addition of rapid catalysts or silicone fluid. The normal overnight cure time can be lowered to a period of minutes with the addition of rapid catalysts such as Silicone's Inc Ultrafast Catalyst or XT-177A. However, there is a trade-off between the amount of catalyst used and the physical properties of the rubber, such as tear strength. A further discussion can be found in (McLaughlin 1999).

It is also possible to lower the durometer of the rubber, i.e., increase the softness, using silicone fluids. Two common silicone fluids which can be used for plasticizing are Dow Corning's DC200 fluid and Shinetsu's DM-50. Each fluid has a viscosity of 200 and 50 centastokes respectively. The lower the viscosity, the thinner the fluid becomes. Similar to the addition of rapid catalyst, there is a trade-off by plasticizing the rubber. The softer the rubber becomes due to the addition of fluid, the lower the tear strength will be but the elongation will increase. In the considerations of how much fluid to add, it is best to first determine the application. Skins which must be driven by less powerful motors should be softer. Skins which are static and are not expected to move can be firmer. Generally, silicone rubber should never be plasticized more than 50% (McLaughlin 1999).

Those readers who are interested in learning more about silicones are highly encouraged to read *Silicone Art* (McLaughlin 1999) available from Burman Industries, www.burmanfoam.com . In this book, are discussions of ways to repair silicone as well as how to attach silicone to metal and other surfaces, which usually pose difficulty due to the reluctance of silicone to stick to anything but itself.

7.3 Molds for the Hand and Fingertips

In order to begin to experiment with how the properties of the silicone skin affect sensor performance, a silicone glove and set of fingertips were created for the new "pixel" hand as shown in Figure 7-4.

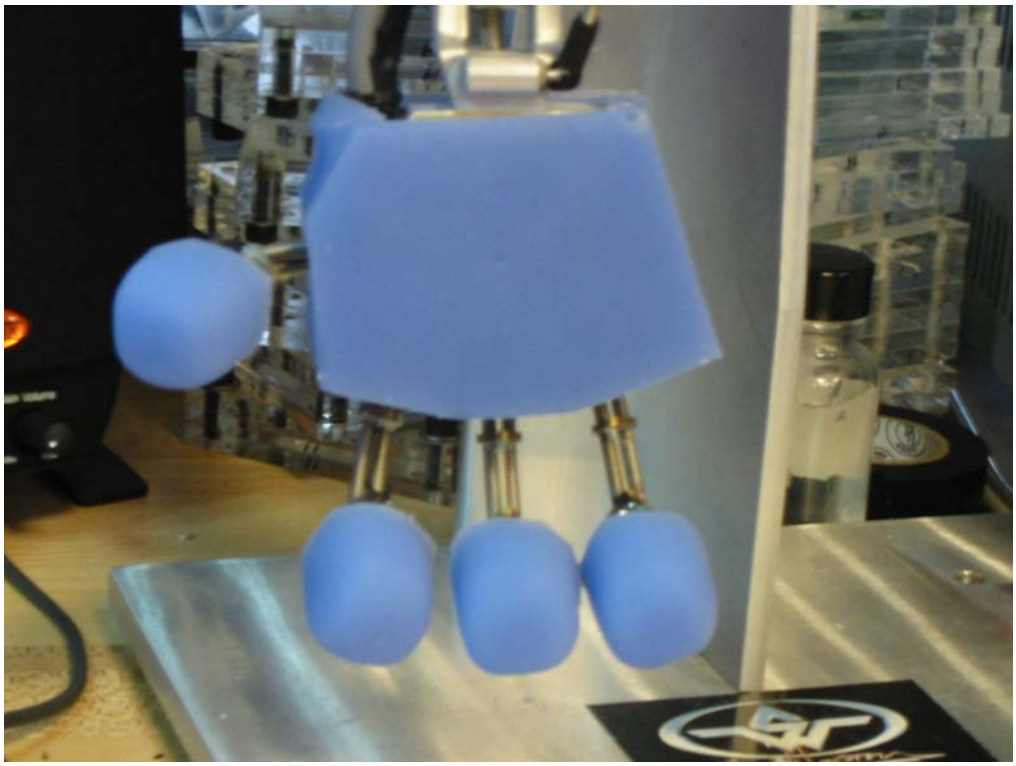

Figure 7-4. The New "Pixel" Hand with Attached Silicone Pieces. The hand is shown in a partial grip pose.

The creation of the silicone pieces can be divided into two parts – the creation of the glove, which slides over the fingers and onto the palm covering the palm, back of hand, and side sensor boards, and the fingertips – which slide over the fingers covering the 5 FSRs on each tip.

The glove mold is designed to be laser cut to reduce the time required to create the mold for the hand. The mold consisted of two pieces as shown in Figure 7-5.

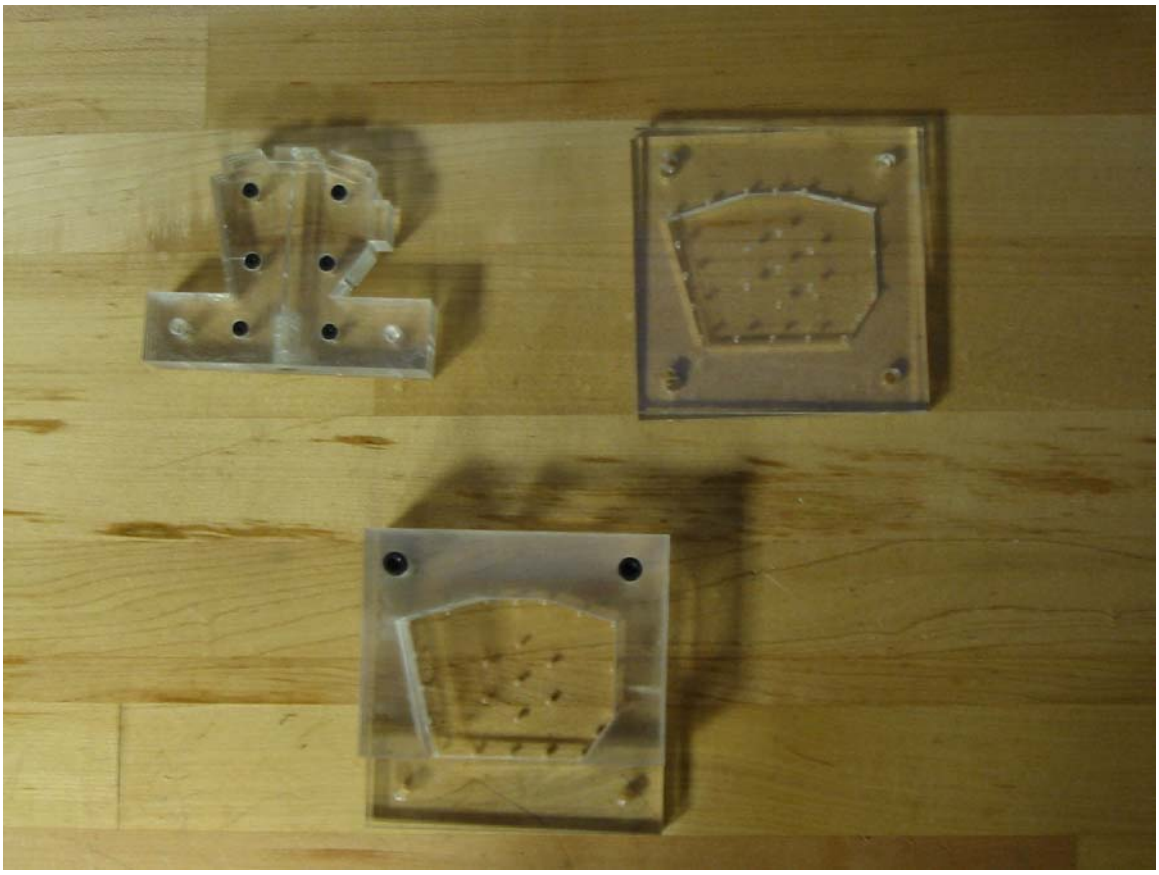

Figure 7-5. The Silicone Glove Mold. The core is shown in the upper left hand corner. The main mold is shown divided into two sections - in the upper right is the top plate, while in the bottom at center is rest of the mold.

The molds are designed to produce uniform skin thickness of ¼." Each part of the mold and core is created by layering individual pieces of laser cut acrylic to produce a 3-dimensional shape. As can be shown in the assembled mold of Figure 7-6, the core features extruded pieces corresponding to the location of each finger. These extrusions create holes in the silicone skin through which the fingers can be passed. A series of vent holes can be seen as well. These holes allow for air to escape to prevent the chance of trapping air bubbles in the skin.

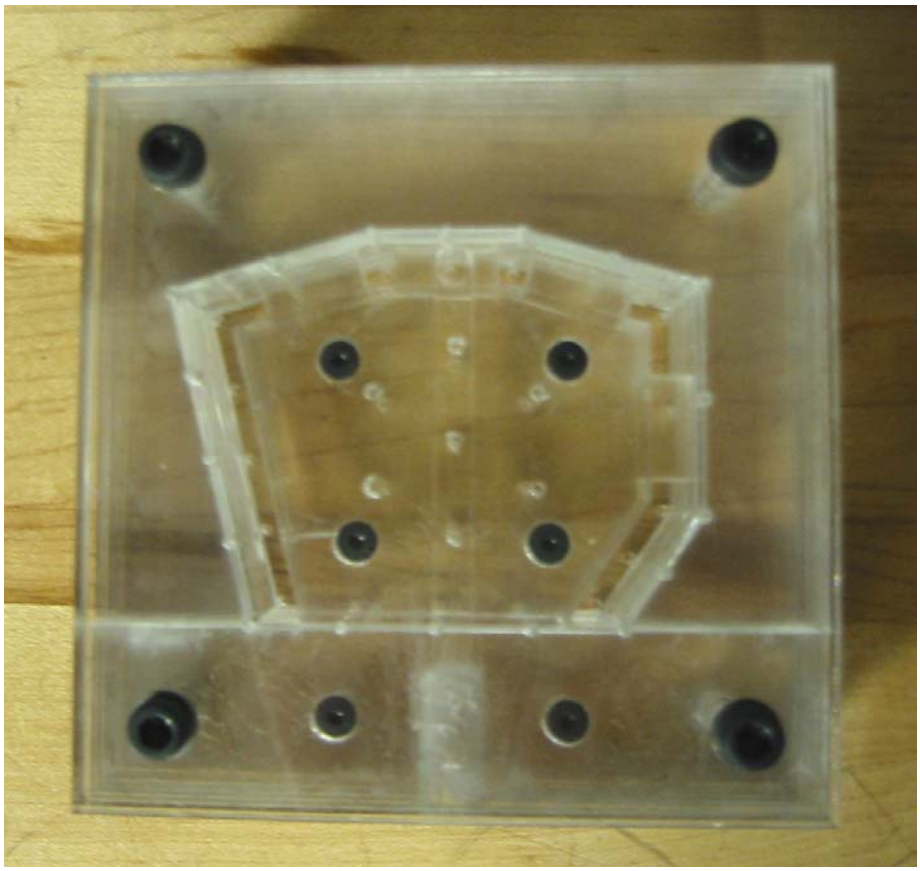

Figure 7-6. The Assembled Glove Mold.

The mold and core are first released using ME-301NS spray Vaseline available from Burman Industries. Then the entire mold is assembled as shown in Figure 7-6. This skin is cast using Walco V-1082 tin silicone consisting of a mixture of 200.0 grams base, 20.0 grams catalyst, and 40.0 grams DC200 silicone fluid. This mixture is placed in a vacuum chamber and pulled at 28 mmHg for 2 minutes. The blue color seen in Figure 7-4 is due to the addition of Factor II Intrinsic colorants. The mixture is injected into the mold and allowed to cure overnight. Kleen Klay is used to prevent silicone from leaking out of the air holes during the overnight cure.

Figure 7-7 shows the finished silicone piece, prior to trimming and cleaning.

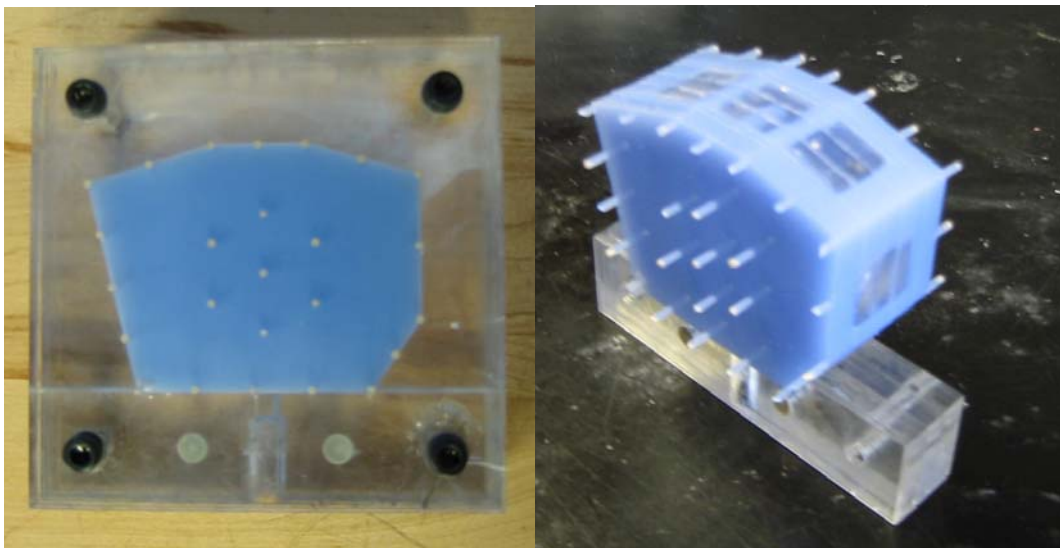

Figure 7-7. The Cured Silicone Glove. At left, the cured glove is shown still in the mold. At right, the glove has been removed from the mold and is still attached to the core. The gaps to allow the fingers to pass through are clearly visible.

Upon removal from the mold, the sprues (the small extrusions of silicone created as it flows into the vent holes and then cures) are pulled off and trimmed down so as to create a smooth surface. The silicone glove is washed with dish soap and water, dried, and then cleaned with acetone. Cabosil, fumed silica, is used both to give the hand a matte finish and to reduce the tacky feel of the skin.

Unlike the glove, which used laser cut pieces of acrylic to create the mold, the fingertips are created using more conventional mold making means. First, a mold of the actual aluminum fingertip is created using V-1065, a mold-making silicone shown in Figure 7-8.

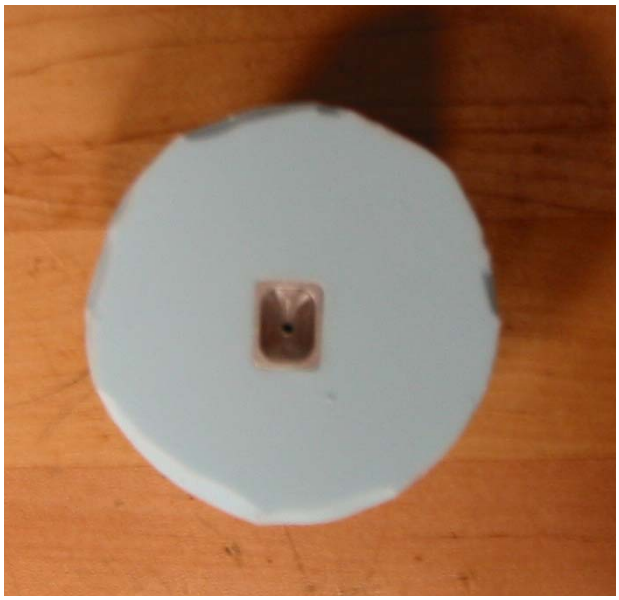

Figure 7-8. Mold of Aluminum Fingertip.

Next, the aluminum finger is removed and Smooth-Cast 300Q, a rapidly setting liquid plastic available from Smooth-On, www.smoothon.com is poured into the cavity to create a plastic copy of the exterior of the aluminum fingertip. The purpose of this is to allow for the creation of many cores which can be used to create many fingertips at once. Next, a set of keys is created on the plastic piece, and another V-1065 mold is created to mass-produce these keyed cores as shown in Figure 7-9.

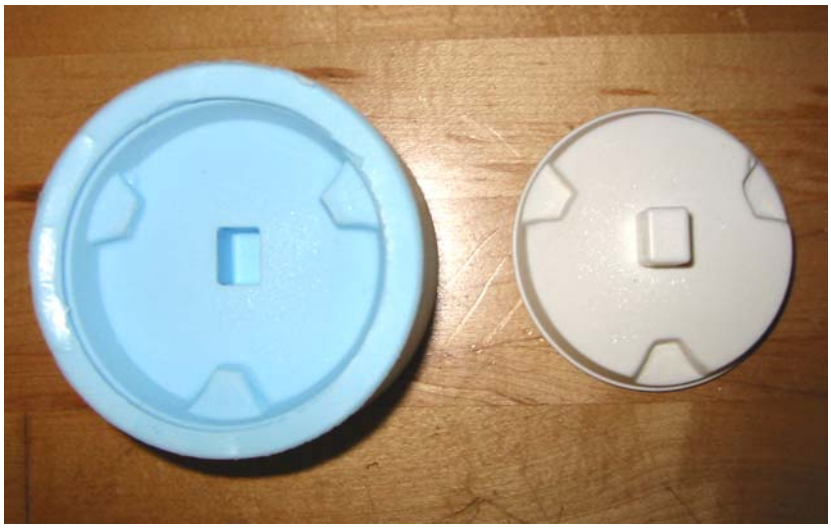

Figure 7-9. The Mold and Cast of the Fingertip Core. The mold (left) used to make the cores (right) features a series of 3 keys which will be used to register the core and the fingertip mold together.

In order to create the thickness and shape of the fingertip, ¼" thick slabs of clay are placed onto the core and then rounded to produce the shape of the fingertip shown in Figure 7-10.

Figure 7-10. The Fingertip Sculpt.

Another V-1065 mold is made of the sculpted fingertip as shown in Figure 7-11.

Figure 7-11. The Silicone Fingertip Mold.

Three additional copies of this mold are created using the method pouring Smooth-Cast 300Q into the V-1065 molds and then making a new V-1065 mold of that cast. Injection ports and vents are drilled into the cores using a 1/8" drill bit for the injection hole and a 1/16" drill for the vents. A similar formula to that which is used to make the silicone

glove is employed using V-1082. The four molds with injected silicone are shown in Figure 7-12. The silicone fingertip is shown in Figure 7-13. Upon removal from the mold, the fingertip was cleaned and trimmed in a similar fashion as previously described for the silicone glove.

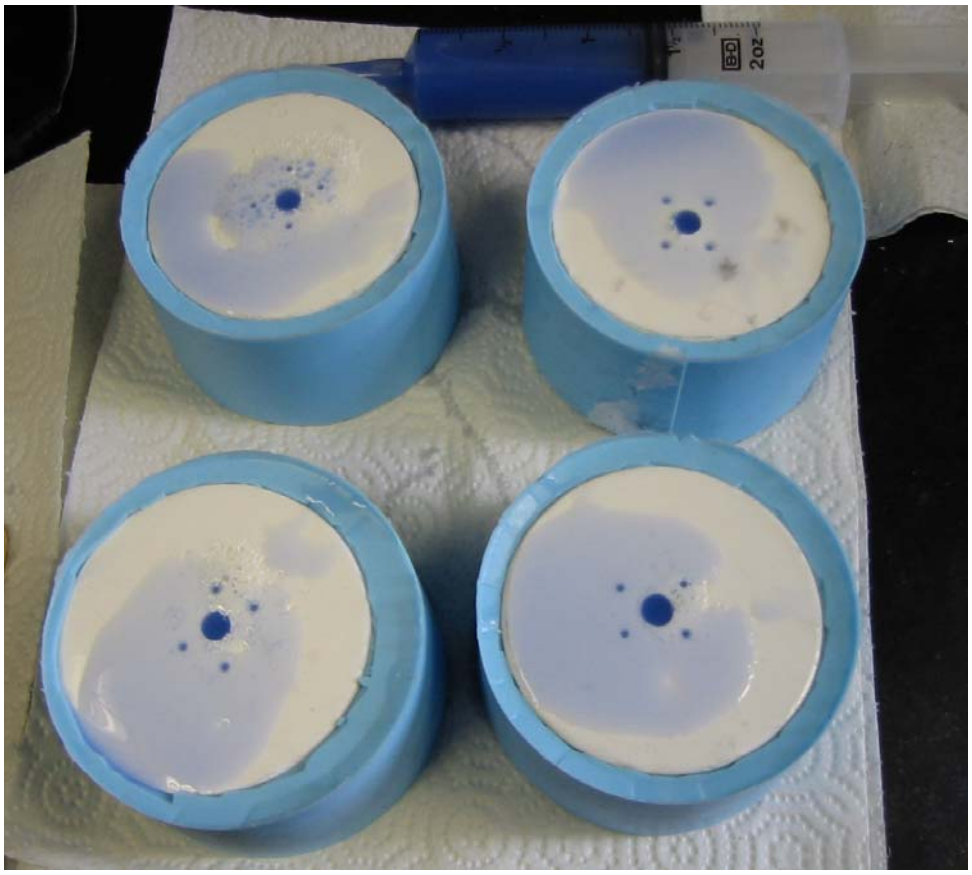

Figure 7-12. Fingertip Molds with Silicone Injected into them.

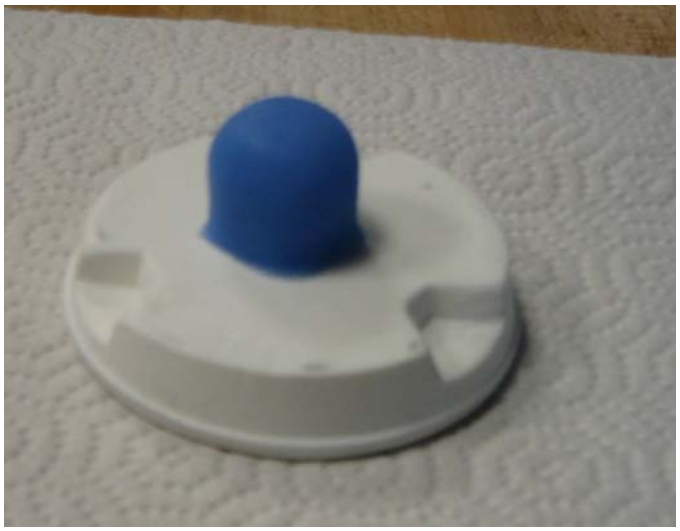

Figure 7-13. The Silicone Fingertip.

7.4 Silicone Formulas for Experimentation and Durometer Tests

The durometer, a measure of hardness, of a silicone rubber decreases as more silicone fluid is added to the mixture. In this section, an experiment will be described in which twelve samples of tin cure silicone are prepared according to the formulas described in Table 7-1. Each sample is placed under a vacuum for a period of 2 minutes under a pull of 28 mmHg. After allowing the samples to cure overnight and powdering the surface with Cabosil to remove the tackiness, they are then tested using the ASTM D 2240 standard for durometer testing (ASTM 2000). Each measurement is conducted using a Shore OO durometer gauge as shown in Figure 7-14.

Figure 7-14. The Measurement of the Durometer of the Twelve Silicone Samples.

Table 7-1. Silicone Formulas used in Experiments. Information about the working time and cure time was taken from (Burman Industries 2000) for the V-1082 and (Silicones Inc. Product Literature) for the XT-298. The use of the Hi Pro catalyst with the GI-245 base was recommended by an industry expert after consultations regarding the problems with using the GI-245 catalyst.

Sample Number	1	2	3	4	5	6	7	8	9	10	11	12
Silicone Base	Walco V-1082	Walco V-1082	Walco V-1082	Silicones Inc. XT-298	Silicones Inc. XT-298	Silicones Inc. XT-298	Silicones Inc. GI-245	Silicones Inc. GI-245	Silicones Inc. GI-245	Factor II FX-308 T	Factor II FX-308 T	Factor II FX-308 T
Mass of Silicone Base	300.0 g	300.0 g	300.0 g	300.0 g	300.0 g	300.0 g	300.0 g	300.0 g	300.0 g	300.0 g	300.0 g	300.0 g
Silicone Catalyst	Hi-Pro Clear	Hi-Pro Clear	Hi-Pro Clear	XT-298 Catalyst	XT-298 Catalyst	XT-298 Catalyst	Hi-Pro Clear	Hi-Pro Clear	Hi-Pro Clear	FX-308 T Catalyst	FX-308 T Catalyst	FX-308 T Catalyst
Mass of Silicone Catalyst	30.0 g	30.0 g	30.0 g	30.0 g	30.0 g	30.0 g	30.0 g	30.0 g	30.0 g	30.0 g	30.0 g	30.0 g
Silicone Fluid	None	DC200	DC200	None	DC200	DC200	None	DC200	DC200	None	DC200	DC200
Mass of Silicone Fluid (% of Base)	0.0 g (0%)	60.0 g (20%)	120.0 g (40%)	0.0 g (0%)	60.0 g (20%)	120.0 g (40%)	0.0 g (0%)	60.0 g (20%)	120.0 g (40%)	0.0 g (0%)	60.0 g (20%)	120.0 g (40%)
Working Time (hrs)	4	4	4	1 to 1.5	1 to 1.5	1 to 1.5	unknown	unknown	unknown	unknown	unknown	unknown
Cure Time (hrs)	16	16	16	18 to 24	18 to 24	18 to 24	overnight	overnight	overnight	overnight	overnight	overnight

The results of the test are shown in Figure 7-15.

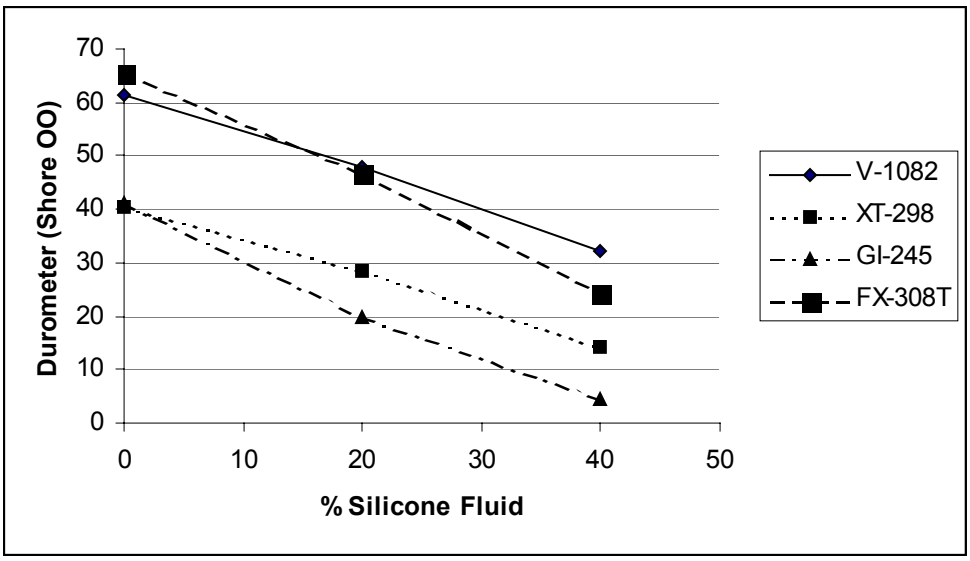

Figure 7-15. Plot of Durometer as a Function of Silicone Fluid Percentage.

These results confirm that increasing the percentage of silicone fluid does lower the durometer of the silicone rubber in a nearly linear fashion. Also softness of these silicone rubbers can be compared against human skin using the Durometer Conversion Chart shown in Table 7-2.

Table 7-2. The Durometer Conversion Chart from (Custom Seal & Rubber Products website)

Hardness Value						
Durometer Scale:	A	B	C	D	O	OO
	100	85	77	58		
	95	81	70	46		
	90	76	59	39		
	85	71	52	33		
	80	66	47	29	84	98
	75	62	42	25	79	97
	70	56	37	22	75	95
	65	51	32	19	72	95
	60	47	28	16	69	93
	55	42	24	14	65	91
	50	37	20	12	61	90
	45	32	17	10	57	88
	40	27	14	8	53	86
	35	22	12	7	48	83
	30	17	9	6	42	80
	25	12			35	76
	20	6			28	70
	15				21	62
	10				14	55
	5				8	45

From this chart a Shore OO value of 55 corresponds to a Shore A value of 10. Human skin has been measured to be softer than a Shore A of 10 (Custom Seal & Rubber Products website). Thus the majority of the silicone samples tested are as soft as, if not softer than, human skin.

For purposes of comparison, Figure 7-16 shows a graph of the varying durometers of common medical silicones used in prosthetics.

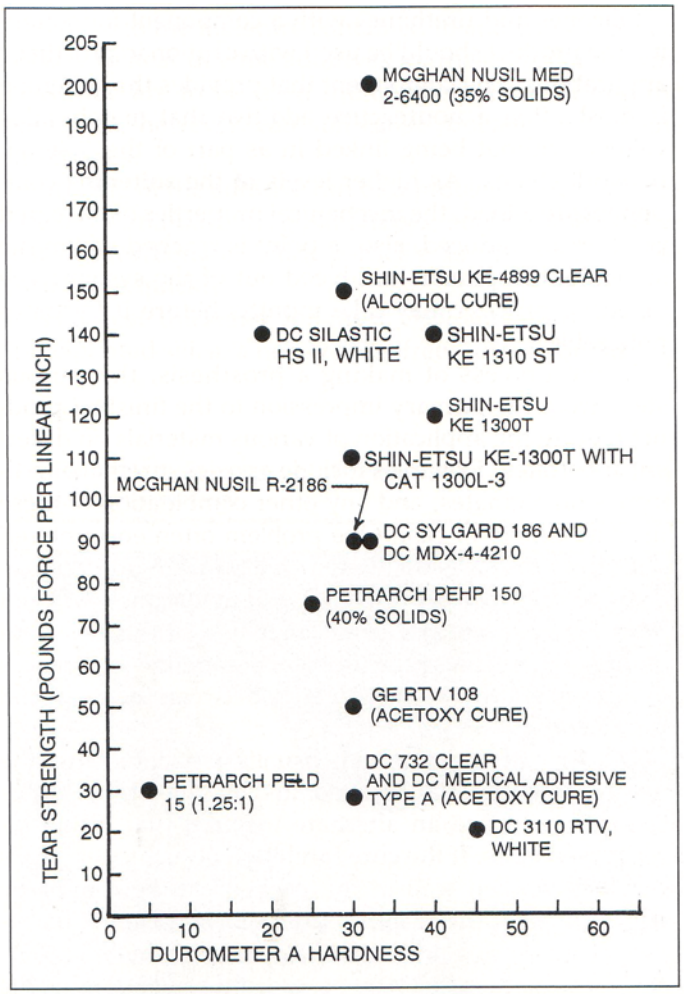

Figure 7-16. Common Medical Grade Silicones Used in Prosthetic Work from (Heller and McKinstry 1995, pg 93).

This graph, while a bit dated, does show that the silicones used in the medical industry are generally harder than those of the special effects industry. One potential explanation for this fact relies upon the fact that the majority of these applications are cosmetic and thus do not have any motion underneath the skin in the sense of motors or other actuators which is inherent in the fields of special effects, animatronics, and robotics. From a survey of a recent maxillofacial prosthetic catalog, (Factor II Inc. Product Catalog 2002), many of the Medical grade and other Platinum silicones are still in the range of 20-30 durometer Shore A.

It is also important to mention that the addition of silicone fluid allowed the silicone to be injected into the molds in a much easier fashion, especially for the very viscous GI-245 Base with a viscosity of 80,000-90,000 cps. While the catalyst does soften the material and allow it to flow, the addition of fluid helps not only to inject the material into the mold but also to lower the risk of trapping air bubbles in the skin.

Thus as can shown from this chapter, silicone has many potential applications for the robotic and sensor community. As the exterior of the robot becomes increasingly

important as a result of human robot interaction, silicone has great potential as a material for a "sensitive skin." The softness of the rubber, especially in the case of the "special effect silicones" tested in this thesis, may allow for improved sensing capabilities and an increased illusion of life.

8. Computation

8.1 Overview

In this Chapter, a theoretical framework will be provided for ways in which the "virtual somatosensory cortex" can process tactile information. While currently not implemented, some initial results do hold the potential for such a framework. This discussion will have applications for both the more global Leonardo framework as well as the new "pixel" hand test platform.

Leonardo is already a complex system spanning many computers. To allow for data transfer between regions of his distributed brain, a networking protocol has been developed by the Robotic Life Group. This protocol allows for efficient and rapid communication between the various nodes in the network. The "virtual somatosensory cortex" is one of these nodes. In the initial framework, it will primarily communicate with the behavior system (which in many ways acts as an attention system) and the motor cortex (for spinal reflex loops). The reflex loops are placed at the "cortex" level to allow for faster processing and easier communication. The speed of processing in rack mount or desktop computer is much faster than that of a PIC or other microcontroller. In addition, serial communication (microcontrollers) is much slower than UDP (networked computers). Figure 8-1 shows the theoretical framework for the computation system.

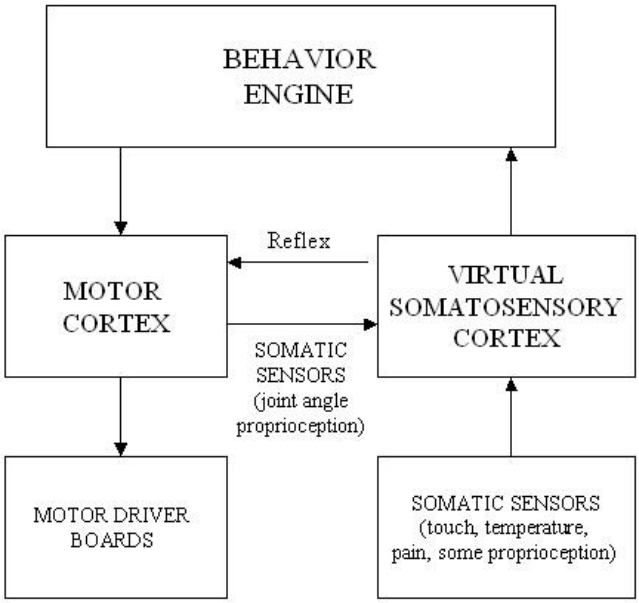

Figure 8-1. The Theoretical Location of the "Virtual Somatosensory Cortex" in Leonardo.

In the current implementation, the "virtual somatosensory cortex" is combined with a "simple motor cortex" as shown in Figure 8-2.

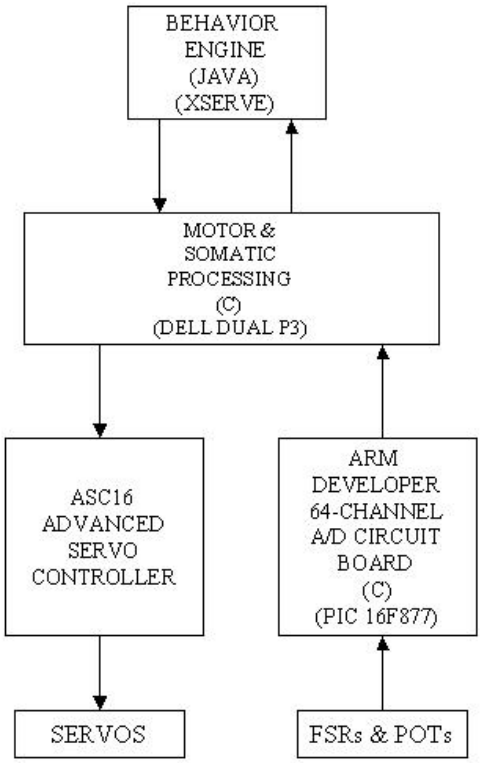

Figure 8-2. Computational Framework of the "Pixel" Arm/Hand.

In the motor output loop, the behavior system sends motor position information via UDP to the "simple motor cortex" which then sends these positions to the ASC16 motor controller card via serial. In the somatic input loop, the "virtual somatosensory cortex" receives information from the Arm Developer A/D circuit board via serial. It then processes this information and both modulates the response of the motion of the arm based on this tactile information and sends this information to the behavior system via UDP.

Already, a reflex loop has been implemented. Initially, the arm performs a pre-scripted animation. However, this animation can be interrupted if the tactile sensors detect the presence of an object, i.e., any sensor rises above a threshold. Immediately the "simple motor cortex" stops the motion of the arm and sends a command to the behavior system that an object is detected and all motion has stopped. The behavior system then sends a command to the "simple motor cortex" that it is safe to begin movement again and plays the animation in reverse, pulling away from the object. Currently, only one direction, i.e. the down movement, shows this reflex loop. However, because both the location of the tactile stimulus and the arm position is known, it will be possible to respond to a wide variety of stimuli presented in any location and pull away accordingly.

8.2 Framework Designed for Expansion

At the center of this effort is the goal of giving Leonardo a fully "sensitive skin," which implies the potential for hundreds of sensors and a large networked processing

system within the body of Leonardo to gather all this sensory data in an efficient fashion. As implemented already, the Arm Developer A/D board allows for up to 64 channels of analog sensory data to be processed in a timely fashion. While the current geometry of the board is much too large, it does provide some key features necessary for expansion.

First, each board is given a unique identifier based on the zone of the body that it receives information from – similar to the dermatome map discussed in Chapter 2. Thus the first pass in processing will be to look at each region, i.e. board, and assess which regions are active. For example, when someone touches Leonardo on his arm, it's extremely important that that location of tactile input be processed quickly and efficiently to prevent damage to Leonardo and to allow other systems, such as vision, the information so they can attend to that location. In many ways, Leonardo will have an internal representation of his skin surface.

Closely linked to the identification of sensor boards is also the identification of receptive fields. As discussed in Chapter 2, populations of single afferents combine to form a larger receptive field. Thus following this framework a hierarchical structure as shown in Figure 8-3 emerges.

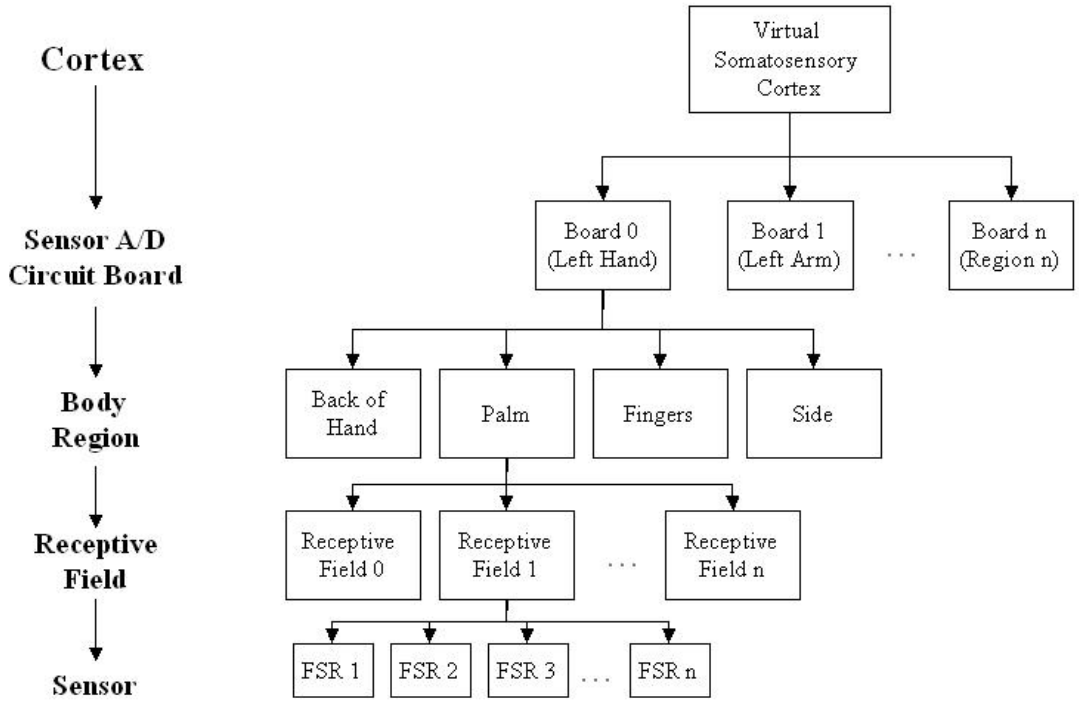

Figure 8-3. Hierarchical Organization from Sensor level to Cortex.

This structure allows for varying levels of processing dependent upon the application. For example, filters can be placed between levels to monitor activity directly below each level. Thus activity at the lowest sensor level, such as FSR 1, will be detected by this filter thus making the receptive field 1 active, etc. Such a filter will also help to conserve processing time in the creation of cortical-neuron-like receptive fields, which will be later discussed in this chapter. In addition, as mentioned previously different systems in the "brain" of Leonardo will need to have access to this information at varying levels depend on their function. Thus, in the previous example of Leonardo looking at the location

where he was touched, the vision system only needs access to the sensor board level of somatic information. However, in the sense of reflexes where a motor must drive the limb in the opposite direction to the location of contact, the body region or receptive field level may be required.

The Arm Developer A/D board also allows for sensors to be ignored in real time, without having to re-program the microprocessor. This is useful for both development and debugging, when a specific sensor or population of sensors is desired. Such on-the-fly selection is also important in the case of damaged sensor so as prohibit false triggering from that sensor.

8.3 Peripheral Coding

As was discussed in Chapter 2, what we perceive about our world through touch is encoded by our somatic sensors. Thus there is not simply one sensor, but rather a variety, with each sensor preferring to encode specific types of stimuli. One of the main divisions of the four mechanoreceptors is based upon how quickly they adapt to changes in stimuli, either rapidly adapting or slowly adapting. Figure 8-4 shows the response of a single FSR to finger taps applied to the silicone skin directly above it.

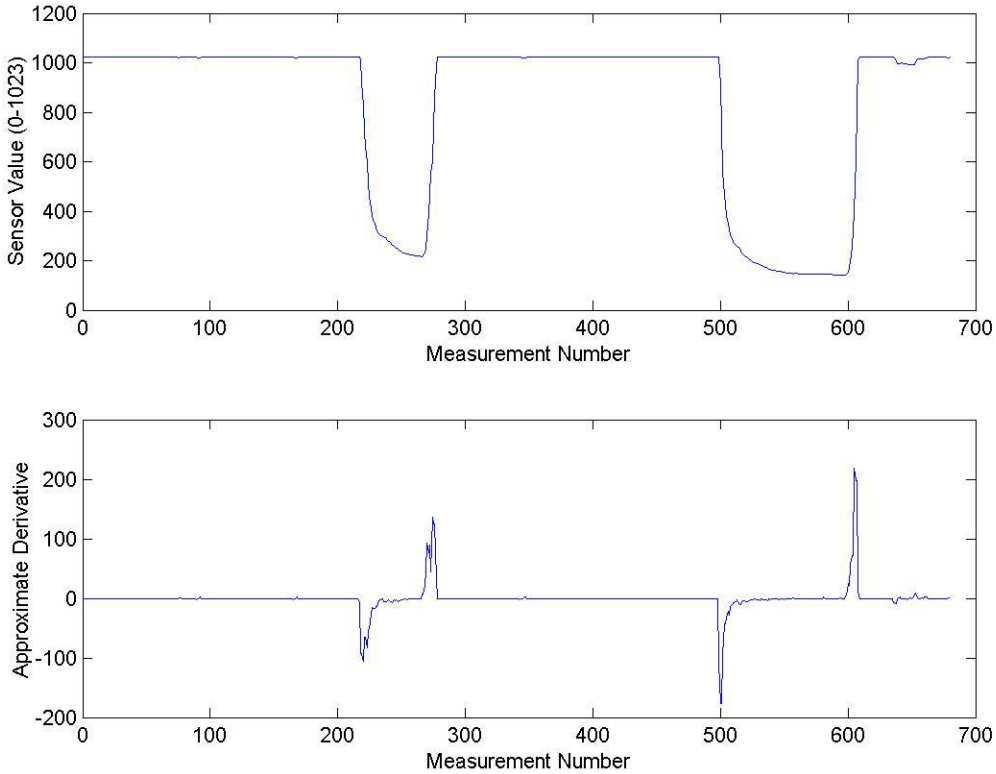

Figure 8-4. The Response of a Single FSR to Finger Taps. At top is the FSR 10-bit sensor value as converted from the analog signal. Below is the approximate derivative of this stimulus as calculated using the diff function in MATLAB.

As can be shown from this figure, the sensor shows the logarithmic response of Figure 6-4. Values decrease with increasing pressure due to the voltage divider relationship shown in Figure 6-9. The sensor functions in a similar manner to a slowly adapting mechanoreceptor, encoding pressure sensed in the skin above. By taking the derivative, as shown in the lower plot, a rapidly adapting profile emerges. The sign of the derivative implies the direction of motion, either increasing or decreasing indentation. Thus one sensor signal can represent two different types of sensory information.

The other division in which mechanoreceptors in glaborous skin are classified is based on the size of their receptive field. While not studied quantitatively in this thesis, the receptive field does appear to expand beyond the center of the sensor. Finger taps were applied to the area of skin around the sensor and the response was observed on an oscilloscope. The FSR showed an increased response as the finger taps were applied closer to its center. However, further testing and quantification of this process will be necessary as the skin chosen will most likely effect the area of the receptive field.

8.4 Higher Cortical Processing

As discussed in Chapter 2, cortical neurons are formed from populations of lower level neurons. Thus the "virtual somatosensory cortex" should employ a similar method by creating receptive fields from populations of sensors of a similar body region, as shown in Figure 8-3. In this section, the theoretical framework for how such sensors could be combined will be described.

For purposes of illustration, an initial test was conducted using a delrin rectangular bar as the stimulus. A palm circuit board, shown in Figure 5-12, was placed on standoffs and covered with a 0236" layer of silicone skin. The formula for this skin is that of sample 2 shown in Table 7-1. The bar was applied by hand and no recordings of force or actual orientation of the bar were made. This test was simply to observe the performance of the sensors and determine if the formation of cortical neurons, as described in this section, could be possible.

Figure 8-5 shows a result from this initial test.

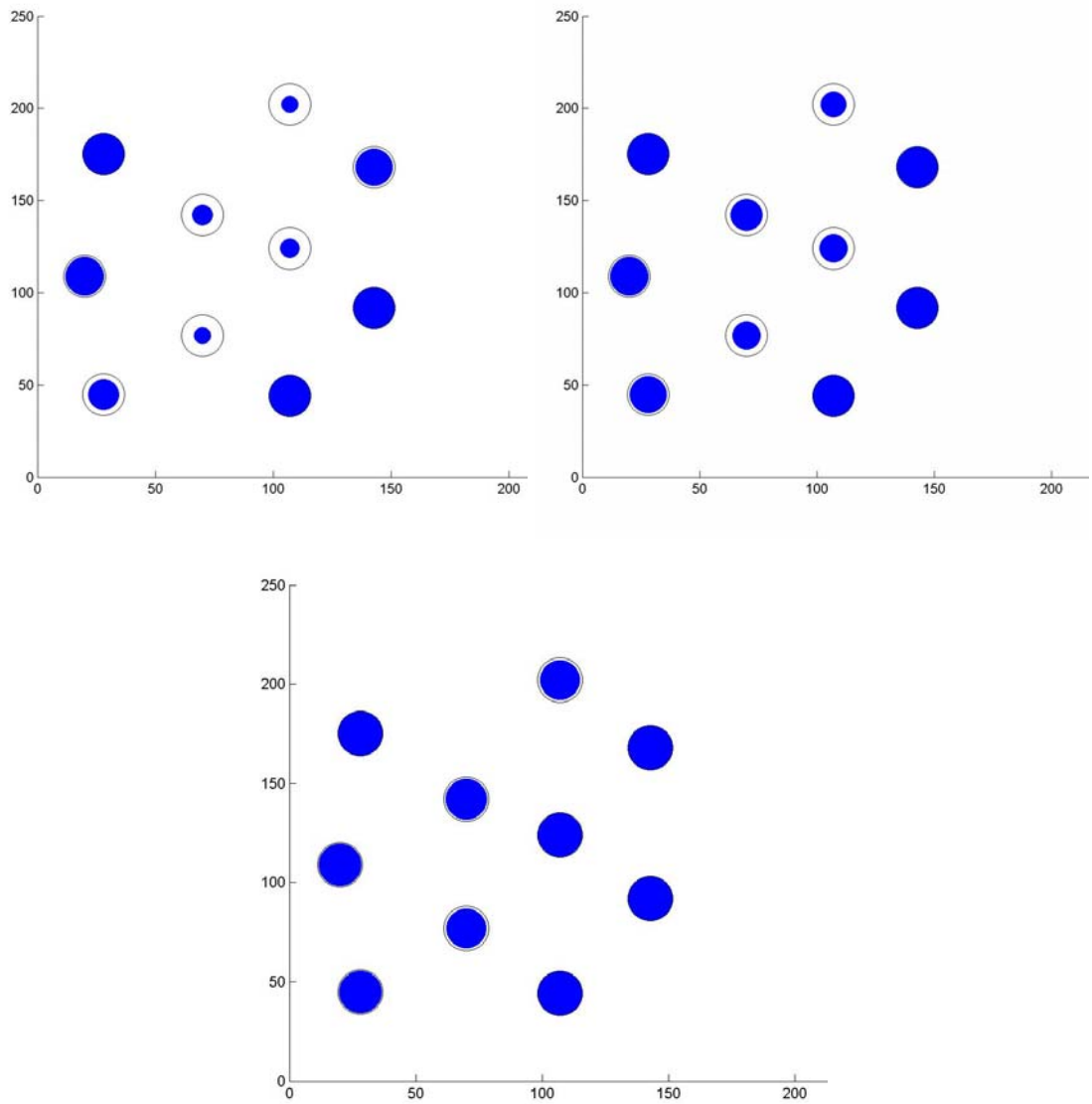

Figure 8-5. An Initial Evaluation of the Possibility of the Formation of Cortical Neurons from Individual Sensors. Each dot is centered at the location of the FSR sensor determined from the circuit board layout in Figure 5-9. The hollow black circles correspond to the size of the sensor. The area of each solid blue dot corresponds to the 10-bit sensor value (0-1023) shown in Figure 8-4. Smaller dots indicate the sensing of higher pressure. The series of images progresses from upper left to upper right to bottom.

As can be shown in the above figure, there does exist the potential for cortical processing of a population of sensors. The cluster of sensors in the center of the figure at the upper left show a similar response, thus implying a uniform pressure. As the stimulus is removed, shown in the progression from the upper left to lower image, these sensors show a similar decrease in their responses to the removal of the stimulus. These

responses are indicative of what should occur in a uniform pressure field. The flat surface of the delrin bar helped to uniformly distribute the applied force across its surface area. Even with the roughness of this initial experiment, the framework for levels of processing exists.

The lowest level is first determining where the centroid of a stimulus is located. As shown in Figure 5-8 through Figure 5-10, each FSR is located at a specific (x, y) location relative to each circuit board. The position of each circuit board on the arm is also known and the location of the hand, or any other part of the arm, can be calculated since the angle of each servo is known due to the internal potentiometer input to the Arm Developer A/D circuit board. Each sensor conveys three coordinates of information: x-location, y-location, and pressure. An initial understanding of the receptive field of the sensor is determined by tapping with a finger over the area of a silicone-covered sensor and watching the response on an oscilloscope. The maximum response is seen for taps applied directly over the sensor and this response trails off as the taps moved away from the center of the sensor. Thus a maximum pressure value is obtained when the stimulus is directly over the sensor. The centroid of the stimulus can then be determined by calculating a weighted average of the active sensors using pressure to weight each sensor. By observing the response in

Figure 8-5, one can see where the bar was pressed into the skin.

In a similar fashion, the orientation of a stimulus can be determined from a population of FSRs. The pressure profile can be broken into x and y coordinates and the angle of orientation can be calculated. The orientation of the bar in

Figure 8-5 is clear to the observer based on the observation of the pressure profile.

Once the orientation and location of the centroid are determined, motion can also be calculated. Motion can potentially be first encoded by observing the responses of the rapidly adapting sensor values, calculated using the methods discussed in the previous section. The sign of the rapidly adapting sensor value will imply direction since the SA sensor decreases as a stimulus is removed and increases as a stimulus is applied. Thus a positive RA value implies movement into the receptive field. In addition, the position of the centroid can be used as well to determine motion across the skin in any direction. If each location of the centroid is recorded in time, each position can be compared to the previous positions to determine movement as well as direction.

In addition, softness may potentially be encoded as well. As force is applied through the material presented, this material may deform. Thus a soft material, such as a sponge, will use some of the force to "squish" and as such the FSRs will register a lower response change in pressure over time than they would register for a hard object. Thus it may be possible to use this information for a comparison of hardness. Additionally, having position information from the potentiometers in the arm will allow for this change in pressure, due to the hardness or softness of the material, to be based on arm position. Thus a soft material will show a lower ramp up in pressure compared to that of a hard material at the same joint positions, provided the objects are of the same size.

9. Conclusions and Future Work

9.1 Conclusions

This thesis provides an overview of initial work towards the ultimate goal of creating a fully "sensitive skin" as first described in (Lumelsky, Shur et al. 2001) for the Leonardo robot introduced in Chapter 4. While much work still needs to be done, the creation of the new "pixel" hand which was the focus of much of this thesis will provide an adequate test bed with which to explore the theoretical framework of giving robots a "sense of touch." It was also deemed that silicone rubbers, specifically those used in the special effects industry, are applicable as a synthetic skin material due to their low durometer, high elasticity, and translucency.

9.2 Future Work

Ultimately, the additional weight of the silicone skin coupled with the increase in size of the new "pixel" hand limited the movement and performance of the "pixel" arm. In addition, both backlash in the servo gearboxes as well as in the mechanism, specifically at the shoulder joint, prohibits much real integration of motion and tactile sensing. This is not a fault of the original design, as it was never meant to be used under any types of load. The "pixel" arm, as described in Chapter 4, was originally designed to show the range of motion being designed into Leonardo's arm. The next step will be to approach the design of a new arm which uses much more powerful actuators with less backlash.

The springs which comprise the fingers ultimately proved much too compliant to be useful for tactile sensing. Much of the load applied to the fingertips actually deflects the fingers rather than compressing the silicone. Thus, the design of more rigid fingers, which constrain motion to one degree of freedom will be explored. In addition to the stiffening of the fingers, the fingers will also be decoupled from one another. This will allow for the exploration of a wider range of haptic exploration methods.

While some initial experimental results were found using silicone, as discussed in Chapter 7, it would be interesting to explore the potential of silicone gels and thermo elastomeric polymers as other synthetic skin materials. These materials are getting much attention in the special effects industry today, especially thermo elastomeric polymers recently mentioned in an article in *Makeup Artist Magazine*(Hedgecock and Wallace 2003). These polymers are softer than the silicones described in Chapter 7 and feature elongations of up to 2800%.

Even with the careful design employed to cleanly route the wires from the FSRs as described in Chapter 5, the number of wires required which much enter into the hand, or other body regions, clearly poses a problem with scalability. Thus in future iterations, the goal will be to retain the functionality of the Arm Developer A/D Board but to reduce its size. Some potential approaches are to place either the multiplexers, microprocessors, or both onto the three sensor boards of the hand – palm, back of hand, and side - as well as other body regions.

Closely coupled to this reduction of wires is the need for the creation of a sensory network. If each region of the body has its own sensing board as described in Chapter 8, then methods to efficiently process information from this large network must be explored. The hope is to leverage some of the work of the Pushpin platform (Lifton, Seetharam et al. 2002) developed in the Responsive Environments Group of the MIT Media Lab to approach this problem.

Even though the new "pixel" hand is similar to the hand of Leonardo, the geometry and sensor placement will be different in the sensor boards of the palm, the back of hand, and the side of the hand. Thus an entire new hand must be designed for integration in Leonardo. An additional complication is that the exterior dimensions of the new hand for Leonardo are fixed due to the fact that the foam latex hands are created to fit the current hand. Any changes in thickness or dimension would necessitate new molds to be created and new hands to be fabricated, a very costly change.

A further understanding of the sensor performance and its relationship to the skin above it must be obtained. To this end, a series of experiments should be conducted to quantify this relationship. Thickness of the skin is one variable which should be studied. Samples of silicone cast using the same formula, but with a different thickness, do not feel the same even though they have the same durometer. Softer samples allow for a greater indentation at increased thickness. Any differences between sensor responses based on the thickness of the skin need to be employed in the design of a silicone skin.

The receptive field of the sensor may also be a function of the silicone skin used above it. The viscoelastic nature of the rubber means that the material retains the same volume during an indentation. The forces generated during indentation in the skin may transmit to the sensor differently based on thickness or durometer. Thus it may be possible that forces which are not applied directly above the sensor may still be detected.

The response of the sensor to indenters of varying curvature should also be studied as a function of skin material and thickness. One would expect to see similar results, that increasing curvature, i.e., smaller radius, would result in an increased response as was found in human skin as shown in Figure 2-10. Thus it may be possible to use this information as another letter in the "somatic alphabet" for object detection.

Finally, it will be important to obtain a greater understanding of the force vs. resistance profile of the FSRs under different skin thicknesses and durometer. Hysteresis and drift have been shown to occur in piezoresistive sensors such as the Interlink FSRs used in this design (Kirtley). Thus it will be important to quantify how different the sensing of the application of a force is from the removal. If the two regimes are different but consistent within the same direction, the rapidly adapting response, described in Chapter 2 and 8, may be used to determine if the force is being applied or removed. A quantification of drift is important to prevent sensors from false triggering by determining how often a baseline should be taken.

As discussed in Chapter 2, our perception of the world around us is created from a wide variety of somatic sensors. These different types of receptors as well as the different ways in which information is processed form a "somatic alphabet." In the current implementation only a small portion of this alphabet is explored, and thus the language of touch in this application is currently limited. Future designs will include a wide variety of sensors throughout the "sensitive skin," each encoding a different

modality. Thus the "somatic alphabet" can be expanded and the language of touch will be much more vivid.

In Chapter 8, a theoretical framework for the creation of cortical neurons, capable of higher level processing, is presented. This framework will be tested through the presentation of a wide variety of stimuli from human touch, to objects of varying shapes, sizes, and material.

9.3 Potential Uses of "Sensitive Skin" Beyond Robotics

The ideas and implementations presented in this thesis are only a small fraction of the potential uses for such a "sensitive skin." Applications from robotics research extend to the fields of special effects, prosthetics, and even commercial products and toys.

In the special effects industry, the organic movements of an animatronic character are due to the coordinated movements of an entire team of puppeteers. This team is usually located far away from the creature they are controlling; yet they must control its eye movements to maintain eye line and display reactions to the human actors. A sense of touch can be beneficial in this case. There are at least two methods in which a sense of touch can be used in an animatronic. In the first method, sensors under the skin of the animatronic could be used to give a visual indicator to the puppeteers of the location on the skin the actor touched. In this method, touch would simply be used as part of a display system which the puppeteers would monitor, and adjust their performance to. A more complicated method would be one in which a level of computation and control would be added. Thus the animatronic would have a layer which is no longer under the sole control of the puppeteers. Thus when the character is touched, it could automatically look to the location on its body where it was touched or execute another response.

Much work has been completed on the control of the motion of prosthetic or robotic arms either through myoelectric activity in humans (Motion Control Inc. website; Abulhaj and Hogan 1990) or through cortical activity in owl monkeys and rats (Chapin, Moxon et al. 1999; Fetz 1999; Wessberg, Stambaugh et al. 2000). Thus an output loop from the brain to a prosthetic device may be possible. However, very little work has been done on the reverse pathway, i.e., going from the prosthetic limb back to the brain. Today, visual information, such as the way in which an object deforms as it is grasped, is the only way a person with a prosthetic limb has for feedback over the control of his or her device (Birchard 1999). One approach of conveying feedback has been to present electrotactilly the output of a specially sensed glove to another location in the body, such as the forehead (Collins and Madey 1974). Another approach is to actually implant touch sensors into the skin of insensate hands (Sabelman, Kovacs et al. 1994). Any work done in the field of touch for robotics, especially one which is based on the human sense of touch described in Chapter 2, may have applications for the creation of a "sensitive" prosthesis.

Finally, a sense of touch can also be applied to the fields of commercial products and toys. A chair can be fabricated with a series of distributed tactile or other somatic sensors to detect the position of the user who is sitting in it. The chair could then use this information to change the position of its frame to better support the user. Toys could

employ a simpler method of a “sensitive skin” through the use of low-cost push button switches located throughout the body of the doll. This information could then be used to increase the illusion of life in the toy.

Clearly, the initial realm of robotics is not the only application for a “sensitive skin” based on the principles described in this thesis.

References

Abulhaj, C. J. and N. Hogan (1990). "Functional assessment of control-systems for cybernetic elbow prostheses, part 1: Description of the technique." IEEE Transactions On Biomedical Engineering **37**: 1025-1036.

ASTM (2000). "D 2240: Standard Test Method for Rubber Property - Durometer Hardness."

Aylett, R. (2002). Robots: Bringing Intelligent Machines to Life? Hauppauge, NY, Barron's Educational Series, Inc.

Banks, J. (unknown year). Design and Control of an Anthropomorphic Robotic Finger with Multi-Point Tactile Sensation. Cambridge, MA, MIT Artificial Intelligence Laboratory**:** 309-310.

Birchard, K. (1999). The science of haptics gets in touch with prosthetics. Lancet. **354:** 52-56.

Breazeal, C. L. (2002). Designing Sociable Robots. Cambridge, MA, MIT Press.

Burman Industries (2000). Product Catalog.

Chapin, J. R., K. A. Moxon, et al. (1999). "Real-time control of a robot arm using simultaneously recorded neurons in the motor cortex." Nature Neuroscience **2**(7): 664-670.

Cholewiak, R. W. and A. A. Collins (1991). Sensory and Physiological Bases of Touch. The Psychology of Touch. M. A. Heller and W. Schiff. Hillsdale, NJ, Lawrence Erlbaum Associates, Inc.**:** 23-60.

Clark, F. J. and K. W. Horch (1986). Kinesthesia. 1986. K. R. Boff, L. Kaufman and J. P. Thomas. New York, Wiley & Sons. **1:** 1-62.

Cole, J. D. (1995). Pride and a Daily Marathon, 1st Edition. Cambridge, Massachusetts, MIT Press.

Collins, C. C. and J. M. J. Madey (1974). "Tactile sensory replacement." Proceedings of the San Diego Biomedical Symposium: 15-26.

Connor, C. E., S. S. Hsiao, et al. (1990). "Tactile Roughness: neural codes that account for psychophysical magnitude estimates." Journal of Neuroscience **10**: 3823-3836.

Connor, C. E. and K. O. Johnson (1992). "Neural coding of tactile texture: comparisons of spatial and temporal mechanisms for roughness perception." Journal of Neuroscience **12**: 3414-3426.

Craig, J. C. and G. B. Rollman (1999). "Somesthesis." Annual Review Psychology **50**: 305-31.

Crowder, R. M. (1998). Tactile Sensors, R.M. Crowder. **2003**.

Custom Seal & Rubber Products website http://www.customsealandrubber.com/charts.html.

Dayan, P. and L. F. Abbott (2001). Theoretical Neuroscience: Computational and Mathematical Modeling of Neural Systems. Cambridge, Massachusetts, MIT Press.

DeRossi, D., F. Carpi, et al. (2002). Electroactive Fabrics for Distributed, Conformable and Interactive Systems. Sensors 2002, Orlando, Florida, IEEE.

Everett, H. R. (1995). Sensors for Mobile Robots: Theory and Application. Wellesley, MA, A.K. Peters.

Factor II Inc. Product Catalog (2002).

Ferrier, N. J., C. Lozano, et al. (2002). A Tactile Sensory-Enhanced Assistive Robot. Sensors 2002, Orlando, Florida, IEEE.

Fetz, E. E. (1999). "Real-time control of a robotic arm by neuronal ensembles." Nature Neuroscience **2**(7): 583-584.

Field, T. (2001). Touch. Cambridge, Massachusetts, MIT Press.

Fraden, J. (1996). Handbook of Modern Sensors. Physics, Designs, and Applications. 2nd Edition. New York, Springer-Verlag.

Gray, H. (1977). Anatomy, Descriptive and Surgical. New York, Gramercy Books.

Gray, P. (1999). Psychology, 3rd Edition. New York, Worth Publishers.

Grupen, R. A., T. C. Henderson, et al. (1989). "A survey of general-purpose manipulation." International Journal of Robotics Research **8**(1): 38-61.

Hakozaki, M., A. Hatori, et al. (2001). A Sensitive Skin Using Wireless Tactile Sensing Elements. 18th Sensor Symposium.

Hara, F. and H. Kobayashi (1997). "State of the art in component technology for an animated face robot: its component technology development for interactive communication with humans." Advanced Robotics **11**(66): 585-604.

Haris, M. B. and R. Asim (2001). New Design of Robotic tactile sensor using dynamic wafer technology based on VLSI technique. Biomedical Research in 2001, Victoria, Australia, IEEE.

Hedgecock, A. and C. Wallace (2003). Lab Tech: New and Interesting Materials. Makeup Artist Magazine**:** 54.

Heller, H. L. and R. E. McKinstry (1995). Facial Materials. Fundamentals of Facial Prosthetics. R. E. McKinstry. Arlington, VA, ABI Professional Publications**:** 79-97.

Heller, M. A. (1991). Introduction. The Psychology of Touch. M. A. Heller and W. Schiff. Hillsdale, NJ, Lawrence Erlbaum Associates, Inc.**:** 1-19.

Hillis, W. D. (1981). Active Touch Sensing. MIT EECS Master's Thesis. Cambridge, MIT.

Hollins, M., R. Faldowski, et al. (1993). "Perpetual dimensions of tactile surface texture: a multidimensional scaling analysis." Perception & Psychophysics **54**: 697-705.

Howe, R. D. (1994). "Tactile sensing and control of robotic manipulation." Journal of Advanced Robotics **8**(3): 245-261.

Hristu, D., N. Ferrier, et al. (2000). The Performance of a deformable-membrane tactile sensor: basic results on geometrically-defined tasks. IEEE International Conference on Robotics and Automation 2000, IEEE.

Hyvarinen, J. and A. Poranen (1978). "Movement-sensitive and direction and orientation-selective cutaneous receptive fields in the hand area of the postcentral gyrus in monkeys." Journal of Physiology (London) **283**: 523-537.

Interlink Electronics product literature. FSR Integration Guide and Evaluation Parts Catalog**:** www.interlinkelec.com.

Johnson, K. O. and S. S. Hsiao (1992). "Neural Mechanisms of Tactual Form and Texture Perception." Annual Review of Neuroscience **15**: 227-50.

Johnson, K. O. and S. S. Hsiao (1994). "Evaluation of the relative roles of slowly and rapidly adapting afferent fibers in roughness perception." Canadian Journal of Physiology and Pharmacology **72**: 488-497.

Johnson, K. O. and G. D. Lamb (1981). "Neural Mechanisms of spatial tactile discrimination: Neural patterns evoked by Braille-like dot patterns in the monkey." Journal of Physiology (London) **310**: 117-44.

Johnson, K. O., J. R. Phillips, et al. (1991). Tactile pattern recognition. Information Processing in the Somatosensory System. O. Franzen and J. Westman. London, Macmillan**:** 308-18.

Johnston, D., P. Zhang, et al. (1996). A Full Tactile Sensing Suite for Dextrous Robot Hands and Use in Contact Force Control. IEEE International Conference on Robotics and Automation, Minneapolis, IEEE.

Jones, J. L., B. A. Seiger, et al. (1999). Mobile Robots. Inspiration to Implementation. 2nd Edition. Natick, Massachusetts, A.K. Peters.

Kandel, E. R., J. H. Schwartz, et al. (2000). Principles of Neuroscience, 4th Edition. New York, McGraw-Hill Health Professions Division.

Karason, S. P., M. A. Srinivasan, et al. (1999). "Encoding and Decoding of Static Information in Tactile Sensing Systems." International Journal of Robotics Research **18**(2): 131-151.

Kirtley, C. Teach-in 2000: Time-dependent behavior of inshoe force sensors http://guardian.curtin.edu.au:16080/cgi/teach-in/hysteresis. **2003**.

Krishna, G. M. and K. Rajanna (2002). Tactile Sensor Based on Piezoelectric Resonance. Sensors 2002, Orlando, Florida, IEEE.

Lamb, G. D. (1983). "Tactile discrimination of textured surfaces: peripheral neural coding in the monkey." Journal of Physiology (London) **338**: 567-587.

LaMotte, R. H. and M. A. Srinivasan (1987). "Tactile Discrimination of Shape: Responses of Rapidly Adapting Mechanoreceptive Afferents to a Step Stroked Across the Monkey Fingerpad." The Journal of Neuroscience **7**(6): 1672-1681.

LaMotte, R. H. and M. A. Srinivasan (1987). "Tactile Discrimination of Shape: Responses of Slowly Adapting Mechanoreceptive Afferents to a Step Stroked Across the Monkey Fingerpad." The Journal of Neuroscience **7**(6): 1655-1671.

LaMotte, R. H. and M. A. Srinivasan (1993). "Responses of cutaneous mechanoreceptors to the shape of objects applied to the primate fingerpad." Acta Psychologica **84**: 41-51.

Lederman, S. J. (1974). "Tactile roughness of grooved surfaces: The touching process and effects of macro- and microsurface structure." Perception & Psychophysics **16**(2): 385-395.

Leigh, D. and P. Dietz "DiamondTouch Characteristics and Capabilities."

Lifton, J., D. Seetharam, et al. (2002). Pushpin Computing System Overview: A Platform for Distributed, Embedded, Ubiquitous Sensor Networks. Pervasive 2002. F. Mattern and M. Naghshineh. Berlin Heidelberg, Springer-Verlag. **LNCS 2414:** 139-151.

Lumelsky, V. J., M. S. Shur, et al. (2001). "Sensitive Skin." IEEE Sensors Journal **1**(1): 41-51.

Madden, S., M. J. Franklin, et al. (2002). TAG: a Tiny Aggregation Service for Ad-Hoc Sensor Networks. Fifth Symposium on Operating Systems Design and implementation (OSDI '02), Boston, MA, IEEE.

Mainwaring, A., J. Polastre, et al. (2002). Wireless Sensor Networks for Habitat Monitoring. Berkeley, Intel Research**:** 1-11.

McKinstry, R. E. (1995). Fundamentals of Facial Prosthetics. Arlington, VA, ABI Professional Publications.

McLaughlin, T. (1999). Silicone Art: Materials, Methods & Techniques for Coloring, Painting, and Finishing Silicone Rubber Version 1.1. Sherman Oaks, California, McLaughlin Productions Publishing.

Menzel, P. and F. D'Aluisio (2000). Robo-Sapians: Evolution of a New Species. Cambridge, MA, MIT Press.

Montagu, A. (1986). Touching. The Human Significance of the Skin, 3rd Edition. New York, Harper & Row.

Motion Control Inc. website www.utaharm.com.

NASA website (2001). http://vesuvius.jsc.nasa.gov/er_er/html/robonaut/MIT_Hand.htm, NASA.

Nolte, J. (2002). The Human Brain: An Introduction to Its Functional Anatomy 5th Edition. St. Louis, Missouri, Mosby Inc.

Papakostas, T. V., J. Lima, et al. (2002). A Large Area Force Sensor for Smart Skin Applications. Sensors 2002, Orlando, Florida, IEEE.

Penfield, W. and T. Rasmussen (1950/1978). The Cerebral Cortex of Man, Macmillan Publishing Co., Inc.

Pohja, S. (1996). Survey of Studies on Tactile Sensing: R96:02. Kista, Sweden, RWCP Neuro SICS Laboratory**:** 1-13.

Positive Logic Engineering (1998). ASC16 Operation Manual.

Robotic Life Group (2003). http://robotic.media.mit.edu/projects/Leonardo/Leo-robot.html.

Rollman, G. B. (1991). Pain Responsiveness. The Psychology of Touch. M. A. Heller and W. Schiff. Hillsdale, NJ, Lawrence Erlbaum Associates, Inc.**:** 91-114.

Rosenzweig, M. R., S. M. Breedlove, et al. (2002). Biological Psychology, 3rd Edition. Sunderland, Massachusetts, Sinauer Associates.

Rosheim, M. E. (1994). Robot Evolution: The Development of Anthrorobotics, John Wiley & Sons Inc.

Sabelman, E. E., G. T. A. Kovacs, et al. (1994). Tactile transducers to replace lost touch sensation, Rehabilitation R&D Center Progress Report.

Sekuler, R. and R. Blake (2002). Perception, 4th Edition. New York, McGraw-Hill.

Sergio, M., N. Manaresi, et al. (2002). A Textile Based Capacitive Pressure Sensor. Sensors 2002, Orlando, Florida, IEEE.

Sherrick, C. and R. W. Cholewiak (1986). Cutaneous Sensitivity. Handbook of Perception and Human Performance. K. R. Boff, L. Kaufman and J. P. Thomas, Wiley-Interscience. **1:** 12-1 - 12-58.

Shigematsu, S., H. Morimura, et al. (1999). "A Single-Chip Fingerprint Sensor and Identifier." IEEE Journal of Solid-State Circuits **34**(12): 1852-1859.

Silicones Inc. Product Literature.

Son, J. S., E. A. Monteverde, et al. (1994). "A Tactile Sensor for Localizing Transient Events in Manipulation." IEEE Transactions **1050-4729/94**: 471-476.

Srinivasan, M. A. and R. H. LaMotte (1987). "Tactile Discrimination of Shape: Responses of Slowly and Rapidly Adapting Mechanoreceptive Afferents to a Step Indented into the Monkey Fingerpad." The Journal of Neuroscience **7**(6): 1682-1697.

Srinivasan, M. A. and R. H. LaMotte (1995). "Tactual discrimination of softness." Journal of Neurophysiology **73**: 88-101.

Stevens, J. C. (1991). Thermal Sensibility. The Psychology of Touch. M. A. Heller and W. Schiff. Hillsdale, NJ, Lawrence Erlbaum Associates, Inc.**:** 61-90.

Thomas, K. F. (1994). Prosthetic Rehabilitation. Quintessence Publishing Co., Ltd., London.

University of Utah School of Computing Website
http://www.cs.utah.edu/~jmh/UMDH.html.

Vega-Bermudez, F., K. O. Johnson, et al. (1991). "Human tactile pattern recognition: Active versus passive touch, velocity effects and patterns of confusion." Journal of Neurophysiology **65**: 531-46.

Warneke, B., M. Last, et al. (2001). "Smart Dust: Communicating with a Cubic-Millimeter Computer." IEEE Computer **0018-9162**(January 2001): 2-9.

Wessberg, J., C. R. Stambaugh, et al. (2000). "Real-time prediction of hand trajectory by ensembles of cortical neurons in primates." Nature **408**: 361-365.

Xu, Y., Y.-C. Tai, et al. (2002). IC-Integrated Flexible Shear-Stress Sensor Skin. Solid-State Sensor, Actuator ad Microsystems Workshop, Hilton Head Island, South Carolina.

Yamada, K., K. Goto, et al. (2002). A Sensor Skin Using Wire-Free Tactile Sensing Elements Based on Optical Connection. SICE 2002, Osaka.

Yamada, Y., T. Maeno, et al. (2002). Identification of Incipient Slip Phenomena Based on the Circuit Output Signals of PVDF Film Strips Embedded in Artificial Finger Ridges. SICE 2002, Osaka.

Appendix A: PIC Code

```
//ArmDeveloperBoard_v3.c
//Dan Stiehl
//wdstiehl@mit.edu
//copyright 2003 MIT Media Lab

//

// PIN OUT of 16f877
//------------------
// PIN 2      AN0 = SENS0
// PIN 3      AN1 = SENS1
// PIN 4      AN2 = SENS2
// PIN 5      AN3 = SENS3
// PIN 7      AN4 = SENS4
// PIN 8      AN5 = SENS5
// PIN 9      AN6 = SENS6
// PIN 10     AN7 = SENS7
// PIN 17     RC6/TX = Serial out to MAX233 chip
// PIN 18     RC7/RX = Serial in from MAX233 chip
// PIN 33     RB0 = Green LED
// PIN 34     RB1 = Red LED
// PIN 35     RB2 = Yellow LED
// PIN 36     RB3 = Blue LED
// PIN 37     RB4 = ENABLE multiplexers
// PIN 38     RB5 = multiplexers A0
// PIN 39     RB6 = multiplexers A1
// PIN 40     RB7 = multiplexers A2


#include <16F877.H>
//#include "string.h"
#include "stdlib.h"
#include "stdio.h"

#device ICD=FALSE
#fuses HS, NOWDT, PUT, NOLVP, NOBROWNOUT

// now we tell the compiler the clock chip is 20MHz.

#use delay(clock=20000000)

// set up the RS232 port:

#use rs232(baud=19200, xmit=PIN_C6, rcv=PIN_C7)

// declare that we will manually establish the data direction of each
// I/O pin on port B (LEDs and multiplexer controlls)

#use fast_io(B)

// define the pins used

#define LED0  PIN_B0
#define LED1  PIN_B1
#define LED2  PIN_B2
#define LED3  PIN_B3
#define EN    PIN_B4
#define A0    PIN_B5
```

```
	#define A1	PIN_B6
	#define A2	PIN_B7

	// Macros

	#define LED0_ON		output_low(LED0)
	#define LED0_OFF	output_high(LED0)
	#define LED1_ON		output_low(LED1)
	#define LED1_OFF	output_high(LED1)
	#define LED2_ON		output_low(LED2)
	#define LED2_OFF	output_high(LED2)
	#define LED3_ON		output_low(LED3)
	#define LED3_OFF	output_high(LED3)
	#define ENABLE		output_high(EN)
	#define A0_1 output_high(A0)
	#define A0_0 output_low(A0)
	#define A1_1 output_high(A1)
	#define A1_0 output_low(A1)
	#define A2_1 output_high(A2)
	#define A2_0 output_low(A2)

	// define all pins on port B as output pins

	#define IRX_B_TRIS  0b00000000

	#define max_num_boards 1 //the maximum number of boards attached
	#define max_num_MUX_Channel 8 //the maximum number of mux channels
	#define max_num_PIC_AD_Channels 8 //the maximum number of A to D channels on
the PIC

	byte binary=1; // binary mode for C program
	byte gauge=0; //Force Gauge attached or not for testing
	byte servo_pot_on=0; //Servos Pots connected (ch0-7)
	byte fsrs_on=0; //FSRs connected (ch8-63)
	byte sense_bool[max_num_boards][max_num_MUX_Channel][max_num_PIC_AD_Channels];
//define the sensor matrix for active sensors as a boolean
	byte quit_s=0;
	byte mux[max_num_MUX_Channel]; //separate the mux bytes
	byte pic_ad[max_num_PIC_AD_Channels]; //separate the pic bytes

	int board=0; //assign this board to 0

	int i,j,k;

	long sensor_num, SENSOR_CH0, SENSOR_CH1, SENSOR_CH2, SENSOR_CH3, SENSOR_CH4,
SENSOR_CH5, SENSOR_CH6, SENSOR_CH7, FG, multiplex_ch; //setup values
	long SENSOR_CH[max_num_PIC_AD_Channels];
	char a_or_b, disp, cc, rr, p, f, g, p_ch, fsrcc, potcc, fgcc, a_or_s, mpq,
m_ch;
	int numbersize=0, temp;
	int fg_mux, fg_pic; //store force gauge location
	int mux_ch, pic_ch;
	byte disp_a=0, disp_s=1; //printf display bytes
	int mux_counter; //to keep track of which mux channel is active

	#SEPARATE fg_setup() {
		printf("Force Gauge Setup: Press 'Y' if Force Gauge is connected");
		printf(" or 'N' if it is not\n\r");
		fgcc=getc();
		if(fgcc=='Y'){
			printf("Select which channel the force gauge is connected ");
			printf("to in the following format: ");
```

```
                    printf("'M'(value 0-7)'P'(value 0-7)\n\r");
                    while(quit_s!=1){//loop until quit
                           mpq=getc();
                           if(mpq=='M'){
                                  m_ch=getc();

      if(m_ch=='0'||m_ch=='1'||m_ch=='2'||m_ch=='3'||m_ch=='4'||m_ch=='5'||m_ch=='6'|
|m_ch=='7'){ //only listen to numbers
                                         //Hand coded since I could not get atoi to
work correctly
                                         if(m_ch=='0'){
                                                mux_ch=0;
                                         }
                                         else if(m_ch=='1'){
                                                mux_ch=1;
                                         }
                                         else if(m_ch=='2'){
                                                mux_ch=2;
                                         }
                                         else if(m_ch=='3'){
                                                mux_ch=3;
                                         }
                                         else if(m_ch=='4'){
                                                mux_ch=4;
                                         }
                                         else if(m_ch=='5'){
                                                mux_ch=5;
                                         }
                                         else if(m_ch=='6'){
                                                mux_ch=6;
                                         }
                                         else if(m_ch=='7'){
                                                mux_ch=7;
                                         }
                                         printf("m_ch=%c M%u",m_ch,mux_ch);

                                  }
                           }
                           else if(mpq=='P'){
                                  p_ch=getc();

      if(p_ch=='0'||p_ch=='1'||p_ch=='2'||p_ch=='3'||p_ch=='4'||p_ch=='5'||p_ch=='6'|
|p_ch=='7'){ //only listen to numbers
                                         //Hand coded since I could not get atoi to
work correctly
                                         if(p_ch=='0'){
                                                pic_ch=0;
                                         }
                                         else if(p_ch=='1'){
                                                pic_ch=1;
                                         }
                                         else if(p_ch=='2'){
                                                pic_ch=2;
                                         }
                                         else if(p_ch=='3'){
                                                pic_ch=3;
                                         }
                                         else if(p_ch=='4'){
                                                pic_ch=4;
                                         }
                                         else if(p_ch=='5'){
                                                pic_ch=5;
```

```
                                        }
                                        else if(p_ch=='6'){
                                               pic_ch=6;
                                        }
                                        else if(p_ch=='7'){
                                               pic_ch=7;
                                        }
                                        printf("p_ch=%c P%u\n\r",p_ch,pic_ch);
                                        sense_bool[board][mux_ch][pic_ch]=1;

      printf("sense_bool[%u][%u][%u]=%d\n\r",board,mux_ch,pic_ch,sense_bool[board][mu
x_ch][pic_ch]);
                                        fg_mux = mux_ch;
                                        fg_pic = pic_ch;
                                        quit_s=1;
                                        //printf("Quit\n\r");
                                 }
                          }
                   }
                   quit_s=0;
            }
            if(fgcc=='N'){
                   //printf("Force Gauge Disconnected\n\r");
                   sense_bool[board][fg_mux][fg_pic]=0;

      //printf("sense_bool[%u][%u][%u]=%d\n\r",board,fg_mux,fg_pic,sense_bool[board][
fg_mux][fg_pic]);
            }
      }

      #SEPARATE fsr_setup() {
            //printf("FSR Setup: Press 'Y' if FSRs are connected or 'N' if they are
not\n\r");
            fsrcc=getc();
            if(fsrcc=='Y'){
                   //printf("Press 'A' if all channels (8-48) are connected or");
                   //printf(" 'S' to select which channels are connected\n\r");
                   a_or_s=getc();
                   if(a_or_s=='A'){
                          //printf("All Sensor Channels (8-48) are connected\n\r");
                          for(i=1;i<6;i++){//for channels 8-47
                                 for(j=0;j<8;j++){
                                        sense_bool[board][i][j]=1; //Set Board 0, Mux
Ch1-5, and Pic Ch0-7 true

      //printf("sense_bool[%u][%u][%u]=%d\n\r",board,i,j,sense_bool[board][i][j]);
                                 }
                          }
                          for(i=0;i<1;i++){//for channel 48
                                 sense_bool[board][6][i]=1; //Set Board 0, Mux Ch6,
and Pic Ch0 true

      //printf("sense_bool[%u][6][%u]=%d\n\r",board,i,sense_bool[board][6][i]);
                          }
                   }
                   else if(a_or_s=='S'){
                          printf("Select which sensor channels are connected in the
following format: ");
                          printf("'M'(value 0-7)'P'(value 0-7)\n\r");
                          printf("Press 'Q' when finished\n\r");
                          while(quit_s!=1){//loop until quit
                                 mpq=getc();
```

```
                                if(mpq=='M'){
                                        m_ch=getc();

        if(m_ch=='1'||m_ch=='2'||m_ch=='3'||m_ch=='4'||m_ch=='5'||m_ch=='6'||m_ch=='7')
{ //only listen to numbers
                                                //Hand coded since I could not get atoi
to work correctly
                                                if(m_ch=='1'){
                                                        mux_ch=1;
                                                }
                                                else if(m_ch=='2'){
                                                        mux_ch=2;
                                                }
                                                else if(m_ch=='3'){
                                                        mux_ch=3;
                                                }
                                                else if(m_ch=='4'){
                                                        mux_ch=4;
                                                }
                                                else if(m_ch=='5'){
                                                        mux_ch=5;
                                                }
                                                else if(m_ch=='6'){
                                                        mux_ch=6;
                                                }
                                                else if(m_ch=='7'){
                                                        mux_ch=7;
                                                }

                                                //printf("m_ch=%c M%u",m_ch,mux_ch);
                                        }
                                }
                                else if(mpq=='P'){
                                        p_ch=getc();

        if(p_ch=='0'||p_ch=='1'||p_ch=='2'||p_ch=='3'||p_ch=='4'||p_ch=='5'||p_ch=='6'|
|p_ch=='7'){ //only listen to numbers
                                                //Hand coded since I could not get atoi
to work correctly
                                                if(p_ch=='0'){
                                                        pic_ch=0;
                                                }
                                                else if(p_ch=='1'){
                                                        pic_ch=1;
                                                }
                                                else if(p_ch=='2'){
                                                        pic_ch=2;
                                                }
                                                else if(p_ch=='3'){
                                                        pic_ch=3;
                                                }
                                                else if(p_ch=='4'){
                                                        pic_ch=4;
                                                }
                                                else if(p_ch=='5'){
                                                        pic_ch=5;
                                                }
                                                else if(p_ch=='6'){
                                                        pic_ch=6;
                                                }
                                                else if(p_ch=='7'){
                                                        pic_ch=7;
```

```
                                                }
                                                //printf("p_ch=%c
P%u\n\r",p_ch,pic_ch);
                                                sense_bool[board][mux_ch][pic_ch]=1;

      //printf("sense_bool[%u][%u][%u]=%d\n\r",board,mux_ch,pic_ch,sense_bool[board][
mux_ch][pic_ch]);
                                                //printf("IN P\n\r");
                                        }
                                }
                                else if(mpq=='Q'){ //Quit loop
                                        quit_s=1;
                                        //printf("Quit\n\r");
                                }
                        }
                        quit_s=0;
                }
        }
        else if(fsrcc=='N'){
                //printf("All FSR Sensors are Disconnected\n\r");
                for(i=1;i<6;i++){//for channels 8-47
                        for(j=0;j<8;j++){
                                sense_bool[board][i][j]=0; //Set Board 0, Mux Ch1-5,
and Pic Ch0-7 true

      //printf("sense_bool[%u][%u][%u]=%d\n\r",board,i,j,sense_bool[board][i][j]);
                        }
                }
                for(i=0;i<2;i++){//for channel 48
                        sense_bool[board][6][i]=0; //Set Board 0, Mux Ch6, and Pic
Ch0-1 true

      //printf("sense_bool[%u][6][%u]=%d\n\r",board,i,sense_bool[board][6][i]);
                }

        }

      }

      #SEPARATE pot_setup() {
        //printf("Servo Pot Setup: Press 'Y' if Pots are connected or 'N' if they
are not\n\r");
        potcc=getc();
        if(potcc=='Y'){
                //printf("Press 'A' if all channels (0-6) are connected or");
                //printf(" 'S' to select which channels are connected\n\r");
                a_or_s=getc();
                if(a_or_s=='A'){
                        //printf("All Sensor Channels (0-6) are connected\n\r");
                        for(k=0;k<7;k++){
                                sense_bool[board][0][k]=1; //Set Board 0, Mux Ch0,
and Pic Ch0-6 true

      //printf("sense_bool[%u][0][%u]=%d\n\r",board,k,sense_bool[board][0][k]);
                        }
                }
                else if(a_or_s=='S'){
                        //printf("Select which sensor channels are connected in the
following format: ");
                        //printf("'P'(value 0-7), note M=0 by default\n\r");
                        //printf("Press 'Q' when finished\n\r");
                        while(quit_s!=1){//loop until quit
```

```
                                mpq=getc();
                                if(mpq=='P'){
                                        p_ch=getc();

        if(p_ch=='0'||p_ch=='1'||p_ch=='2'||p_ch=='3'||p_ch=='4'||p_ch=='5'||p_ch=='6'|
|p_ch=='7'){ //only listen to numbers and E (for end)
                                                //Hand coded since I could not get atoi
to work correctly
                                                if(p_ch=='0'){
                                                        pic_ch=0;
                                                }
                                                else if(p_ch=='1'){
                                                        pic_ch=1;
                                                }
                                                else if(p_ch=='2'){
                                                        pic_ch=2;
                                                }
                                                else if(p_ch=='3'){
                                                        pic_ch=3;
                                                }
                                                else if(p_ch=='4'){
                                                        pic_ch=4;
                                                }
                                                else if(p_ch=='5'){
                                                        pic_ch=5;
                                                }
                                                else if(p_ch=='6'){
                                                        pic_ch=6;
                                                }
                                                else if(p_ch=='7'){
                                                        pic_ch=7;
                                                }
                                                //printf("p_ch=%c
P%u\n\r",p_ch,pic_ch);
                                                sense_bool[board][mux_ch][pic_ch]=1;

        //printf("sense_bool[%u][%u][%u]=%d\n\r",board,mux_ch,pic_ch,sense_bool[board][
mux_ch][pic_ch]);
                                                //printf("IN P\n\r");
                                        }
                                }
                                else if(mpq=='Q'){ //Quit loop
                                        quit_s=1;
                                        //printf("Quit\n\r");
                                }
                        }
                        quit_s=0;
                }
        }
        else if(potcc=='N'){
                //printf("All Sensor Channels Are Disconnected\n\r");
                for(k=0;k<7;k++){
                        sense_bool[board][0][k]=0; //Set Board 0, Mux Ch0, and Pic
Ch0-6 false

        //printf("sense_bool[%u][0][%u]=%d\n\r",board,k,sense_bool[board][0][k]);
                }
        }
        }

        #SEPARATE setup(cc) {
        //printf("IN SETUP\n\r");
```

```
		//printf("cc=%c\n\r",cc);
		while(cc!='N'){ //Send an 'N' to start the sampling
			cc=getc();
			switch(cc){
				case 'P': //Servo Pot Setup
					pot_setup();
				break;
				case 'F': //FSR Setup
					fsr_setup();
				break;
				case 'G': //Force Gauge Setup
					fg_setup();
				break;
				case 'V': //check values of sense_bool for debug
					for(i=0; i<max_num_MUX_Channel;i++){
						for(j=0;j<max_num_PIC_AD_Channels;j++){

	printf("sense_bool[%d][%d][%d]=%d\n\r",board,i,j,sense_bool[board][i][j]);
						}
					}
				break;
				case 'M': //Analog or Binary
					//printf("Press 'A' for Analog or 'B' for Binary
mode\n\r");
					a_or_b=getc();
					if(a_or_b=='A'){
						binary=0;
						}
					else if(a_or_b=='B'){
						binary=1;
					}
					//printf("binary=%d\n\r",binary);
				break;
				case 'D': //Display Modes
					printf("Select the Printout Display Mode\n\r");
					printf("Press 'E' for Expert - no printouts\n\r");
					printf("Press 'S' for Setup - only setup printouts
(default)\n\r");
					printf("Press 'A' for all printouts\n\r");
					disp=getc();
					if(disp=='E'){
						disp_a=0;
						disp_s=0;
					}
					if(disp=='S'){
						disp_a=0;
						disp_s=1;
					}
					if(disp=='A'){
						disp_a=1;
						disp_s=1;
					}
				break;
			}
		}
	}

	#SEPARATE ch_on_off(){
		for(i=0;i<max_num_MUX_Channel;i++){
			for(j=0;j<max_num_PIC_AD_Channels;j++){
				if(sense_bool[0][i][j]==1){
					mux[i]=1;
```

```
                                pic_ad[j]=1;
                            }
                            //printf("sense_bool[%u][%u][%u]=%d mux[%u]=%d
pic_ad[%u]=%d\n\r",board,i,j,sense_bool[board][i][j],i,mux[i],j,pic_ad[j]);
                        }
                }
        }

        #SEPARATE initialize(){
                //initialize all sensor values to be zero
                for(i=0; i<max_num_MUX_Channel;i++){
                        for(j=0;j<max_num_PIC_AD_Channels;j++){
                                sense_bool[board][i][j]=0;

        //printf("sense_bool[%d][%d][%d]=%d\n\r",board,i,j,sense_bool[board][j][k]);
                        }
                }
                //initialize all on_off values to zero
                for(i=0;i<max_num_MUX_Channel;i++){
                        mux[i]=0;
                        //printf("mux[%u]=%d\n\r",i,mux[i]);
                }
                for(i=0;i<max_num_PIC_AD_Channels;i++){
                        pic_ad[i]=0;
                        //printf("pic_ad[%u]=%d\n\r",i,pic_ad[i]);
                }
        }

        void main()
        {
                reset: printf("Reset\n\r");
                // set up portb
                set_tris_b(IRX_B_TRIS);

                setup_port_a(ALL_ANALOG);
                setup_adc(adc_clock_internal);

                // Blink the LEDs on and off to show we're alive
                LED0_ON;
                LED2_ON;
                delay_ms(50);
                LED1_ON;
                delay_ms(50);
                LED0_OFF;
                delay_ms(50);
                LED1_OFF;
                LED2_OFF;



                //printf("Arm Developer Board - 64 Channel A/D Converter\n\r");


                //INITIALIZE
                initialize();

                //SETUP
                setup(cc);

                //Turn Channels on or off
                ch_on_off();
```

```
LED0_OFF;
LED1_OFF;

// Enter main loop
while (1) {
	if(kbhit()){//check for a keyboard input
		if(getc()=='R'){
			//printf("Got and R");
			GOTO reset;
		}
	}

	LED0_ON;
	LED1_ON;

	//printf("multiplex_ch=%ld\n\r",multiplex_ch);

	//MUX CHANNEL SELECTION
	if(multiplex_ch==0){
		if(mux[multiplex_ch]==1){
			LED0_OFF;
			LED1_OFF;
			LED2_OFF;
			LED3_OFF;
			ENABLE;
			A0_0;
			A1_0;
			A2_0;
			//printf("A2=0 A1=0 A0=0\n\r");
		}
		//Send out 'DATA' Header
		if(binary){
			putc('D');
			putc('A');
			putc('T');
			putc('A');
		}
		else{
			printf("DATA\n\r");
		}
		mux_counter=0; //current channel
		multiplex_ch=1;	//next channel
		delay_us(2);}
	else if(multiplex_ch==1){
		if(mux[multiplex_ch]==1){
			LED0_OFF;
			LED1_OFF;
			LED2_ON;
			LED3_OFF;
			ENABLE;
			A0_1;
			A1_0;
			A2_0;
			//printf("A2=0 A1=0 A0=1\n\r");
		}
		mux_counter=1;
		multiplex_ch=2;
		delay_us(2);}
	else if(multiplex_ch==2){
		if(mux[multiplex_ch]==1){
			LED0_OFF;
			LED1_ON;
```

```
                LED2_OFF;
                LED3_OFF;
                ENABLE;
                A0_0;
                A1_1;
                A2_0;
                //printf("A2=0 A1=1 A0=0\n\r");
        }
        mux_counter=2;
        multiplex_ch=3;
        delay_us(2); }
else if(multiplex_ch==3){
        if(mux[multiplex_ch]==1){
                LED0_OFF;
                LED1_ON;
                LED2_ON;
                LED3_OFF;
                ENABLE;
                A0_1;
                A1_1;
                A2_0;
                //printf("A2=0 A1=1 A0=1\n\r");
        }
        mux_counter=3;
        multiplex_ch=4;
        delay_us(2);}
else if(multiplex_ch==4){
        if(mux[multiplex_ch]==1){
                LED0_ON;
                LED1_OFF;
                LED2_OFF;
                LED3_OFF;
                ENABLE;
                A0_0;
                A1_0;
                A2_1;
                //printf("A2=1 A1=0 A0=0\n\r");
        }
        mux_counter=4;
        multiplex_ch=5;
        delay_us(2);}
else if(multiplex_ch==5){
        if(mux[multiplex_ch]==1){
                LED0_ON;
                LED1_OFF;
                LED2_ON;
                LED3_OFF;
                ENABLE;
                A0_1;
                A1_0;
                A2_1;
                //printf("A2=1 A1=0 A0=1\n\r");
        }
        mux_counter=5;
        multiplex_ch=6;
        delay_us(2);}
else if(multiplex_ch==6){
        if(mux[multiplex_ch]==1){
                LED0_OFF;
                LED1_ON;
                LED2_ON;
                LED3_OFF;
```

```
                                ENABLE;
                                A0_1;
                                A1_1;
                                A2_0;
                                //printf("A2=0 A1=1 A0=1\n\r");
                        }
                        mux_counter=6;
                        multiplex_ch=7;
                        delay_us(2);}
                else if(multiplex_ch==7){
                        if(mux[multiplex_ch]==1){
                                LED0_ON;
                                LED1_ON;
                                LED2_ON;
                                LED3_OFF;
                                ENABLE;
                                A0_1;
                                A1_1;
                                A2_1;
                                //printf("A2=1 A1=1 A0=1\n\r");
                        }
                        mux_counter=7;
                        multiplex_ch=0;
                        delay_us(2);}
                else {
                        multiplex_ch=0;
                        delay_us(1);
                        }
                //printf("mux[%u]=%d\n\r",mux_counter,mux[mux_counter]);

                for(i=0;i<max_num_PIC_AD_Channels;i++){
                        if(mux[mux_counter]==1){
                                //READ SENSORS
                                //printf("MUX_CH=%04ld\n\r", mux_counter);
                                //printf("pic_ad[%u]=%d\n\r",i,pic_ad[i]);

        //printf("sense_bool[%u][%u][%u]=%d\n\r",board,mux_counter,i,sense_bool[board][
mux_counter][i]);
                                if(sense_bool[board][mux_counter][i]==1){
                                        //Read adc_ch0
                                        LED3_ON;
                                        set_adc_channel( i );
                                        delay_us(50); //allow time for conversion
                                        SENSOR_CH[i]=read_adc();
                                        LED3_OFF;
                                        if(binary){
                                                putc(SENSOR_CH[i]>>8);
                                                putc(SENSOR_CH[i]&0x00ff);
                                        }
                                        else{
                                                sensor_num=(mux_counter*8)+i; //for
output sensor number for ascii text debug
                                                //printf("s%02ldv%04ld\n",sensor_num,
SENSOR_CH0);
                                                printf("s%02ldv%04ld ",sensor_num,
SENSOR_CH[i]);
                                        }
                                }
                                if(!binary){
                                        printf("\n\r");
                                }
                        }
```

```
                    }
            }
    }
```